CHAPTER I

INTRODUCTION

Gene therapy involves the introduction of exogenous genes into target cells where production of the encoded protein will occur. In the case of acquired or inherited genetic disorders, this enables the replacement of a missing or defective gene, leading to normal cell function (Corsi et al., 2003). The direct delivery of genes is uncompleted by low bioavailability, indication of toxicity, a short half-life (Han et al., 2000) and low transfection efficiency. Transfection is the expression of genes which are introduced into the target cell or the target tissue to modify a presenting function or to establish a renewed function.

The development of gene delivery system is optimization of efficient and safe carriers that are called the vectors. The viral or non-viral vectors deliver gene to cells target. Viral vectors are retroviruses, adeno-viruses, adeno-associated viruses, herpes simplex viruses and lentiviruses (Oligino et al., 2000). Viral vectors have been commonly effective in clinical trials because of their high transfection efficiency compared with non-viral vectors, their application to the human body is often restricted by immunogenicity, potential infectivity, complicated production, and inflammation (Smith A., 1995). Furthermore, obstacles involve their rapid clearance

from the circulation and the reduced capacity to carry a large amount of genetic information.

Non-viral delivery systems together with cationic liposome and polymeric system have been estimated. The advantage of the non-viral method resides in its being a safer alternative, demonstrating no immunogenicity, slight toxicity, having the ability to carry large therapeutic genes and a reduced production cost (Romano et al., 2000). The most generally used non-viral vectors are complexes composed of plasmid DNA and cationic lipids (Monck et al., 2000; Maurer et al., 1999). Improving their clearance from the circulation, they are reasonably large in size with positive charges. Despite they show an increased tranfection efficacy in vitro, they have evidenced toxicity both in vitro and in vivo (Li et al., 1997; Brown., 2001). Besides, polymers present various specific advantages in excess of cationic lipids. The efficiency with which cationic polymers bind and condense plasmid DNA permits the protection of the nucleic acids during the intracellular transport (Dunlop et al., 1997). Due to protein expression, polymers control gene release in the course of their biodegradation. Another important aspect is the possibility to modify the polymer surface, raising the prospect of targeting specific cellular receptors. This specificity is essential to avoid side effects resulting from expression of the gene in sites other than those intended (Corsi et al., 2003). Generally used polymers consist of polyethyleneimine (PEI) (Weiss et al., 2006), polylysine (Yamagata et a1., 2007), polyamidoamine dendrimer (Choi et al., 2006) and chitosan (Rolland,1998;Borchard,2001). Both PEI and the dendrimers are effective gene carriers, but both are synthetic and not biodegradable, which means that their potential

toxicity is a concern. Although biodegradable, PLL forms polyplexes with lower transfection efficiency than that of PEI and the dendrimers (T.-H. Kim et al., 2007).

Additionally, cell membranes perform as barriers can cause a problem in genes delivery by selectively allowing only certain structures to pass based on hydrophilicity : hydrophobicity ratios (Bianco et al., 2007). Through the currently available delivery systems which include liposome, emulsions, polymers and microparticles (Allen et al., 2004; Kosterelos et al., 2003; Merdan et al., 2002), carbon nanotubes (CNTs) have lately gained high attractiveness as potential drug carriers, therapeutic agents and for applications in diagnosis (Blanco et al., 2005; Lin et al., 2004; Pastorin et al., 2005; Katz et al., 2005; Fortina et al., 2005).

Carbon nanotubes (CNTs) are cylindrical molecules, hexagonal arrangement of sp^2 hybridized carbon atoms. The hollow cylinders are formed by rolling single or multiple layers of graphene sheet. Functionalized single-walled carbon nanotubes (f-SWCNTs) have been reported for protein and DNA delivery that they could transfect cultured cells. Pantarotto determined that CNTs covalently functionalized with ammonium groups ($CNT\text{-}NH^{3+}$) were able to associate with pDNA through electrostatic interactions. The delivery of pDNA and expression of b-galactosidase in CHO cells was found to be approximately 10 times higher than naked pDNA. Liu et al. suggested that the CNT–PEI–pDNA conjugates were found the level of gene (pCMV-Luc) expression to be much higher than those of DNA alone. Rasti K. et al. developed SWNTs with hexamethylenediamine (HMDA) to bind negatively charged siRNA. siRNA were able to cross the cell membrane and to suppress expression of

the ERK target proteins in primary cardiomyocytes by about 75%. Weiling Q. et al. showed the interaction between MWCNT-PAMAM with plasmid DNA of enhanced green fluorescence protein (pEGFP-N1). They found that the MWCNT-PAMAM hybrid possessed good pEGFP-N1 immobilization ability and could efficiently deliver GFP gene into cultured HeLa cells. Moreover, many investigations showed SWCNTs were nontoxic. Multiwalled carbon nanotubes (MWCNTs) are easily synthesized and the production cost is much less than that of SWCNTs. MWCNTs can be functionalized at the surface to have positive charge for DNA transport. The purpose of this study was to develop f-MWCNTs for plasmid DNA delivery.

Chitosan is derived from deacetylation of chitin, the main organic component of crustacean shells, cuticles of insects and cell walls of fungi. Chitosan is known as a biocompatible, biodegradable and low toxic material with high cationic potential (Lee et al., 1998). Chitosan is appropriate material for effective non-viral gene therapy which many in vitro and in vivo studies have publicized. The chemical modification of chitosan should be improved for efficacy transfection and cell specificity.

In this study, multiwalled carbonnanotubes (MWCNTs) were modified and used as carrier for gene delivery. The MWCNTs were functionalized by treating with concentrated acid to improve solubility and to obtain anionic particles. The morphology of f-MWCNTs was investigated. The obtained f-MWCNTs were then attached with cationic chitosan nanoparticles (CS). f-MWCNTs/CS were further formed complex with plasmid DNA (plasmid Enhanced Green Fluorescence Protein-C_2 (pEGFP-C_2)). The characteristics of nanoparticles were evaluated. For in vitro

studies, f-MWCNTs/CS/pDNA nanoparticles were examined for cytotoxicity and transfection in HeLa cell culture and compared with commercial vectors.

Therefore, the purposes of this study were as follows:

1. To form the nanoparticles of fMCNTs/CS/pDNA complexes.
2. To determine the physical properties fMCNTs/CS/pDNA complexes.
3. To determine the cytotoxicity of fMCNTs/CS/pDNA complexes in HeLa cell.
4. To determine the transfection effect of fMCNTs/CS/pDNA complexes in HeLa cell.

CHAPTER II

LITERATURE REVIEW

A. Gene therapy and Gene delivery system

Gene therapy

The introduction of exogenous genes was into target cells where production of the encoded protein will occur. In the case of acquired or inherited genetic disorders, this enables the replacement of a missing or defective gene, leading to normal cell function (Corsi et al., 2003). Gene therapy is the way of accurate genes to the target cells to replace malfunctioning genes fading.

Gene therapy was used for treating the cause of a disease rather than the symptom. The competence of management of protein expression in humans presents the treatment with many diseases that are currently untreatable by conventional drug therapy. The diseases are appropriate for treatment by gene therapy, there were divided into genetic and acquired disease (Sullivan, 2003). Genetic diseases are caused by a single gene mutation, deletion of normal metabolic pathways, receptor function or regulation of cell cycle. There are the examples of genetic disease such as

severe combined immunodeficiency, hemophilia, familial hypercholesterolemia, cystic fibrosis, hemoglobinopathies, Gaucher's disease, inherited emphysema, muscular dystrophy. The acquired disease, no single gene has been identified as the only cause of the disease such as cancer, neurological diseases, cardiovascular diseases, infectious diseases. The expression of a proper single gene in target cells can get rid of the diseases of acquired diseases.

A disease of the immune system called severe combined immunodeficiency disease (SCID), the cells have a defective gene that cannot encode a particular enzyme. This enzyme is adenosine diaminase (ADA). The ADA deficiency causes the body to lose the protection of lymphocytes that the patient cannot increase a defense against infectious disease and soon dies. The gene for ADA production is located on chromosome number 20 and has 32,000 base pairs and twelve exons. In 1990, a research team from the National Institutes of Health (NIH) received approval to use gene therapy for the reason of relieving ADA deficiency. The lymphocytes were taken out from the patient and exposed the cells to billions of retroviruses carrying the genes for ADA production. This is the *ex vivo* approach compared to the *in vivo* approach where cells remain in the patient's body. On September 14, 1990, the first gene therapy was used in 4-year-old girl. The amount of ADA produced by the lymphocytes appeared to be increasing, and the ability to produce antibodies had increased significantly (Alcamo, 2001).

In addition, the accomplishment was detected *in vivo* human gene therapy for treatment of hemophilia. Adeno-associated virus, as gene delivery vector, was delivered intramuscularly to patients lacking functional clotting Factor IX. The decreasing in the amount of bleeding for the treated patients was also monitored (Sullivan, 2003). *In vivo* gene therapy consists of a gene and vector that is directly administered to the patient via conventional. *Ex vivo* approach requires isolating the patient's cells for introducing the gene into those cells and then reintroducing the modified cells back into the patient. *In vivo* gene therapy is a more acceptable approach than *ex vivo* approach. As a result, *ex vivo* gene therapy is not an attractive approach for pharmaceutical companies but may be a service that can be provided for person treatment.

A cystic fibrosis (CF) symptom is the cells lining the body's organs and vessels increase the chloride ions. These ions usually pass out of cells through a cystic transmembrane conductance regulator (CTCR) protein which is channel-shaped and tunnel-like protein. The CTCR protein is not produced due to gene defect in cystic fibrosis patient and the ions continue in the cells. For that reason, the water is drawn into the cells and departs dehydrated, sticky mucus in the body's passageways, especially its airways. This condition can conduct the infection. Most CF patients die from respiratory tract and lung infections. The adenovirus is suitable vector because of its ability to penetrate cells of human respiratory tract (Alcamo, 200l).

Gene therapy was attempted to correct inheritable disorders resulting from a single gene defect in the begin of development. For example, adenosine deaminase deficiency in severe combined immunodeficiency disease (SCID), cystic fibrosis transmembrane conductance regulator gene mutation in cystic fibrosis, hypoxanthine-guanine phosphoribosyl transferase deficiency in Lesch-Nyhan disease and glucocerebrosidase enzyme deficiency in Gaucher's disease. Presently, gene therapy was a promising treatment for a broad range of disease, including cancer, AIDS, neurological disorders such as Parkinson's disease, Alzheimer's disease, cardiovascular disorders, the corneal gene therapy, thalassemia.

Gene therapy for thoracic malignancies represents a novel therapeutic approach and has been evaluated in several clinical trials. Strategies have included induction of apoptosis, tumor suppressor gene replacement, suicide gene expression, cytokine-based therapy, various vaccination approaches, and adoptive transfer of modified immune cells (Anil et al, 2011).

Gene therapy was also used to relieve the effects of acquired immunodeficiency syndrome (AIDS) by attaching genes for HIV proteins to the vector and then administer into the patients. The HIV genes stimulated the normal body cells to produce HIV proteins. Then, these proteins should stimulate the immune system to secrete anti-HIV antibodies.

Mohan et al, 2011 studies showing substantial targeted gene delivery into corneal endothelium are particularly exciting as it has potential as an effective therapy for endothelial dystrophies in the future.

Human globin gene therapy with autotransplantation of transduced human hematopoietic stem cells is an exciting alternative approach to a potential cure. One patient with thalassemia has recently been reported to have clinical benefit after lentiviral human β-globin gene therapy. He has not required blood transfusions for almost 2 years (Arthur, 2010).

Gene delivery system

Even though gene therapy has many benefits, the process of gene therapy involves much difficulty. DNA was poor cellular uptake and rapid degradation. The delivery systems of DNA should defend them from enzymes. The charge, size, and poor stability of DNA were effective problems to cellular uptake. The negatively charged phosphate backbone of the DNA is the primary cause of its inefficient cellular association, due to electrostatic repulsion between DNA and negatively charged cell surface. In addition, naked DNA has extremely low stability because of degradation by nuclease. Nucleases recognize the phosphodiester linkage in the DNA backbone and induce hydrolytic degradation of the DNA molecule. Nuclease degradation of DNA can be circumvented by chemical derivatization of the backbone or by using gene delivery system.

The delivery system must use the carrier molecule or particle called vector to deliver genes to targeted cells. The vector is a molecule, particle, organism, or other carrier that transports genes to the targeted cells.

The image below represented the schematic representation of the delivery, uptake, and intracellular trafficking of DNA during delivered by gene delivery system. First of all, the complexation between DNA and vectors or the entrapment of DNA in delivery system is occurred. When DNA-vector complex is within tissue, avoiding interactions with exbacellular matrix, and then they must go to the target cell. After targeting the delivery system to the target cell, the DNA-vector complex is associated with the cell membrane and is internalized into the cytoplasm via endocytosis. In the endosomal vesicles, the DNA can be inactivated or degraded by lysosomal enzyme.

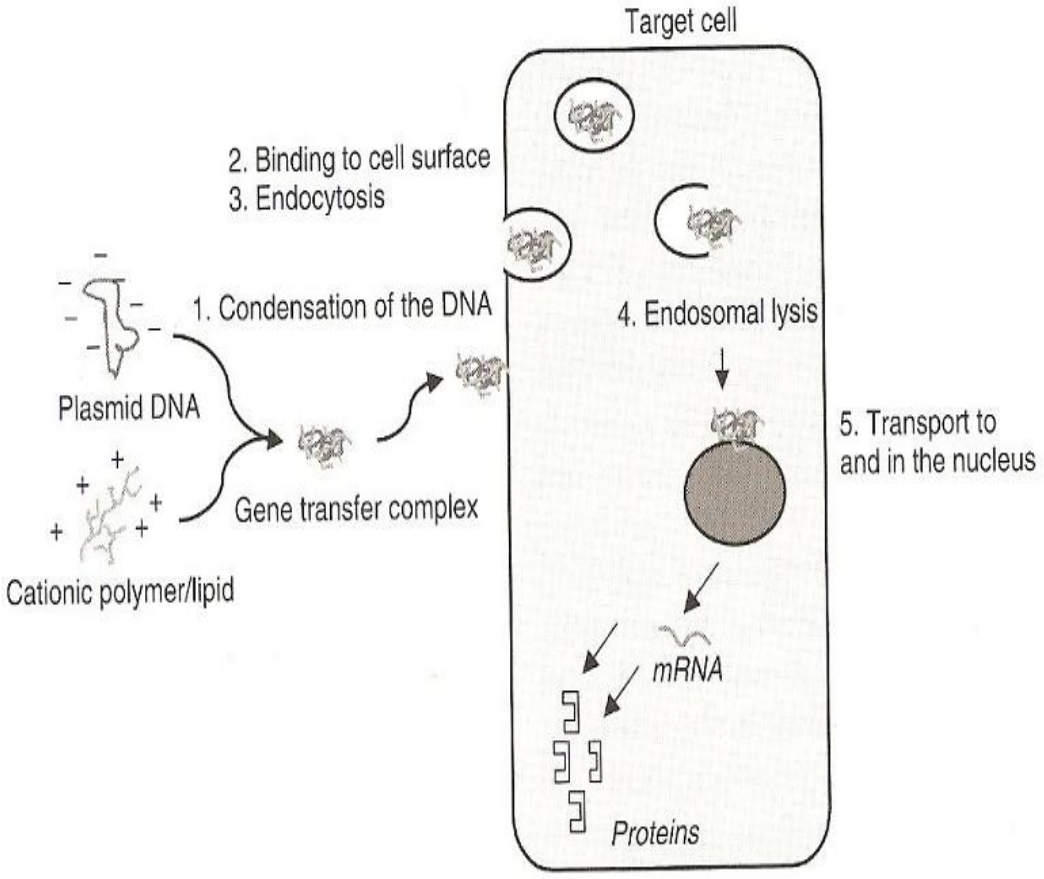

Figure 1 The image represented the schematic representation of the delivery, uptake, and cellular trafficking of DNA during delivered by gene delivery system.

If the DNA-vector complex escapes from the endosome, it can enter the cytoplasm of the cell. Therefore to ensuring activity of the DNA, it is essential to ensure their rapid escape and protect the DNA from degradation in endosome because the endosome is a major site of DNA metabolism. In the cytoplasm, DNA undergoes dissociation from the vector and passes into the nucleus through the nuclear pores, or during mitosis, when the nuclear envelope is weakened. Therefore the internalization of DNA is controlled by the pores of nuclear membrane. Lastly, when the DNA has entered the nucleus, long-lived gene expression must be ensured.

In the systemic application, particle size is the critical parameter for successful delivery playing a role in transport of DNA-vector complex through capillaries, passing out of the blood vessels (extravasation) and passing through the intertissue space. Furthermore, complex must remain stable and not aggregating in the blood. Moreover, complex should be designed not to interact with components of the blood system, such as plasma, erythrocytes, cell of the reticuloendothelial system (RES), extracellular matrix and other non-target cells (Wightman et al., 2003).

B. Viral and Non-viral gene delivery

Viral gene delivery

Gene expression using viral vectors is achieved with extremely high transfection efficiencies in a variety of human tissues (Schmid et a1., 2004). However, there are several drawbacks over the use of viruses as vectors to deliver DNA therapeutics in humans. The major drawbacks are the toxicity of the viruses and the potential for generating immune response because of their proteinaceous capsid and not allowing repeated *in vivo* transfection the same carrier (Kay et al., 2001) Moreover, the insertion of therapeutic genes into the host genome by the takes place in a random way. There is no control over the exact location of the insertion that may inhibit expression of normal cellular genes or activate oncogenes. This may other problems, such as mutagenesis and carcinogenesis (Simon et al., 1993; Kamiya et a1., 2001). Many other factors may limit the use of viral vectors for gene delivery. Because the viral envelope has a finite capacity, there is a limit on the size of the expression plasmid that it can incorporate.

The direct delivery of genes is uncompleted by low bioavailability, indication of toxicity, a short half-life (Han et al., 2000) and low transfection efficiency. Transfection is the expression of genes which are introduced into the target cell or the target tissue to modify a presenting function or to establish a renewed function.

The development of gene delivery system is optimization of efficient and safe carriers that are called the vectors. The viral or non-viral vectors deliver gene to cells target. Viral vectors are retroviruses, adeno-viruses, adeno-associated viruses, herpes simplex virus and lentivirus (Oligino et al., 2000). In spite of the viral vectors have been commonly effective in clinical trials because of their high transfection efficiency compared with non-viral vectors, their application to the human body is often restricted by immunogenicity, potential infectivity, complicated production, and inflammation (Smith A., 1995). Furthermore, obstacles involve their rapid clearance from the circulation and the reduced capacity to carry a large amount of genetic information.

a

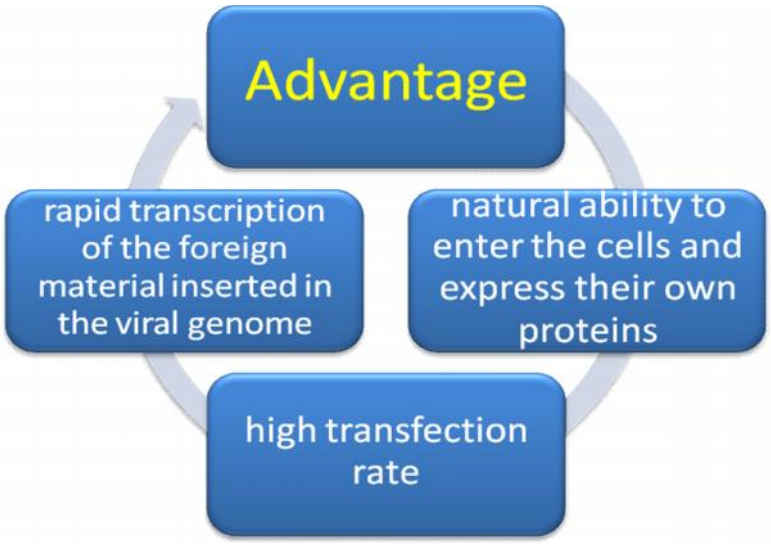

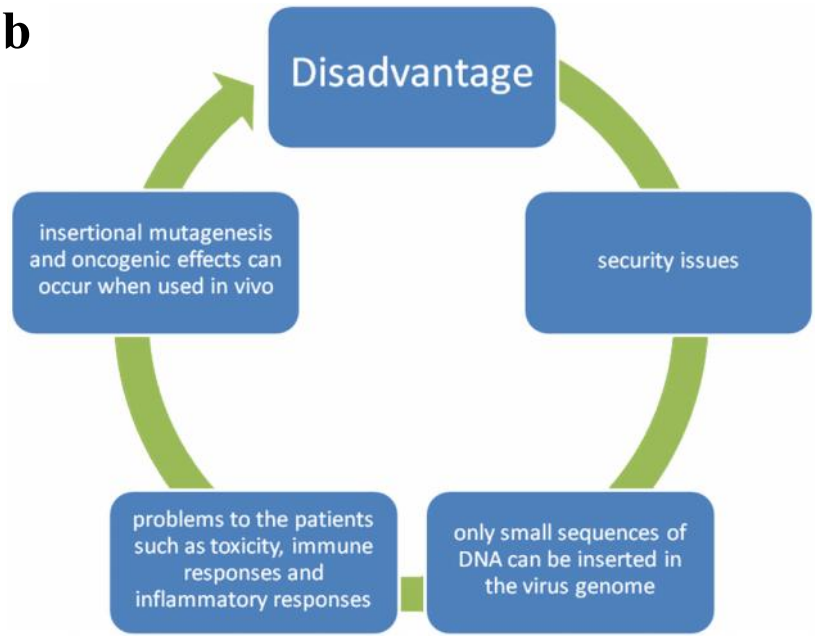

Figure 2 The advantage (a) and disadvantage (b) of viral vector

Non-viral gene delivery

Non-viral delivery can overcome some of the problems associated with viral vectors and are emerging as favorable alternatives to viral vectors owing to their biosafety (Seymour, 1998) and lack of immune response. Unlike viral delivery, non-viral delivery will not insert the therapeutic genes into the host genome. Moreover, other advantages of non-viral gene delivery vectors are ease of formulation, stability and ability to be produced in large quantities. Additional, non-viral vector provide flexibility in the size and sequence of DNA that can delivered (Kreiss et al., 1999). Furthermore, the low cost and consistence of production, as compared to the growth of viruses followed by purification, attract the use of non- viral delivery. However,

non-viral gene delivery systems mediate moderate to high gene expression. Levels in vitro, but often fail to induce significant levels of gene expression in vivo.

Generally used non-viral vectors for gene delivery can be classified into 2 major types on the nature of the synthetic material, cationic phospholipids and cationic polymers. Because of their permanent cationic charge, both types interact electrostatically with negatively charged DNA and form complexes (Tang et al., 1997; Mao et al., 2001). Then gene transfer complexes with electropositively charge bind ionically to the electronegative surface of the cells composed of proteoglycans or sialylated glycoproteins results in the internalization and ultimately the transfection of the cells.

Catonic phospholipids

Cationic phospholipids have been widely used as gene delivery vectors. Liposomes are vesicles that consist of an aqueous compartment enclosed in phospholipids bilayers. The head group of cationic phospholipids is protonated affording binding to DNA, this complex is called lipoplexes. Cationic phospholipids offer several advantages over viral vector, such as low immunogenicity and ease of preparation. The phospholipids composition in the liposome bilayers can be varied therefore liposomal delivery systems can be easily designed to yield a desired size.

a

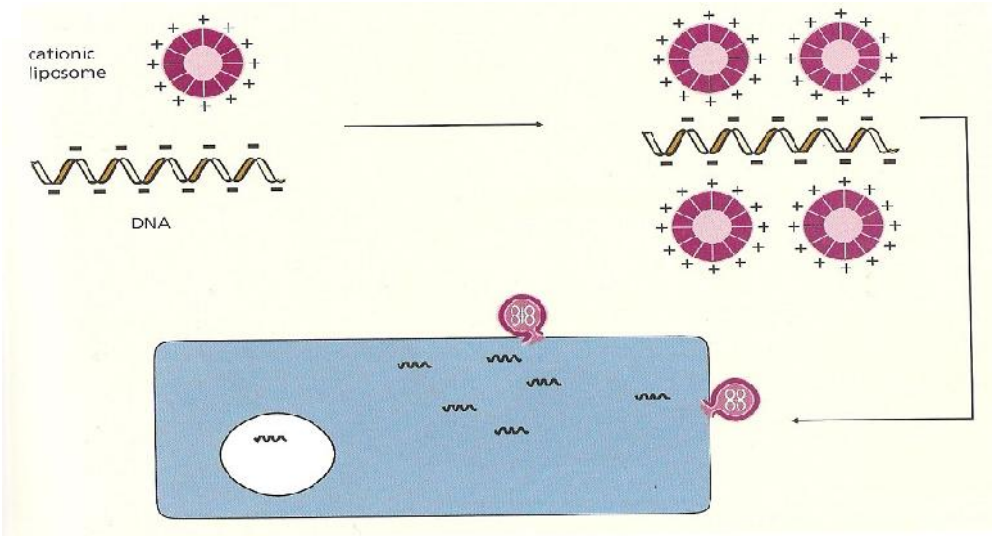

b

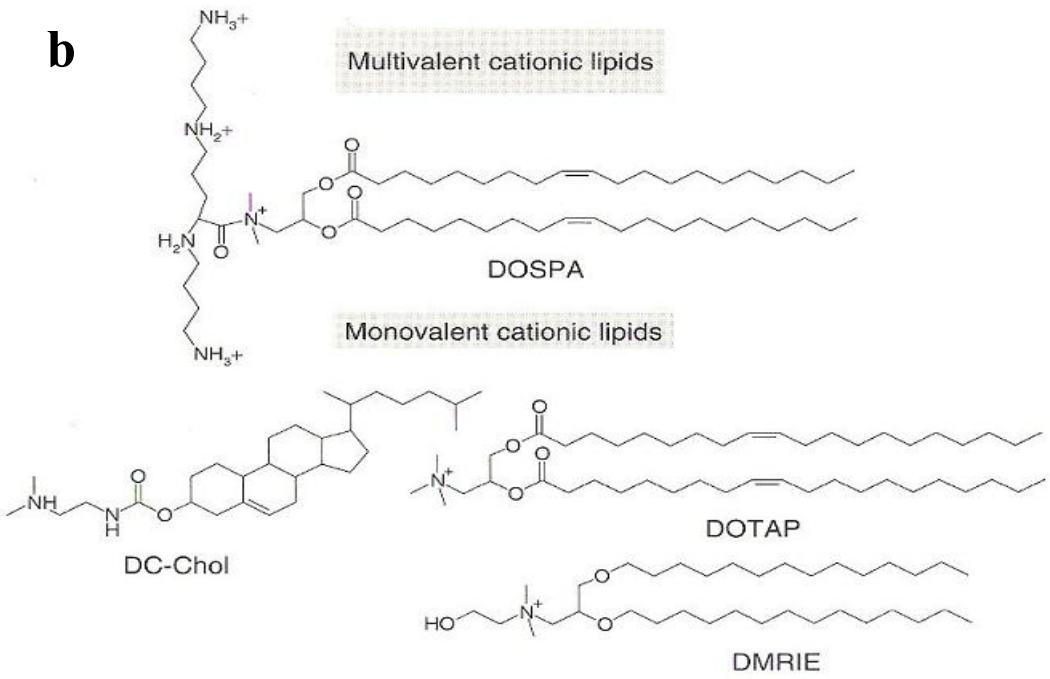

Figure 3 The image of delivery by cationic phospholipid (Dann et al., 2002) (a), the image of cationic phospholipid structures (Kayser et al., 2004) (b).

Therapeutic genes and a reduced production cost (Romano et al., 2000). The most generally used non-viral vectors are complexes composed of plasmid DNA and cationic lipids (Monck et al., 2000; Maurer et al., 1999). Improving their clearance from the circulation, they are reasonably large in size with positive charges. Despite they show an increased tranfection efficacy in vitro, they have evidenced toxicity both in vitro and in vivo (Li et al., 1997; Brown, 2001). Besides, polymers present various specific advantages in excess of cationic lipids.

Cationic polymers

The efficiency with which cationic polymers bind and condense plasmid DNA permits the protection of the nucleic acids during the intracellular transport (Dunlop DD et al., 1997). Ought to protein expression, polymers control gene release in the course of their biodegradation. Another important aspect is the possibility to modify the polymer surface, raising the prospect of targeting specific cellular receptors. This specificity is essential to avoid side effects resulting from expression of the gene in sites other than those intended (K. Corsi et al., 2003). Generally used polymers consist of polyethyleneimine (PEI) (Weiss et al., 2006), polylysine (Yamagata et a1., 2007), polyamidoamine dendrimer (Choi et al., 2006) and chitosan (Rolland AP,1998;Borchard,2001). Both PEI and the dendrimers are effective gene carriers, but both are synthetic and not biodegradable, which means that their potential toxicity is a

concern. Although biodegradable, PLL forms polyplexes with lower transfection efficiency than that of PEI and the dendrimers (T.-H. Kim et al., 2007).

Chitosan is derived from deacetylation of chitin, the main organic component of crustacean shells, cuticles of insects and cell walls of fungi. Chitosan is known as a biocompatible, biodegradable and low toxic material with high cationic potential (Lee KY et al., 1998). Chitosan is appropriate material for effective non-viral gene therapy which many in vitro and in vivo studies have publicized. The chemical modification of chitosan should be improving for efficacy transfection and cell specificity.

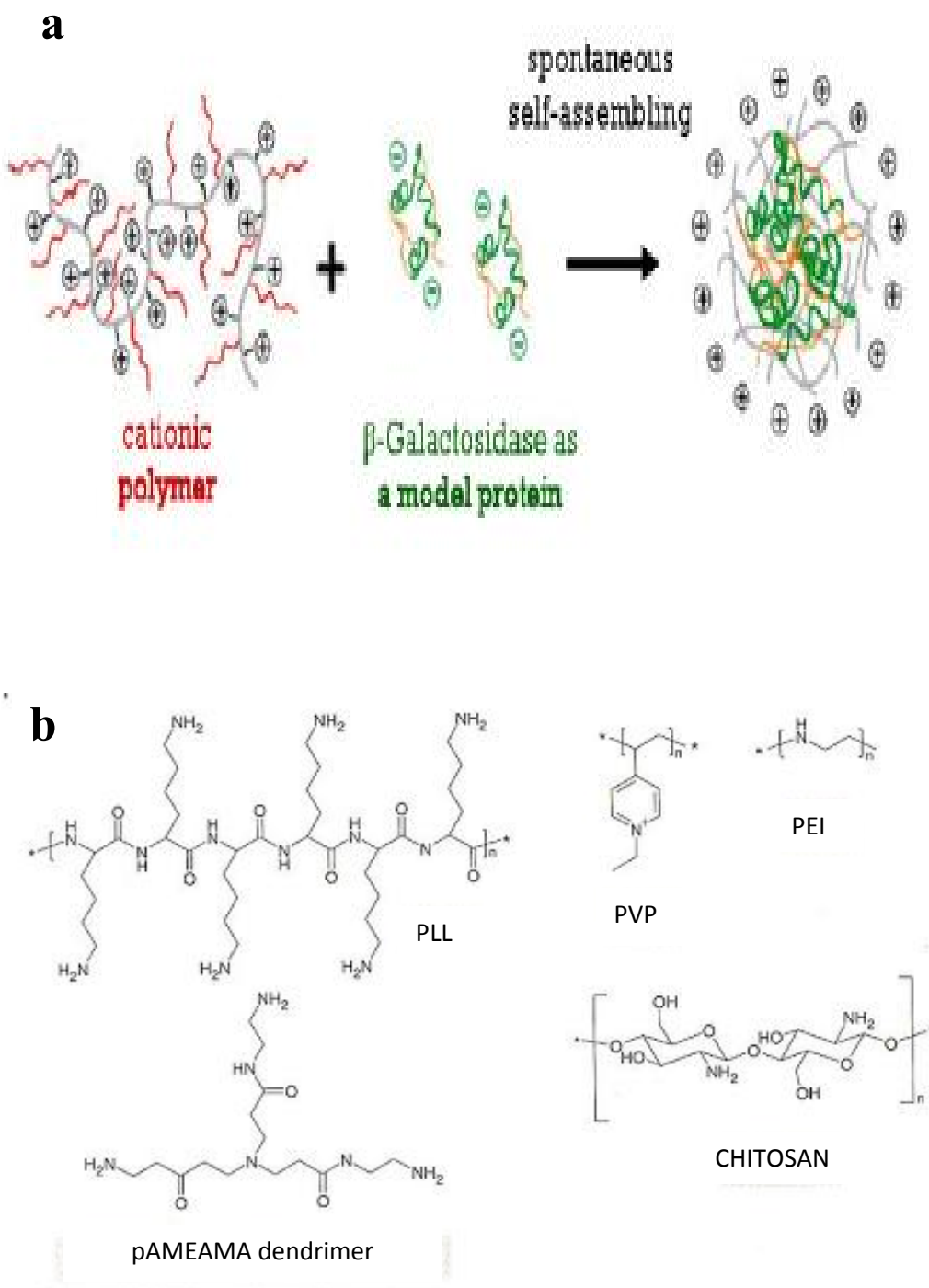

Figure 4 The complexation of protein-cationic polymer (a), the images of cationic polymers (b).

C. Carbon nanotube

The review of Sobhi et al., 2006, Carbon nanotubes (CNTs) are a newallotrope of carbon originated from fullerene family, which will revolutionalize the future nanotechnological devices. CNTs can be imagined as rolled graphite sheets held together by van der Waal's bonds. These nanosized near perfect whiskers were first noticed and characterized in 1991 by Iijima of NEC Corporation in Japan. CNTs are elongated fullerenes that can be produced with exactly pentagons and millions of hexagons. They have a long cylinder made of hexagonal honey comb of lattice of carbon, bound by two pieces of fullerenes at the ends. The first nanotubes observed were multiwalled CNTs (MWCNT) which consist of more concentric cylindrical shells of graphene sheets ocoaxially arranged around a central hollow area with a spacing between the layers which is close to that of the interlayer separation as in graphite (0.34 nm). In contrast, single shell single walled nanotubes (SWCNT) are made of single grapheme (one layer of graphite) cylinders and have a size distribution (1–2 nm). Both types of nanotubes have the physical characteristics of solids and are microcrystals, although their diameters are close to molecular dimensions.

Carbon nanotubes (CNTs) are cylindrical molecules, hexagonal arrangement of sp^2 hybridized carbon atoms. The hollow cylinders are formed by rolling single or multiple layers of graphene sheet. Functionalized single-walled carbon nanotubes (f-SWCNTs) have been reported for protein and DNA delivery that they could transfect cultured cells.

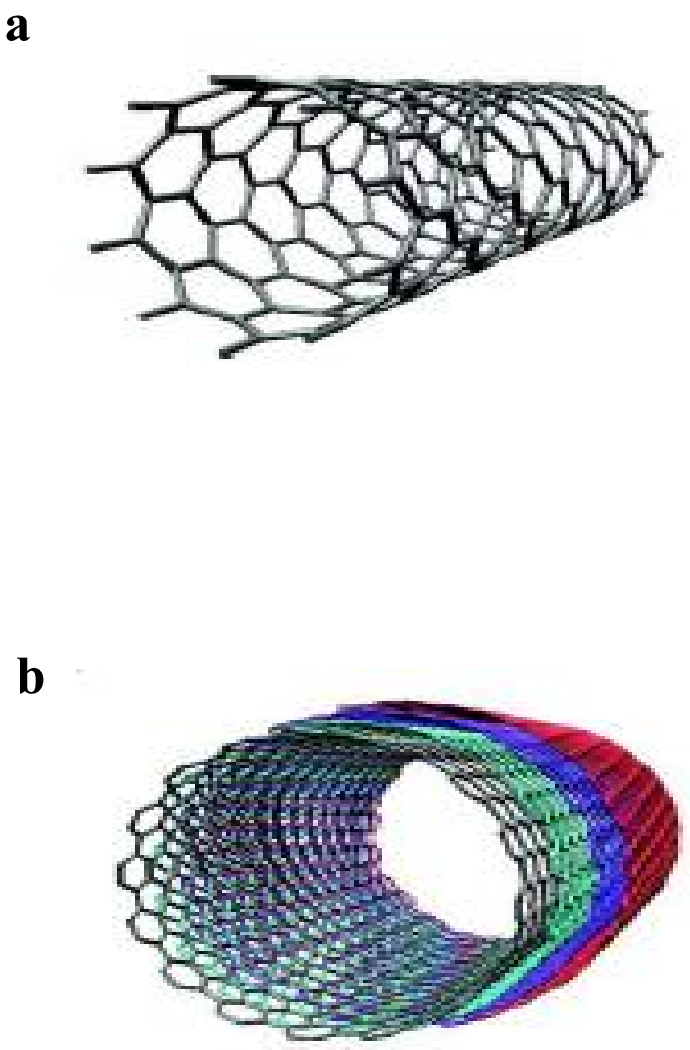

Figure 5 Computer-generated images of carbon nanostructures; the cylindrical structure of a single-walled carbon nanotube (SWNT) (a), the cylindrical structure of a multiwalled carbon nanotube (MWNT) (b) using Nanotube Modeler© 2005 from JCrystalSoft (Livermore, California) (Foldvari et al., 2008).

Pantarotto determined that CNTs covalently functionalized with ammonium groups (CNT-NH^{3+}) were able to associate with pDNA through electrostatic interactions. The delivery of pDNA and expression of b-galactosidase in CHO cells was found to be approximately 10 times higher than naked pDNA. Liu et al. suggested that the CNT–PEI–pDNA conjugates were found the level of gene (pCMV-Luc) expression to be much higher than those of DNA alone. Rasti K. et al. developed SWNTs with hexamethylenediamine (HMDA) to bind negatively charged siRNA. siRNA were able to cross the cell membrane and to suppress expression of the ERK target proteins in primary cardiomyocytes by about 75%. Weiling Q. et al. showed the interaction between MWCNT-PAMAM with plasmid DNA of enhanced green fluorescence protein (pEGFP-N1). They found that the MWCNT-PAMAM hybrid possessed good pEGFP-N1 immobilization ability and could efficiently delivery GFP gene into cultured HeLa cells.

Moreover, many investigations showed SWCNTs were nontoxic. Multiwalled carbon nanotubes (MWCNTs) are easily synthesized and the production cost is much less than that of SWCNTs. MWCNTs can be functionalized at the surface to have positive charge for DNA transport. The purpose of this study was to develop f-MWCNTs for plasmid DNA delivery.

Alberto Bianco et al. reported that Administration of drugs is very often limited by problems of insolubility, inefficient distribution, lack of selectivity and

side-effects raising health concerns. Currently, most of these problems are the subject of very intense studies, aiming to improve efficiency, availability and toxicity profiles. In addition, cell membranes that act as barriers can pose a problem in drug delivery by selectively allowing only certain structures to pass based on hydrophilicity:hydrophobicity ratios.

Additionally, cell membranes perform as barriers can cause a problem in genes delivery by selectively allowing only certain structures to pass based on hydrophilicity : hydrophobicity ratios (A. Bianco et al., 2007). Through the currently available delivery systems which include liposome, emulsions, polymers and microparticles (Allen T.M. et al., 2004; Kosterelos K. et al., 2003; Merdan T. et al., 2002), carbon nanotubes (CNTs) have lately gained high attractiveness as potential drug carriers, therapeutic agents and for applications in diagnosis (Blanco A. et al., 2005; Lin Y. et al., 2004; Pastorin G. et al., 2005; Katz E. et al., 2005; Fortina P. et al., 2005)

CNTs possess a unique and fascinating one-dimensional nanostructure, which imparts intriguing properties to the nanomaterial, such as tremendous strength, high thermal conductivity and amazing electronic properties ranging from metallic to semiconducting. These all-carbon hollow graphitic tubes with high aspect and nanoscale diameter can be classified by their structure into two main types: single-walled CNTs (SWNTs), which consist of a single layer of graphene sheet seamlessly

rolled into a cylindrical tube, and multiwalled CNTs (MWNTs), which comprise multiple layers of concentric cylinders with a space of about 0.34 nm between the adjacent layers.

Several techniques, e.g. arc-discharge, laser ablation, chemical vapor deposition (CVD) or the gas-phase catalytic process (HiPCO), have been used to synthesize CNTs. However, up to now, the CNTs prepared by all currently known methods are mixtures of different tubes with a broad distribution in diameter and chirality, and often contaminated by impurities (mainly including amorphous carbon and catalyst particles). Various methods have been developed to purify CNTs, such as oxidation of contaminants, microfiltratio, chromatographic procedures and microwave irradiation.

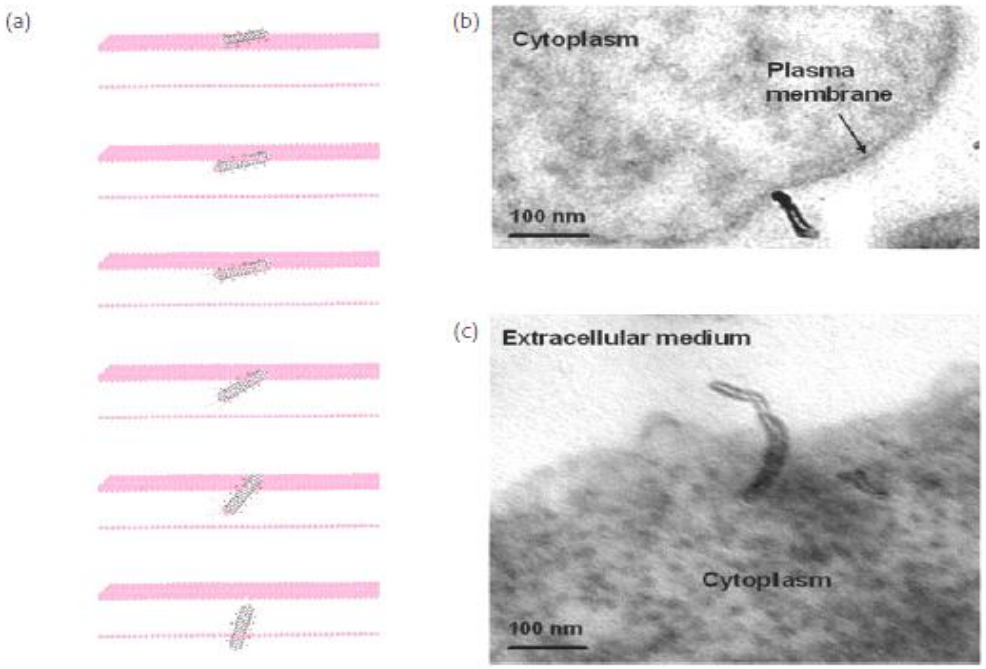

Figure 6 Image CNTs acting as nanoneedles (kostarelos et al., 2006) (Lacerda et al., 2007).

(a) Schematic of a CNT crossing the plasma membrane
(b) TEM image of MWNT-NH^{3+} interacting with the plasma membrane of A549 cells
(c) TEM image of MWNT- NH^{3+} crossing the plasma membrane of HeLa cells.

D. Carbon nanotube for drug/protein delivery (CAI S.Y. et al., 2009)

Vector

CNTs are able to carry peptides, proteins, as well as nucleic acids and other bioactive molecules into cells without toxicity, which can serve as an effective vehicle of therapeutic agents in the treatment of tumors.

Peptides

Peptides have received prominence in molecular biology. The immunological properties of peptides have been proved to retain after their conjugation to the surface of SWNTs whereas the presence of peptides can disperse CNTs to achieve their biomedical application. The first successful trial was accomplished by Pantarotto in 2004. They observed the transportation of small peptides into the cells by fluorescent labeled SWNTs under a confocal fluorescence microscope. This pioneering work has laid a foundation for the following researches in the delivery of biomolecules.

Proteins

Immobilization of proteins on the surface of SWNTs can be completed by noncovalent or covalent interaction. In the case of noncovalent interaction, nonspecific adsorption could be inhibited by surfactants and polymers. Kam utilized fluorescent labeled streptavidin to interact with biotin-SWNTs and found the uptake of those conjugates into cells by endocytosis. Various proteins can be adsorbed onto the surface of acid-treated SWNTs by nonspecific adsorption and perform its biological functions after internalization into living cells. The real pathway of CNTs into the cells is unclear now; however, there are two prevalence views (1) energy-

independent mechanism involved active insertion-diffusion process and (2) energy-dependent mechanism entitling endocytosis.

Nucleic acids

Nucleic acids play an important role in biomedicine. Nearly 2000 kinds of hereditary diseases, as well as tumor occurrence, viral infection, and radiation to human body are found to be associated with DNA structure. Nucleic acids can conjugate to the surface of CNTs by covalent bonding, then hybridize selectively with complementary sequences.

Functionalized carbon nanotubes are able to interact with plasmid DNA through the electrostatic interaction and penetrate cell membranes with low cytotoxicity, and the amount to bind DNA is dependent on the surface area and charge density of CNTs. Bianco's study proved that SWNTs are able to bring oligodeoxynucleotide with CpG motif (CpG-ODN) into the target cells effectively and enhance the immune activation.

Moreover, transfection of the plasmid DNA could be achieved effectively with nickel-embedded carbon nanotubes in magnetic field, and its transfection efficiency is equivalent to that of viral vector approach. This so-called nanospearing technique

interaction, which could only provide a metastable complex for gene transfection, and the efficiency is determined by the chemical groups on the surface of CNTs.

The application of polymers such as polyethylenimine (PEI), polyamidoamine(PAMAM) dendrimers can solve this problem. Liu immobilized DNA on the surface of MWNTs firmly with PEI, and its transfection efficiency was three times higher than that of PEI and four orders of magnitude higher than that of DNA alone. Pan investigated the delivery of Survivin antisense shows fairly high biocompatibility. In most cases, the immobilization of DNA onto CNTs is achieved by electrostatic oligonucleotide (ASOND) into the hepatic cancer cells mediated by

CNTs-PMAMA dendrimer and its effect on liver cancer cells. They found that the compound can serve as an efficient gene vector with high inhibition to the proliferation of cancer cells. Jia and coworkers functionalized PEI-MWNTs with quantum dots tagged ASODN. Those bifunctional compounds that with treatment and tracking effects showed high efficiency of intracellular delivery, nuclear localization, and transfection.

Similarly, the translocation of RNA into the cells could be achieved with CNTs. Lu characterized the delivery of RNA polymer into cells with radio-labeled SWNTs. Thanks to the nonspecific interaction between RNA polymers and CNTs, the intracellular release of RNA could be realized. The complexes were found to across

the cellular and nuclear membrane in the confocal fluorescent microscope images in different sections.

Controllable release of intracellular biomolecules could be performed via special chemical linkage. Kam attached the biological cargos such as DNA, RNA to the surface of SWNTs and demonstrated the transportation, release, and nuclear translocation of DNA with cleavable disulfide linkage, which allow the gene silencing of specific intracellular proteins by highly efficient delivery of siRNA .

Subsequently, efficient RNA interference of HIV-specific cell-surface receptors CD4 and coreceptors CXCR4/CCR5 was carried out with SWNTs. The transfection efficiency of SWNTs was superior to that of several nonviral agents such as liposome and was dependent on the surface functionalization and hydrophilicity of CNTs.

Suppression of tumor growth could also be implemented by gene silence through the delivery of SWNTs. In Zhang's study, positively charged CNTs interacted with negatively charged human telomerase reverse transcriptase (TERT-siRNA) via electrostatic interaction, those complexes enhanced the stability and transfection efficiency of siRNA, silenced the targeted gene of the immunoregulatory cells.

Drugs

The development of CNTs as drug delivery system is of great importance for improving the pharmacological properties of many drugs. Murakami investigated the adsorption and intracellular release of antiinflammatory glucocorticoid dexamethasone (DEX) onto the surface of oxidated CNHs. Venkatesan studied the adsorption of erythropoietin (EPO) in a variety of porous carbon nanomaterials, including CNTs.

In vivo results indicated that CNTs show the highest performance and biological effect in the presence of an appropriate surfactant. Bianco functionalized MWNTs with fluorescein (FITC) and antibiotic amphotericin B (AmB), AmB with its antifungal activity retained was delivered into the cells effectively. Thereafter, anticancer drugs methotrexate (MTX) was also translocated into the cells with MWNTs by the same method.

Yu and coworkers synthesized gonadotropin releasing hormone (GnRH)-MWNTs complexes and verified their anticancer effect to the prostate cancer cells. Feazell's study shows that a nontoxic platinum (IV) complex could be covalently conjugated to the surface of SWNTs and delivered into the cells, which released toxic anticancer drug cisplatin by means of the reduction of Pt^{4+} at low pH value within cells. Its delivery efficiency was 6–8 times that of cisplatin.

A subsequent study was the modification of platinum complex with folic acid and CNTs. Such a complex killed the cancer cells selectively, delivery efficiency of which was two orders of magnitude higher than that of platinum complexes. In addition, anticancer drugs could be loaded into the interior of CNHs by the nanoprecipitation, and its anticancer effect was 4–6 times that of cisplatin. Besides folic acid, biotin could be utilized as target group to modify CNTs.

Chen realized the delivery of paclitaxel toxoid (Taxoid) into the cancer cells specifically with biotin-SWNTs and the intracellular release due to cleavable linking. As the large hydrophobic surface, functionalized carbon nanotubes are able to interact with aromatic molecules by -stacking supermolecular interaction.

In Liu's study, anticancer drug doxorubicin (DOX) was conjugated to SWNTs by covalent bending and noncovalent bonding, respectively. CNTs showed higher loading capacity than the conventional liposomes. The loaded DOX was released in acidic environment, while its loading and release behavior was relevant to the diameter of CNTs. After functionalized with cyclic arginine-glycine-aspartic acid (RGD) peptide as targeted moiety, the complex showed relatively high specific delivery and destruction efficiency to the RGD receptors-positive cells. Similar results obtained by Ali-Boucetta show MWNTs are able to enhance the destruction efficiency of DOX to cancer cells.

CHAPTER III

MATERIALS AND METHODS

Materials

Agarose, Lot No.AG6431, Vivantis, Malaysia

1 kb DNA Ladder, Lot No.6011, Vivantis, Malaysia

6x Loading Dye, Lot No.4101, Vivantis, Malaysia

Acetic acid, Lot No.K34739317521, AnalaR, England

Antibiotic-Antimycotic, Lot No.907169, Gibco, USA

Chitosan 50kDa 75-85% deacetylaion, Lot No.MKBD3830, Sigma, Singapore

Dulbecco's Modified Eagle Medium High Glucose, Lot No.935949, Gibco, USA

Ethidium bromide, Lot No.1376B017, Vivantis, Malaysia

Feotal bovine serum, Lot No.41G8397K, Gibco, USA

HeLa cell, human epithelial cervix carcinoma cell lines, were kindly provided from the Department of Biochemistry and Microbiology, Faculty of Pharmaceutical Sciences, Chulalongkom University.

Kanamycin sulfate, Lot No.4063, Meiji, Japan

LB Broth, Miller (Luria-Bertani), Lot No. 6080249, Becton Dickinson, France

Lipofectamine, Lot No.862000, Invitrogen, USA

OPTI-MEM@I Reduced Serum Medium, Lot No.930012, Gibco, USA

Plasmid EnhancedGreen Fluorescence Protein-C2 (pEGFP-C2), 4.7 kb, Clontech, USA

Plasmid midi kit, Lot No.TK17902, Geneaids,Taiwan

Sulfuric acid, Lot.No.7664939, J.T.Baker, USA

Thiazolyl blue tetrazolium bromide (MTT), Lot.No.MKBD4834, Sigma, USA

Trypsin-EDTA, Lot.No.917993, Gibco, Canada

Tween 80, Lot.No.809861, Srichand, Japan

Equipments

Analytical balance, Model AGZ0, Mettler Toledo, Switzerland

Analytical balance, Model PB3002, Mettler Toledo, Switzerland

Centrifuge, Model 2K15, Sigma, Germany

Flow cytometer, FACS Calibur CellQuest Pro Software, Becton Dickinson, USA

Fluorescence microscope, IX5 1, Olympus, Japan

Laminar air flow, Model HBB 2448, Holten, USA

Microplate reader, Model3550, Bio-Rad, USA

Orbital Shaker, ModelSO3, Stuart scientific, UK

pH meter, Model 2L0A, Thermo Orion, USA

Transmission Electron Microscope, Model JEM-1230, JEOL, Japan

UV/VIS Spectrophotometer, Model V-530, Jasco, Japan

Methods

1. Plasmid DNA and preparation of plasmid DNA

1.1 Plasmid DNA (pDNA)

Plasmid Enhanched Green Fluorescent Protien-C2 (pEGFP-C2) (Clonetech®) encodes a red-shifted variant of wild-type GFP which has been optimized for brighter fluorescence and higher expression in mammalian cells. Modified Alkaline Lysis method (Birnboim et al., 1979) was used to extract Plasmid Enhanched Green Fluorescent Protien-C2 (pEGFP-C2) from 100 ml of cultured *Escherichia coli*.

1.2 Preparation of plasmid DNA

pEGFP-C2 was propagated in *Escherichia coli* that grown in suitable nourishment medium. LB Broth, Miller (Luria-Bertani) was used for maintenance and propagation of *E.coli*. LB Broth solution was prepared by dissolving 25 g. of LB Broth in purified water and adjusted to 1 L. LB Broth solution was completely mixed and autoclaved at 121°C for 15 minutes. The 50 µg/µl of kanamycin was added at amount of 100 µl: 100 ml liquid medium. The 7% agar was added in kanamycin-liquid medium for agar plates and 20 ml kanamycin-liquid medium agar was poured into plate.

pEGFP-C2 was purified by using the Geneaid Plasmid Midi Kit (Endotoxin Free). Modified Alkaline Lysis method (Birnboim, and Doly, 1979) was used to extract plasmid DNA (pDNA) from 100 ml of cultured *Escherichia coli*. The bacterial culture was harvested by centrifugation at 6000 x g for 15 minutes. Supernatant was discarded totally. The nucleic acid was precipitated then ribonuclease A (RNase A) was added to digest RNA. Selective alkaline denaturation of high molecular weight chromosomal DNA while covalently closed circular DNA remains double stranded is the principle method. Chromosome DNA was renatured to form an insoluble clot when neutralization. Plasmid DNA was left in the supernatant. Phenol/chloroform/isoamyl alcohol was added to remove the lasting protein. DNA was precipitated by adding isopropanol and DNA pellet was air-dried for 10 minutes. Then, the DNA was dissolved in water.

1.3 DNA concentration and purity determination

The plasmid DNA was measured for the concentration and purity by a UV specrophotometer. The 600 µl of solvent was a control and the 600 µl of the pDNA dissolved in this solvent was sample. The concentration of pDNA was defined by measuring UV absorbance at 260 nm (1 OD = 50 µg/ml) (equation 1). The purity of pDNA was determined by equation 2. The value was in the range of 1.8 to 2.0 (Huang et a1., 2005; Jean-Pierre,2005).

The concentration of pDNA = OD_{260} x 50 (µg/ml) (1)

The purity of pDNA = OD_{260}/OD_{280} (2)

2. M/C/D Nanocomposites

2.1 Surface modification of functionalized multiwalled carbon nanotubes (f-MWCNTs)

The preparation was modified from Seung-Hoon et al. (2008). MWCNTs were added with mixture of 65% nitric acid and 95% sulfuric acid (1:3 ratio). All Pristine MWCNTs were sonicated for 6 hours and 12 hours. The obtained f-MWCNTs were filtered through a 0.2 µm filter and washed with ultrapurified water until neutral then dried at 80°C over night. Dried f-MWCNTs 0.005%, 0.01%, 0.015% and 0.02% w/v were then added with ultrapurified water.

Production yield percentage of f-MWCNTs was determined as the following equation. M_o was the initial pristine multiwalled carbon nanotube dry weight. M_f was the functionalized multiwalled carbon nanotube dry weight.

Production yield percentage (%y) = (M_f / M_o) x100 (3)

2.2 Preparation of chitosan nanoparticles (CS)

The 0.05% w/v and 0.25% w/v of low molecular weight chitosan was dissolved in the solution of 2%v/v acetic acid containing 1%TWEEN 80 (Seung-Hoon et al, 2008). The CS solution was sonicated at 100% transmittion in sonicator bath (Elma®, Germany) for 45 min.

2.3 Preparation of f-MWCNTs/CS (M/C) nanoparticles

f-MWCNTs/CS were prepared by varying preferred weight ratios of 3:1 and 1:3. The mixtures were stirred overnight at room temperature. f-MWCNTs/CS nanoparticle were sterile filtered through a 0.2 μm filter.

2.4 Preparation of f-MWCNTs/CS/pDNA (M/C/D) nanoparticles

The nanoparticles were prepared by complex method (Mao et al., 2001). f-MWCNTs/CS nanoparticle were formed complexes with 100μg/ml of pDNA concentration in water. Ultrapurified water was added to equal volume. All solutions were separately heated to 55˚C for 10 min. The solutions were instantly mixed together and vortexed for 30 sec. The nanoparticles were left at room temperature for 30 minutes to form complete complexes. All nanoparticles were freshly prepared before used.

3. Physical characterization of nanoparticles

3.1 Measurement of particle size and zeta potential

Particle size measurement of the obtained complex nanoparticles was determined by photon correlation spectroscopy (PCS) under a laser diffractometer (model: Mastersizer 2000, Malvern, UK). The 1 ml sample was filled into a cuvette then was characterized nanoparticles in nanometer (nm) using a zetasizer. The zeta potential measurements were determined in millivolt (mV) with the same method. The samples were reported mean±standard deviation (SD).

3.2 Morphological Observation

3.2.1 Transmission electron microscopy (TEM)

A drop of the freshly prepared nanoparticle samples was put on a copper grid. To test negative charge of f-MWCNTs and pDNA, the sample was negatively stained with 0.5% w/v uranyl acetate solution (UA) (UO_2^{2+}). To test positive charge of CS, the sample was positively stained with 0.5% w/v phosphotungstic acid solution (PTA) ($PW_{12}O_{40}^{3-}$). The samples were dried under room temperature. Observation was undertaken using a transmission electron microscope (JEM-2100 200KV, JEOL, Japan).

As for Negative Contrast, the background area neighboring the specimen was made electron-dense so the specimen appears lighter than contrary to the darkly-stained background. Phosphotungstic acid (PTA) stain is a stain that used for TEM. Positive Contrast is heavy metal salts attach to various organelles or macromolecules within the section to increase their electron density and they appear dark against a lighter background. Uranyl Acetate (UA) reacts strongly with phosphate groups of pDNA in order that nucleic acids are highly stained. Negatively stain, uranyl ions will bind to nucleic acid phosphate groups or carboxyl groups. TEM images showed surface modification of negatively charged f-MWCNTs and f-MWCNTs with chitosan nanoparticles-coated indicating the complex formation by ionic charge.

3.3 Chemical structure characterization

To remove spectral interference peak of water, the samples were lyophilized using freeze dryer. The condition for this experiment was shown in table 1.

Table 1 The process of freeze-drying

Process	Temperature (ºC)	Time (min.)	Vacuum (mT)
Freeze	0	0	600
	-5	0	600
	-10	0	600
	-15	0	600
	-20	0	600
Extra freeze	-20	60	600

Primary drying	-20	0	600
	-20	120	600
	-10	0	600
	-10	120	600
	0	0	600
	0	120	600
	10	0	600
	10	120	600
	20	0	600
	20	120	600
	30	0	600
	30	60	600
Secondary drying	20	60	600

3.3.1 Fourier transform infrared (FT-IR) spectroscopy

Lyophilized samples and anhydrous KBr were composed with hydraulic press. FT-IR spectra were recorded on the spectral region 4000-400 cm^{-1} using FT-IR spectroscopy (model Spectrum One, Perkin Elmer). FT-IR was determined for functional groups of molecules.

4. Gel retardation assay

The M/C/D nanoparticles formation was estimated by using agarose gel electroporesis. The f-MWCNTs/CS/pDNA complexes were used in this study. The samples were mixed with 6x loading dye to a final loading dye concentration of lx. Then, 15 µl of the mixtures were loaded onto a 0.8% agarose gel in TAE buffer (Tris-acetic-EDTA buffer). The samples were run on the gel at a constant voltage of 80 volts for 50 minutes. Then gel was stained with 0.5 µl/ml ethidium bromide and visualized under UV light. The naked pDNA was used as a control and a 1 kb DNA ladder was used as a reference.

5. Cytotoxicity of f-MWCNTs, CS, pDNA, M/D, M/C/D nanocomposites and commercial vectors.

5.1 Morphology of HeLa cells observed by inverted microscope

The cytotoxicity of all sample solutions were evaluated morphological observation by inverted microscope.

5.2 Cell viability tests

Cell viability tests were determined by thiazolyl blue tetrazolium bromide (MTT) viability assay. HeLa cells were seeded in 96-well plate at a density of $1x10^4$cells/well in 100 µl of complete medium. HeLa cells were incubated in the 5% CO_2 humidified incubator at 37°C until the cells was 80-100% confluent. Non-serum

DMEM, 100µl, containing the sample solutions or commercial-pDNA complexes were added to each well. The incubation was continued for 72 hours. Cell viability was determined by the ability of the cells to cleave the tetrazolium salt MTT. The mitochondrial enzyme, succinate dehydrogenase, showed a blue formazan crystal.

MTT was dissolved in PBS at a concentration of 5 mg/ml and sterile filtered through 0.2 µm filter. Then, 100 µl of 1:10 the MTT solution was added to each well and incubated at 37^{o}C under 5% CO_2. After incubation for 4 h, 100 µl of DMSO solution was added to each well and mixed thoroughly using orbital shaker at 150 rpm to dissolve the blue formazan crystals. The plates were protected from light and estimated immediately. Then, the plates were read on microplate reader, using a test wavelength of 570 nm.

Cell viability percentage of sample was calculated according to the following equation. OD_o was the optical density from the well treated with only DMEM. OD_s was the optical density from the well treated with the sample solutions.

$$\text{Cell viability percentage (\%)} = (OD_s / OD_o) \times 100 \qquad (4)$$

6. *In vitro* transfection in HeLa cells culture

HeLa cells were seeded 24 hours into a 24-well plate at a density of $5x10^4$ cells per well in 1 ml of complete medium. HeLa cells culture were incubated in the 5%

CO_2 humidified incubator at 37°C until the cells was 80-100% confluent. The day of transfection, the complete medium was removed and the cells were rinsed with PBS.

6.1 Transfection with naked pDNA and M/C/D nanoparticles

The medium containing pDNA 1μg was used as a negative control. The M/C/D nanoparticles containing 1μg of pDNA were mixed with non-serum DMEM and added to each well. The medium contained not more than 40% of whole serum DMEM and non-serum DMEM. The cells were incubated with the formulations for 48 hours in the 5% CO_2 humidified incubator at 37°C. The day after transfection, they were washed once with PBS. The cells were suspended in 1 ml of DMEM and assayed for reporter gene expression.

6.2 Transfection with Polyfect® (positive control)

The method was applied from QIAGEN® user manual. The medium containing pDNA 1μg was added 2.4 μl Polyfect® reagent. Then, the samples were mixed by pipetting up and down 5 times. They were incubated for 10 min at room temperature (20–25°C) to allow complex formation. While complex formation was taken place, the growth medium was gently aspirated from the wells. Cells were washed once with PBS and added 1 ml of the fresh cell growth medium (containing serum and antibiotics). 600 μl of cell growth medium (containing serum and antibiotics) were added to the reaction tube containing the transfection complexes.

The mixture was mixed by pipetting up and down twice, and immediately transferd the total volume to the cells in 24-well plate. 24-well plate was gently swirled to ensure uniform distribution of the complexes. The cells were incubated with the formulations for 48 hours in the 5% CO_2 humidified incubator at 37°C. The day after transfection, they were washed once with PBS. The cells were suspended in 1 ml of DMEM and assay for reporter gene expression.

6.3 Transfection with Lipofectamine® (positive control)

The method was applied from INVITROGEN® user manual. Lipofectamine®-pDNA complexes were prepared with a 2: l ratio of Lipofectamine (µl): pDNA (µg). HeLa cells were seeded 24 hours into a 24-well plate at a density of $5xl0^4$ cells per well in 1 ml of non serum medium. pDNA were diluted in 50 µl of Opti-MEM I Reduced Serum Medium without serum. Lipofectamine were mixed gently before use, then were diluted the appropriate amount in 50 µl of Opti-MEM I Medium. The mixture were mixed gently and incubated for 5 minutes at room temperature. After the 5 minute incubation, the diluted DNA were combined with the diluted Lipofectamine. They were mixed gently and incubated for 20 minutes at room temperature to allow the DNA-Lipofectamine complexes to form. The 500 µl of cell growth medium (containing serum and antibiotics) were added to the reaction tube containing the transfection complexes. The mixture was mixed by pipetting up and down twice, and immediately transferred the total volume to the cells in 24-well plate.

24-well plate was gently swirled to ensure uniform distribution of the complexes. The cells were incubated with the formulations for 48 hours in the 5% CO_2 humidified incubator at 37°C. The day after transfection, they were washed once with PBS. The cells were suspended in 1 ml of DMEM and assayed for reporter gene expression.

Chapter IV

RESULTS AND DISCUSSION

3. Plasmid DNA and preparation of plasmid DNA

The concentration of first batch of pDNA was 100.85 µg/ml. The obtained DNA was dissolved in water. The purity ratio of first batch of DNA was 2.54. The concentration of second batch of pDNA was 97.9µg/ml while the purity ratio of DNA was 1.61. There was some other OD of impurity that resulted in decrease of the OD ratio between 260 and 280 nm (Jean-Pierre, 2005). The OD ratio was less than 1.8 indicated that then was an impurity in the second batch. Therefore, the pDNA of the first batch was selected to use in this studies. The plasmid DNA may be contaminated with protein, genomic DNA and RNA during purification methods.

2. M/C/D Nanocomposites

2.1 Surface modification of functionalized multiwalled carbon nanotubes (f-MWCNTs)

The MWCNTs showed poor soluble in most solvents and often contaminated by impurities including amorphous carbon and catalyst particles (Alberto et al., 2007). Tong et al. found the method of the purification and modification at the end of carbon nanotubes. The f-MWCNTs was functionalized MWCNTs to improve the solubility. Following solubility test, pristine MWCNTs showed the poor solubility while the f-MWCNTs was dispersed completely in ultrapurified water. Insoluble pristine MWCNTs particles precipitated at the bottom of the bottle (figure 7 a). Contrarily, the stable solution with well-dispersed of f-MWCNTs could be seen in figure 7 b. The result showed, the functionalization could increase the solubility of MWCNTs.

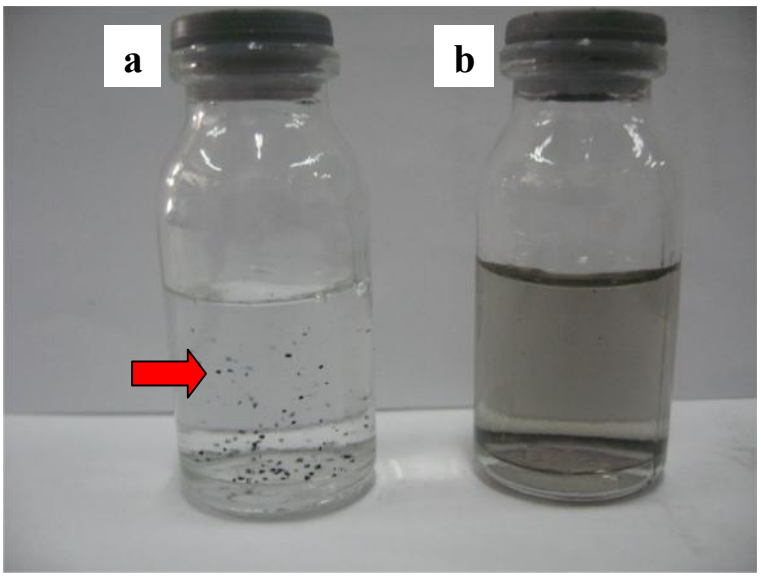

Figure 7 Pristine MWCNTs (a) and the f-MWCNTs (b) at concentrations of 1% w/v were shaken.

The functionalized process was performed by the oxidative digestion of graphene caps and layers generated polycyclic aromatic substances of the MWCNTs and the formation of oxygen-containing surface functional groups (Zhaowei et al., 2009).

Generally, an acid was used as the functionalizing agent. The figure 8 represented the attack of an acid to the MWCNTs during oxidation process.

Tsang et al. used the HNO_3 acid for oxidation of carbon nanotube. In addition, the mixtures of H_2SO_4/HNO_3 (3:1) by volume were also used in previous study for pristine MWCNTs functionalizing to improve the solubility. (Zhenglong Yang et al., 2005). Therefore, the H_2SO_4/HNO_3 was used in this study.

The carboxylic acid groups were formed on the MWCNTs surface by acid. The f-MWCNTs were obtained anionic particles. For treating with acid, the formation of oxygen-containing surface functional groups, the oxidative digestion of graphene caps and layers generated polycyclic aromatic substances (Zhaowei et al., 2009). There was agreed with Schematic representation **(**Figure 8) of the attack to the MWCNTs during the oxidation process by Goyanes et al., 2007.

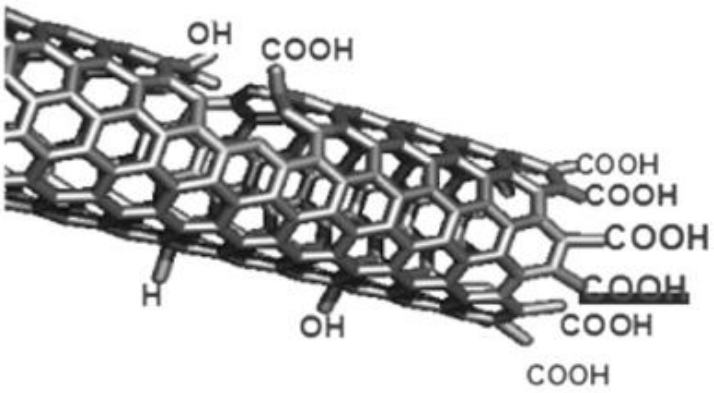

Figure 8 Schematic representation of the attack to the MWCNTs during the oxidation process (Goyanes et al., 2007).

2.2 Production yield of functionalized multiwalled carbon nanotubes (f-MWCNTs)

Pristine MWCNTs that were sonicated with acid for 6 hours showed incomplete reaction. There were remained pieces of pristine MWCNTs after sonicating for 6 hours. The images were shown in figure 9a-e. The solutions of 0.005% (a) and 0.02% (d) w/v f-MWCNTs could be seen that they were not dispersed absolutely. The dark solutions of 0.01% (b) and 0.015% (c) w/v f-MWCNTs was more solubilized that couldn't see the pieces of pristine MWCNTs.

At sonication times of 12 hours, the production yield of f-MWCNTs at 5 mg/100ml, 10mg/100ml, 15mg/100ml and 20 mg/ml were 101.4±10.18, 102.77±7.46, 100.82±3.26 and 100.98 % ±2.02 respectively (table 2 and figure 9f). There was not significant difference ($p=0.05$) of the percentage yield in each formation.

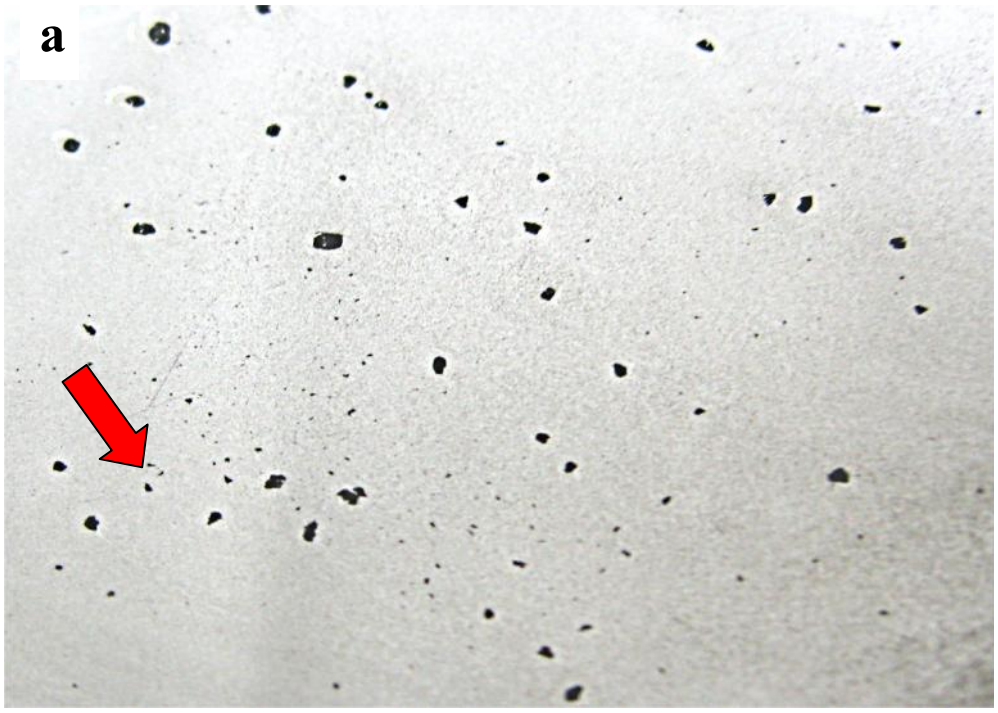
a

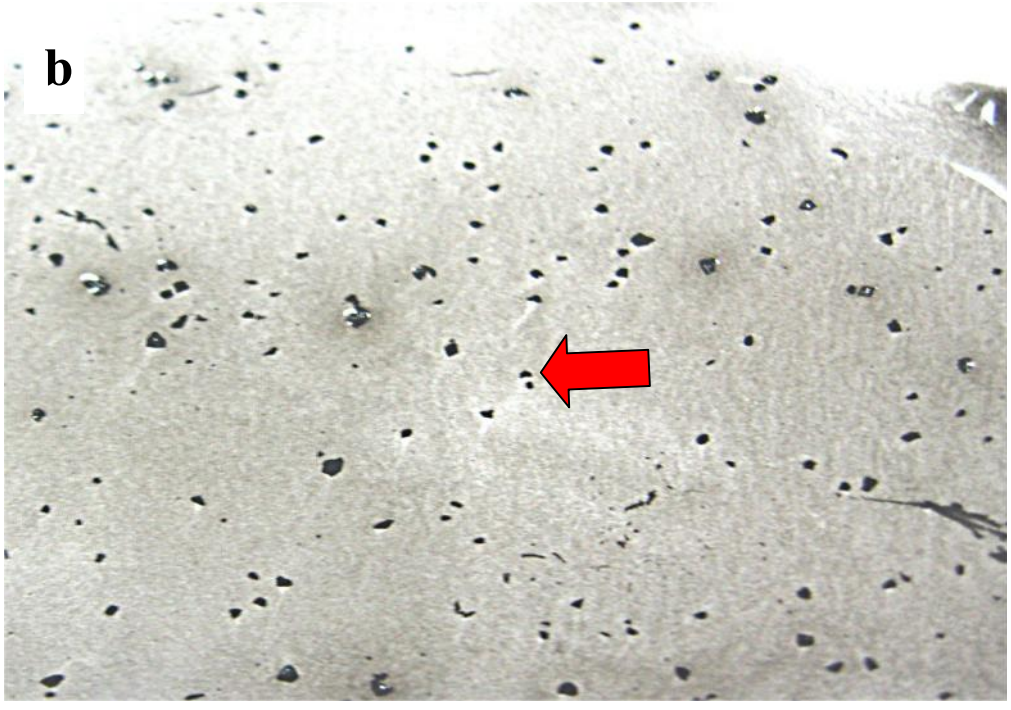
b

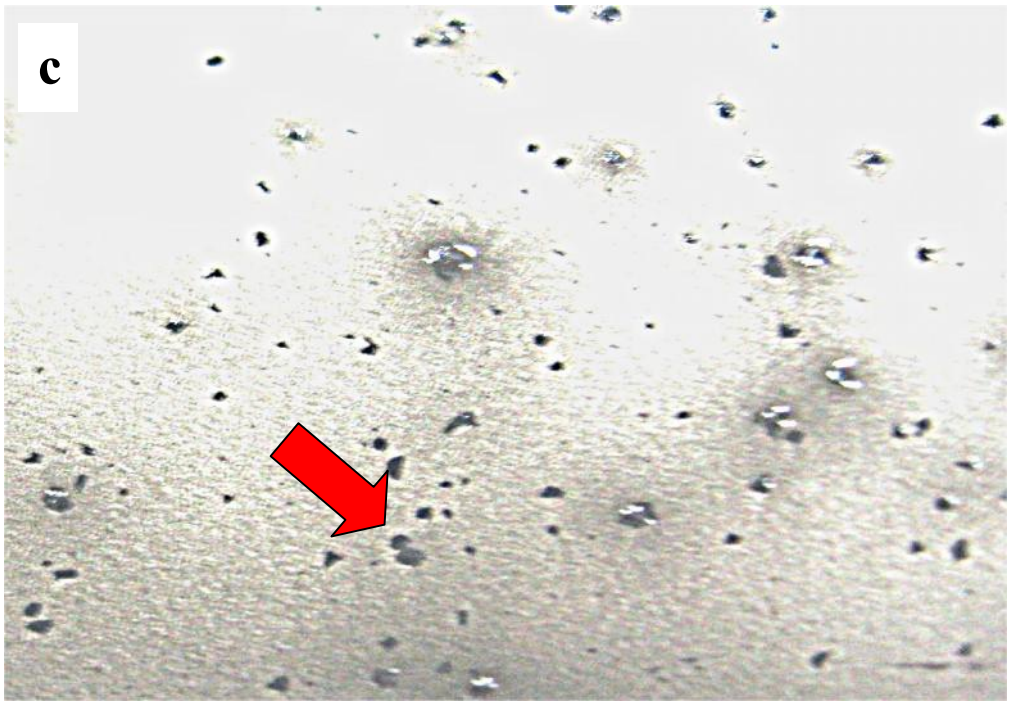
c


d

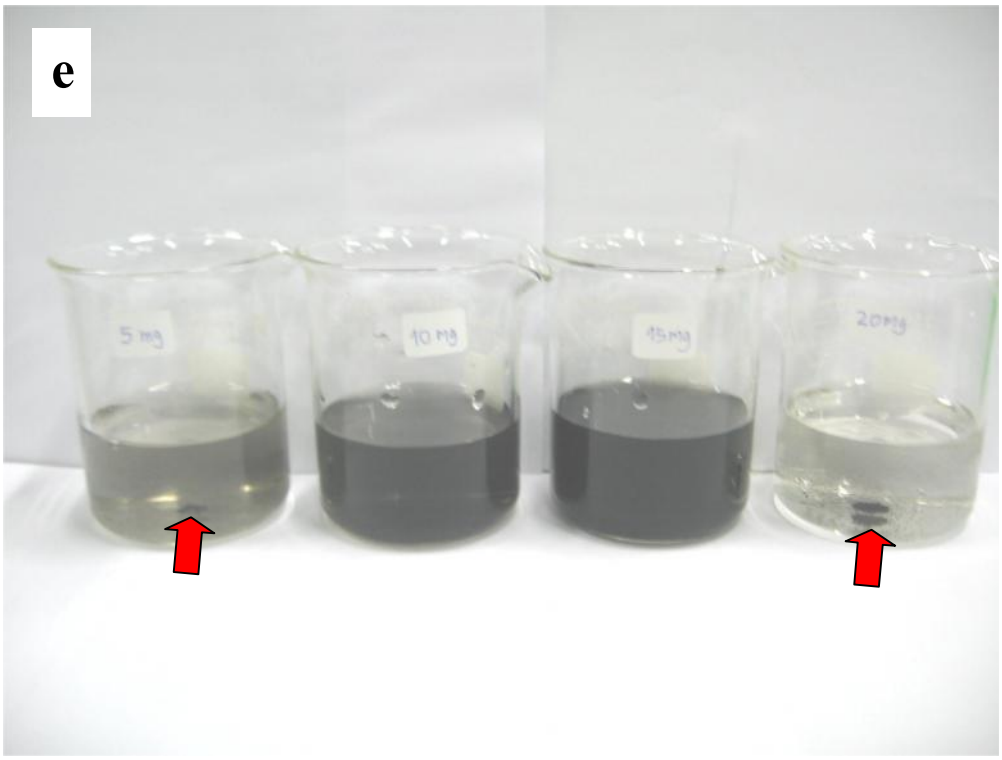

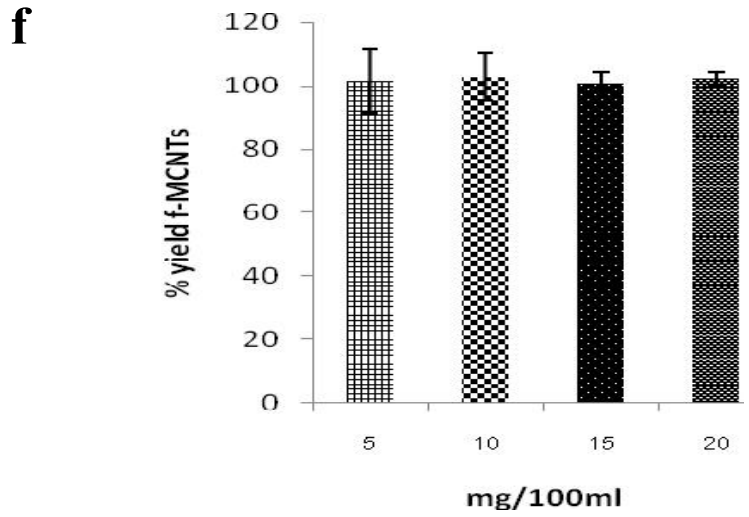

Figure 9 The images of 5 mg (a), 10 mg (b), 15 mg (c) and 20 mg (d) f-MCNTs in 1:3 nitric acid:sulfuric acid were shown after sonicating for 6 hours, The images of 5 mg, 10 mg, 15 mg and 20 mg f-MCNTs in 100 ml ultrapurified water after sonicating for 6 hours(e), The production yield percentage of each f-MWCNTs in the mixture solvents of H_2SO_4/HNO_3 for 12 hours(f).

Table 2 The production yield percentage of each f-MWCNTs in the mixture solvents of H_2SO_4/HNO_3 (3:1) for 12 hours.

Formulation (mg/100ml)	% yield f-MWCNTs
5	101.4±10.18
10	102.77±7.46
15	100.82±3.26
20	100.98±2.02

3. Physical characterization of nanoparticles

3.1 Measurement of particle size and zeta potential

3.1.1 Functionalized multi-walled carbon nanotube

The comparison between two concentrations of f-MWCNTs at 0.010%w/v and 0.015%w/v showed that f-MWCNTs with a lower concentration could undergo complete reaction when compared with the higher concentration f-MWCNTs. There were some different properties, such as size and zeta potential of f-MWCNTs with two concentration. The 0.010%w/v f-MWCNTs exhibit the average size of 68.00±4.64 nm and the zeta potential of -22.44±3.85 mV while the average size and the zeta potential of 0.015%w/v f-MWCNTs are 84.63±2.91 nm, -9.58±3.32 mV respectively (table 3) (figure 10a-b). These results were potentially described to a decrease in pristine MWCNTs to oxidizing agent ratios, which lead to the smaller particles size and the lower zeta potential due to agglomeration effect.

Table 3 Particle size and zeta potential of functionalized carbon nanotube (mean±SD,n=3)

Concentration of functionalized carbon nanotube			
0.010%w/v f-MWCNTS		0.015%w/v f-MWCNTS	
Particle size (d.nm.)	Zeta potential (mV)	Particle size (d.nm.)	Zeta potential (mV)
68.00±4.64	-22.44±3.85	84.63±2.91	-9.58±3.32

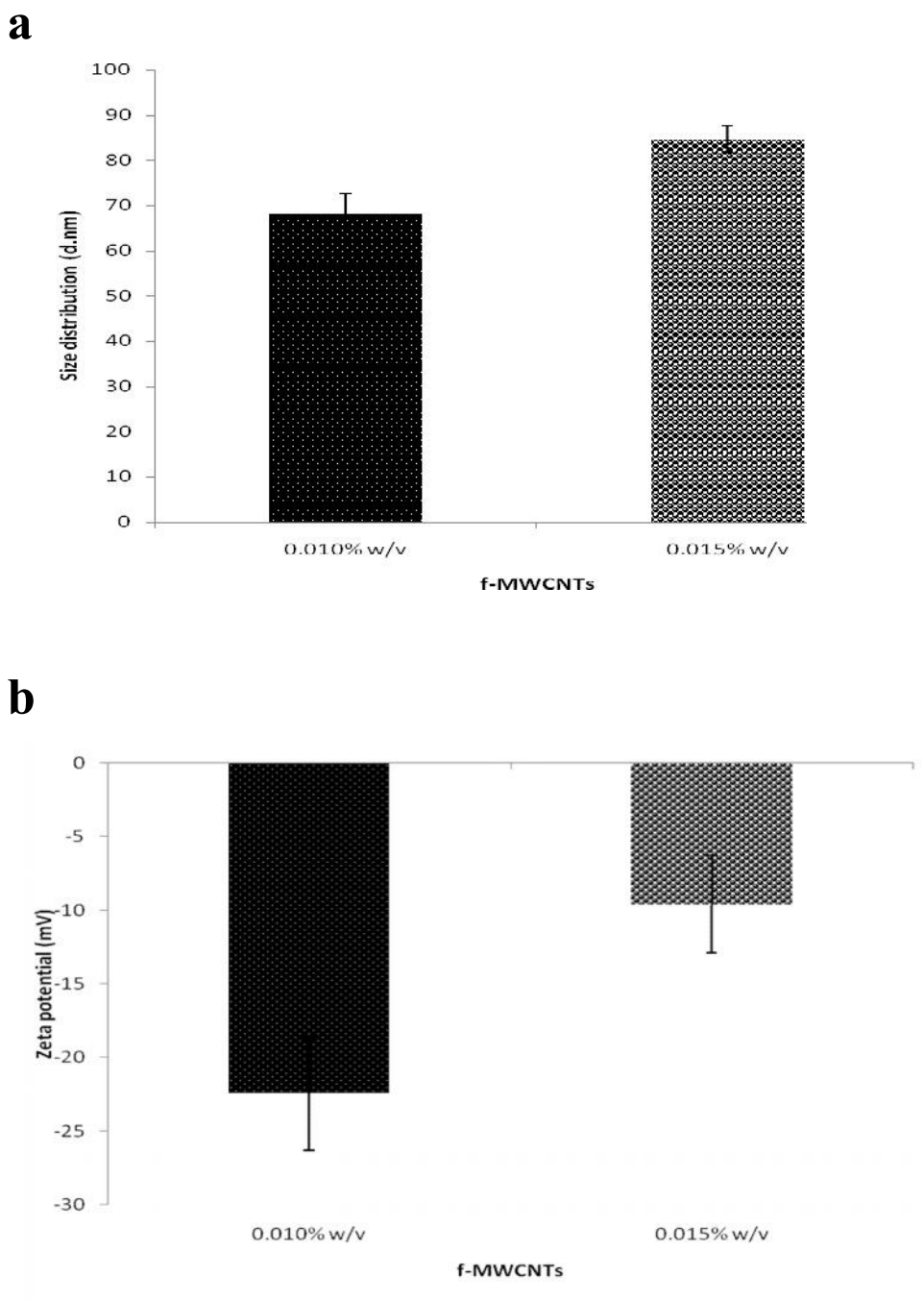

Figure 10 The size distribution (a) and zeta potential (b) of 0.01%w/v f-MWCNTs and 0.015%w/v f-MWCNTs.

3.1.2 Chitosan nanoparticles

The comparison between concentrations of chitosan at 0.005%w/v, 0.025%w/v, 0.045%w/v and 0.065%w/v were compared. The results indicated those concentrations of chitosan at 0.045%w/v and 0.065%w/v was more positive charge. However, both concentrations had large size distribution which was undesirable (in Appendix c). Following this study, the selected formulations were CS concentration at 0.005%w/v and 0.025%w/v.

Physical properties including, particle size and zeta potential of chitosan nanaparticles are present in Table 4a and 4b respectively. The necessary for selecting the suitable particle size is the ability of nanoparticle to penetrate across the nucleopore. As the method described earlier chapter III, the concentration of chitosan was separated in to two concentrations (0.005%w/v and 0.025%w/v) at each concentrations which was exposed with different condition in order to reduce the size of nanoparticle.

According to the previous study (Seung-Hoon et al., 2008), the sonication was the method of choice for size reducing. So three intensity of sonication was selected at 100%, 120% and 140% ultrasound power with variation of duration at 15, 30, 45, 60 and 90 min.

From the result, in the samples containing 0.005%w/v of chitosan was treated with different both factors (sonication intensity and duration) gave no statistical significant (95% confidence interval) in size and zeta potential as well as samples

containing 0.025% w/v. Therefore the selected condition was chitosan at 0.005% w/v exposed to 100% ultrasound power at 15 min. because of the gentlest condition.

Increasing CS, the particles size and the zeta potential were increased. The primary amines in chitosan becomes positively charged in acid solution. The transfection efficiency of the complexes was largely depend on protonate amine of chitosan facilitate its binding to negatively charge DNA (Kim et al., 2007)

Table 4 Particle size of chitosan nanoparticles (mean±SD,n=3) (a), Zeta potential of chitosan nanoparticles (mean±SD,n=3) (b)

Time (min.)	Concentration of chitosan					
	0.005%w/v			0.025%w/v		
	100%T	120%T	140%T	100%T	120%T	140%T
15	9.70±0.03	11.23±0.02	12.50±1.62	29.05±19.15	24.33±7.72	24.40±1.77
30	11.22±0.67	13.03±2.21	12.48±0.44	18.30±3.82	31.62±13.01	23.73±3.92
45	11.12±0.41	11.50±0.42	11.35±0.95	19.95±3.05	22.06±2.46	20.13±5.18
60	20.15±9.28	11.77±0.54	14.71±5.72	24.95±13.37	25.80±5.89	21.42±0.82
90	10.66±0.45	11.59±0.31	13.97±4.54	33.91±17.90	22.26±5.13	20.35±1.83

(a)

Time (min.)	Concentration of chitosan					
	0.005%w/v			0.025%w/v		
	100%T	120%T	140%T	100%T	120%T	140%T
15	19.04±7.53	18.57±5.83	8.20±3.23	26.84±17.30	28.50±6.46	19.52±5.17
30	16.38±10.20	22.48±9.32	24.73±16.26	29.90±6.23	21.07±8.32	38.31±6.80
45	25.18±8.35	24.76±3.61	13.47±7.68	36.48±2.78	22.99±9.99	38.98±2.87
60	16.19±11.89	19.88±7.90	21.51±13.07	29.86±8.86	28.06±6.23	32.71±5.81
90	12.85±8.58	23.83±13.75	18.55±5.39	29.36±4.32	30.80±3.87	28.39±5.17

(b)

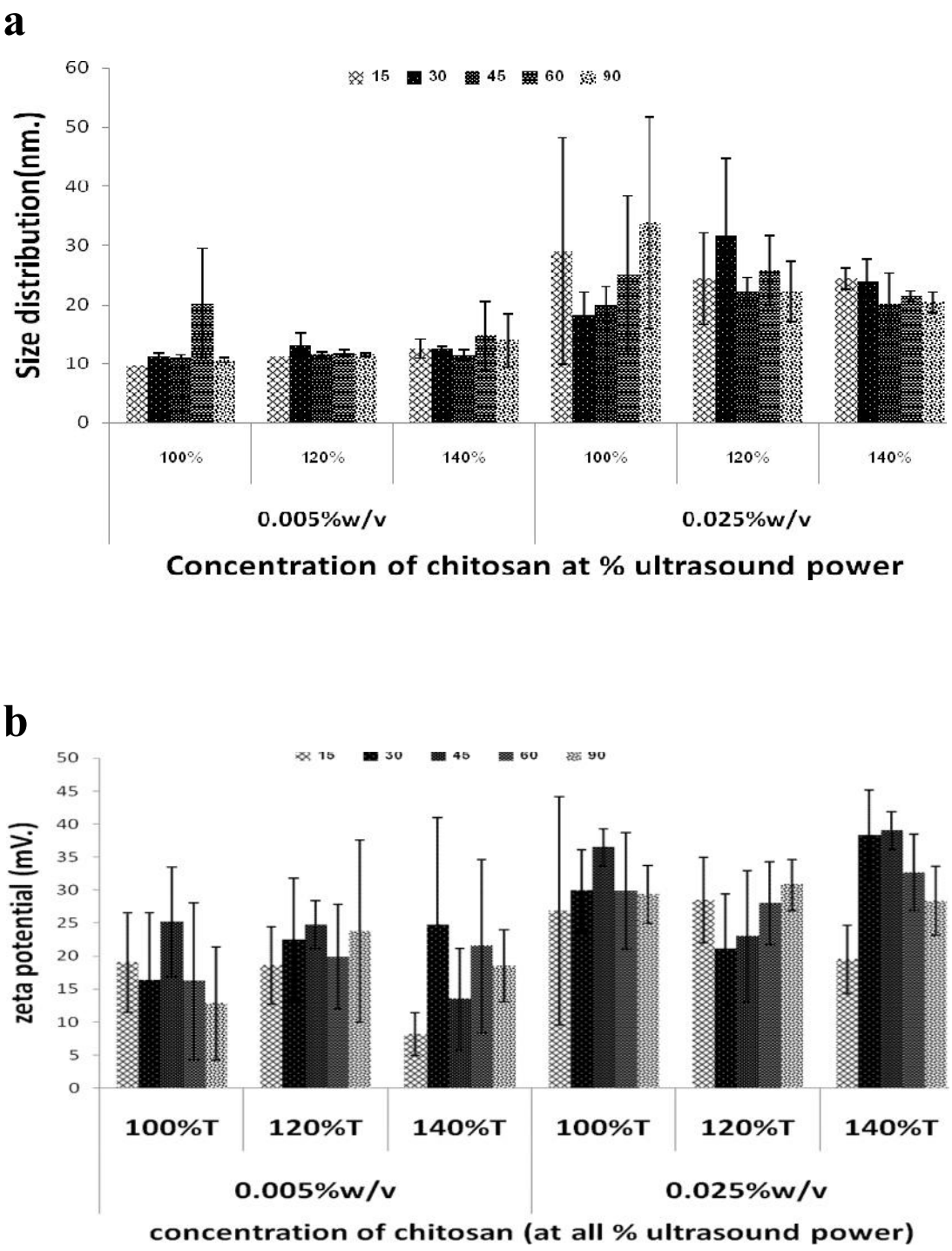

Figure 11 The size distribution (a) and zeta potential (b) of 0.005%w/v and 0.025%w/v chitosan by vary % ultrasound power at 15, 30, 45, 60 and 90 min.

3.1.3 M/C nanoparticles

f-MWCNTs/CS (M/C) nanoparticles were prepared by mixing f-MWCNTs with CS since mechanism of attachment is electrostatic interactions between positive charge on CS and negative charge on f-MWCNTs. From figure 12a and 12b, there were demonstrated the zeta potential of f-MWCNTs/CS complex.

There were two concentration of M/C at 2:1 and 1:2.5 in figure 6a. In 2:1 ratios, the high concentration of f-MWCNTs had low zeta potential that they showed decreasing zeta potential of M/C electrostatic complex at 100% ultrasound power 45min. and 120% ultrasound power 30min. They were the same effect at 3:1 ratios with all methods in figure 12b.

Chitosan nanoparticles were harmonized with f-MWCNTs. Electrostatic interaction between negatively carboxyl moieties and positively amines head groups were determined by decreasing the zeta potential of f-MWCNTs/CS.

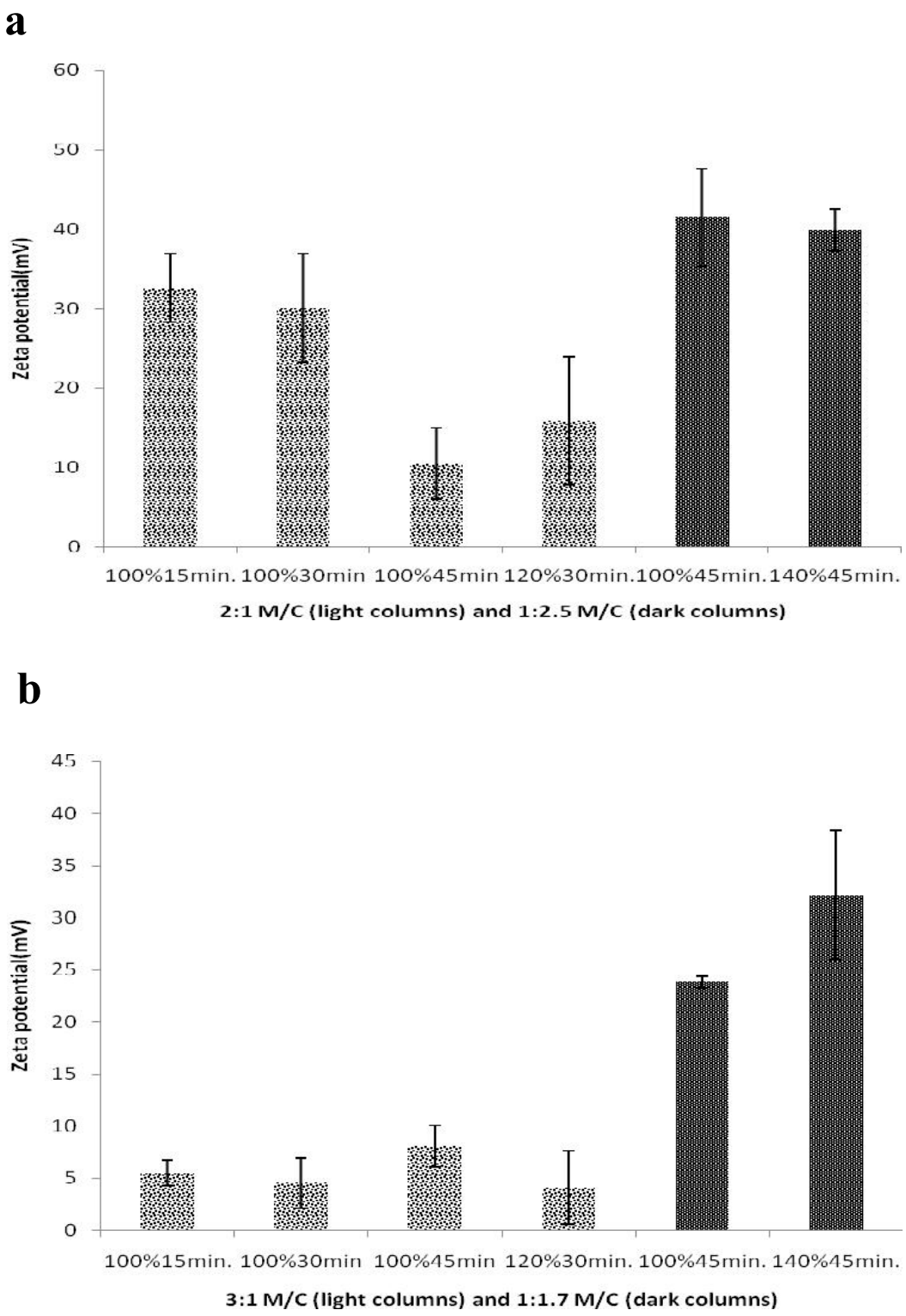

Figure 12 The zeta potential of 2:1 and 1:2.5 f-MWCNTs/CS complex (a), the zeta potential of 3:1 and 1:1.7 f-MWCNTs/CS complex (b)

3.1.4 M/D/C nanocomposites

For pDNA binding, electrostatic interaction between negatively phosphate groups and positively amines head groups were examined by decreasing the zeta potential of M/C/D that showed the condensation of pDNA in figure 13a-b. They showed decreasing zeta potential of 2:1:1 M/C/D electrostatic complex at 120% ultrasound power 30min in figure 13a. They were the same effect at 3:1:1 ratios at 100% 15min., 100% 30min., 120% 30min. and at 1:1.7:1 ratios 140% ultrasound power 45min in figure 13b. The method of 120% ultrasound power 30 min. presented the most decreasing zeta potential. The results agreed with expectation that the primary amines in the chitosan were protonated positively charged without f-MWCNTs attachment became to bind to negatively charged pDNA by electrostatic interaction.

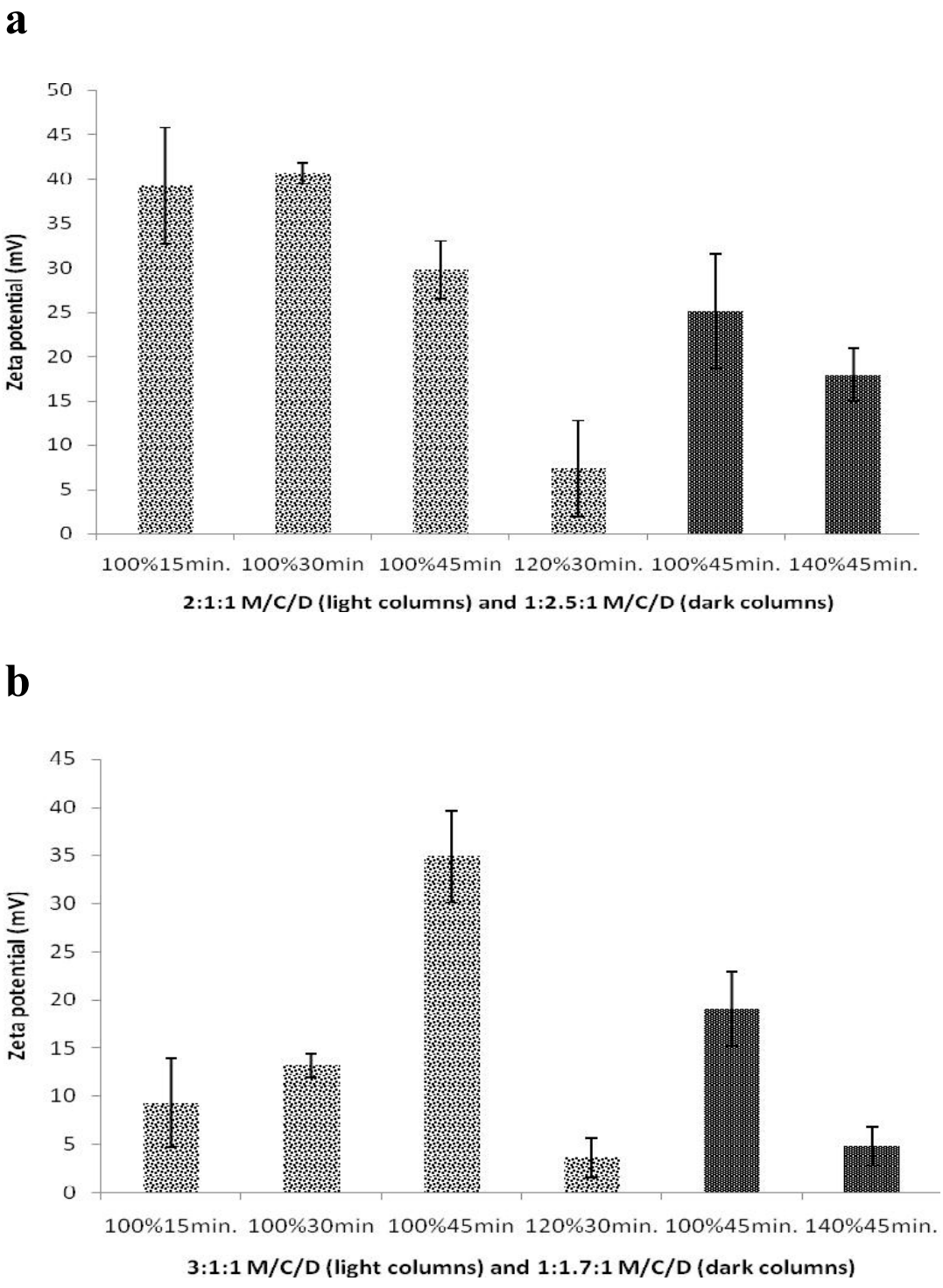

Figure 13 The zeta potential of 2:1:1 and 1:2.5:1 f-MWCNTs/CS/pDNA complex (a), the zeta potential of 3:1:1 and 1:1.7:1 f-MWCNTs/CS/pDNA complex (b).

3.2 Morphological Observation

3.2.1 Transmission electron microscopy (TEM)

TEM indicated that the f-MWCNTs, CS, pDNA, M/C and M/C/D complexes correspond to aggregates containing globular substructures. For sharp imaging of structure, the samples must be counterstained with heavy-metal salts which bind to components at the surface. Therefore the staining samples were enhanced electron density, sharp and contrasting electron images.

Generally, phosphotungstic acid (PTA) and uranyl acetate (UA) were use as staining agent. The PTA would bind with the positive substances while the UA bound with negative substances such as f-MWCNTs at carboxylic group position. The figure 14a showed the TEM images of f-MWCNTs without UA staining. When f-MWCNTs was stained with UA (figure 14b), the dark area of f-MWCNTs indicated the binding between UA and carboxylic group on the f-MWCNTs resulting to the darker specimen comparing the lighter background. As comparing between figure 14a and 14b, the image result showed that the carboxylic group formed after the functionalization located around MWCNTs.

As the figure 14c, the red arrow pointed to the darker specimen determining the UA could strongly react with phosphate group (negative ion) of pDNA. The CS nanoparticles (figure 14d), PTA was use as the staining agent to bind with the cation ion of CS. When compare the TEM image between figure 14b and 14e, the chitosan

coated f-MWCNTs showed the continuous tube which revealed that chitosan coated on the f-MWCNTs and acts as barrier to protect the reaction between the carboxylic group and UA.

a

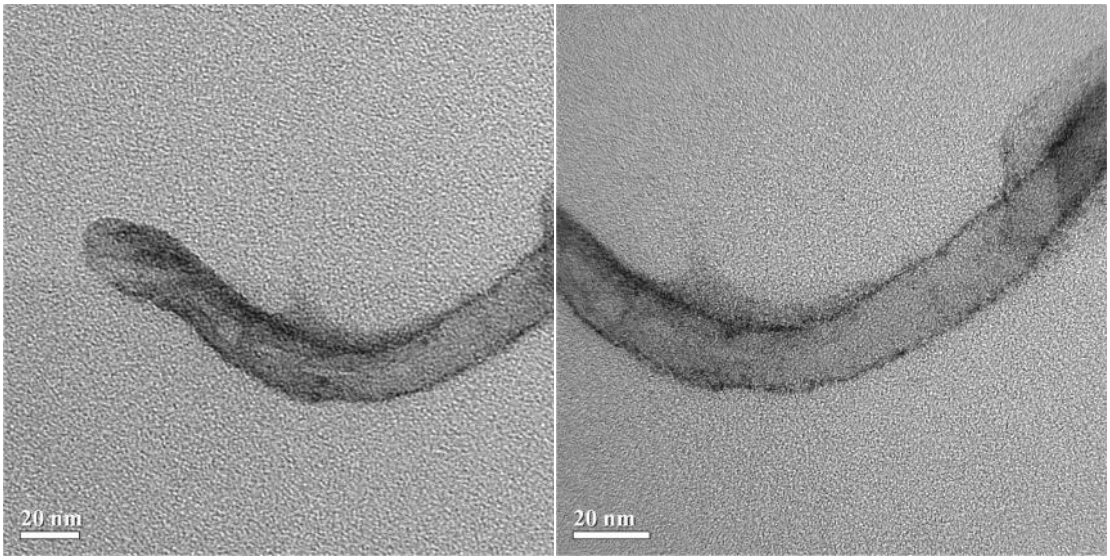

b

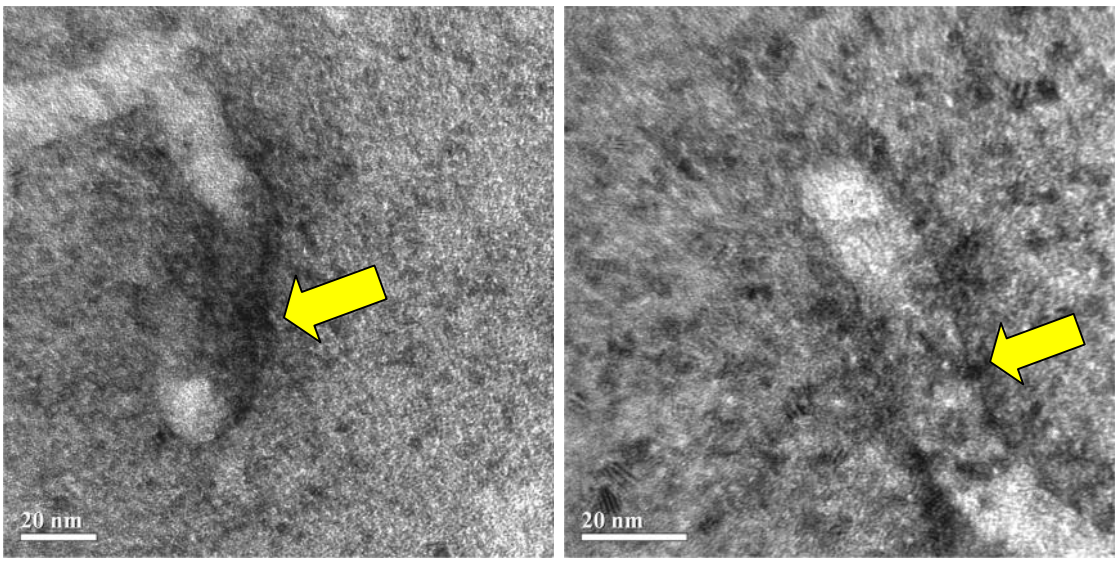

c

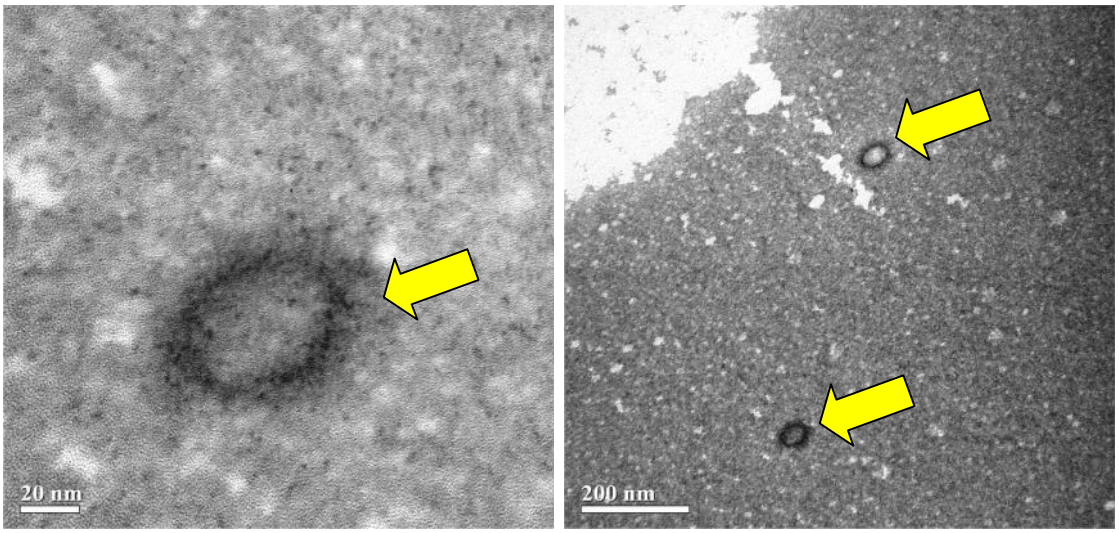

d

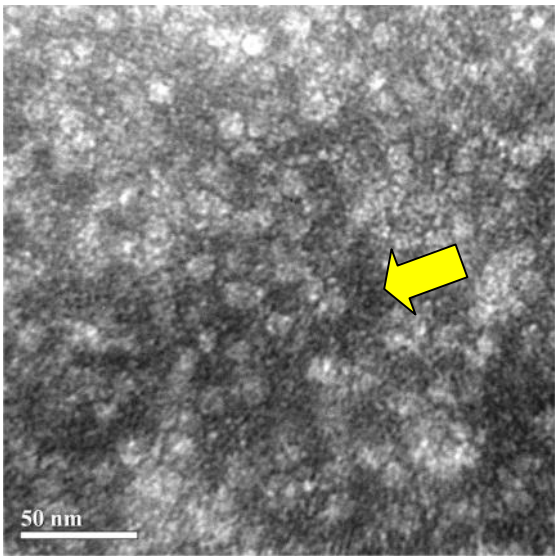

e

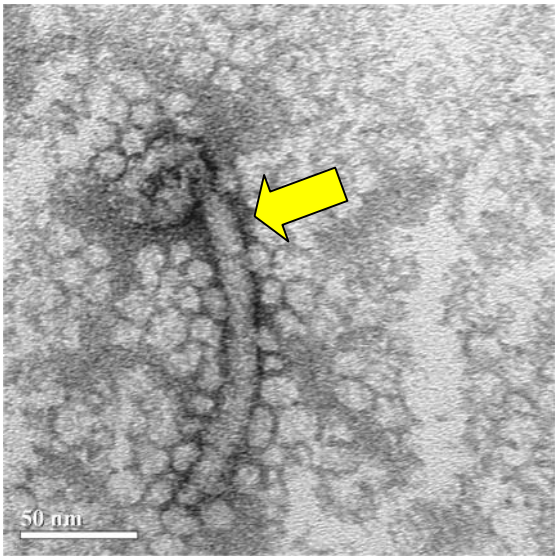

f

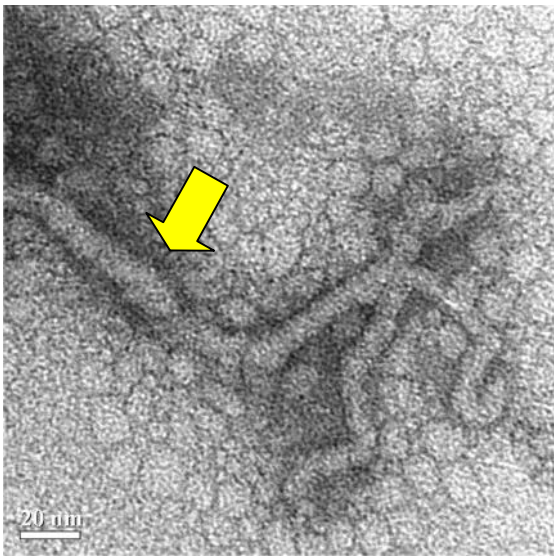

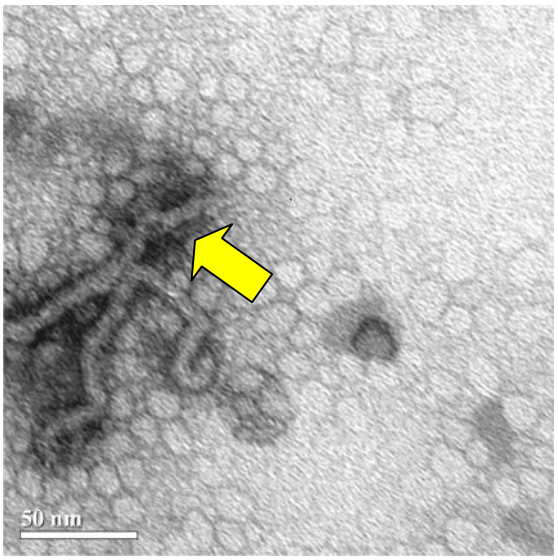

g

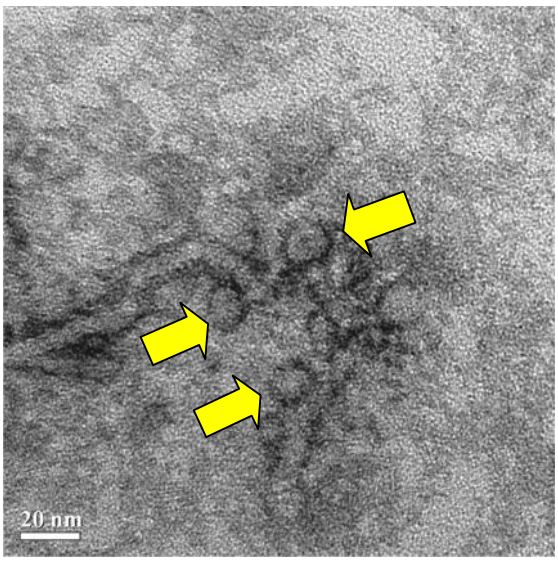

Figure 14 TEM images of f-MWCNTs without UA 1% or PTA 1% label (a), TEM images of f-MWCNT nanocomposites with UA 1% label (b), TEM images of naked pDNA (pEGFP-C_2) with UA 1% label (c), TEM images of the CS nanoparticles with PTA 1% label (d). TEM images of f–MWCNTs/CS composite with UA 1% label (e), TEM images of f-MWCNT/CS nanocomposites with PTA 1% label (f), TEM images of f-MWCNT/CS/pDNA nanocomposites with PTA 1% label (g).

3.1 Chemical structure characterization

3.1.1 Fourier transform infrared (FT-IR) spectroscopy

The band of CS (C) and f-MWCNTs/CS (D) showed the region 2879 cm^{-1} that were assigned to amines (C=N). The region 1631, 1649, 1635 cm^{-1} of f-MWCNTs (B), CS and f-MWCNTs/CS of indicated the carbonyl group (C=O).

The regions that assigned to amines (C=N) of CS (C) were 2870.44 cm^{-1}(a). The infrared spectra of the treated CS formulations were decreased of the band intensity of C=N that was showed in the infrared spectra of f-MWCNTs/CS (D). This band suggested damages of amine bonds.

Generally, FT-IR spectra analysis of DNA is divided in three principal regions (Brewer S.H. et al, 2002). The first region from 1750 to 1600 cm^{-1} essentially due to C=O, C=N, C=C stretching and exocyclic–NH_2 bending vibrations in the DNA bases. The second region from 1600 to 1500 cm^{-1} results mostly from the purine and pyrimidine ring modes (Falk et al., 1963; Liquier et al., 1991; Zhou-Sun et al., 1997) and the last region from 1250 to 950 cm^{-1} correspond to the symmetric and asymmetric PO_2^{-1} groups of the phosphodiester-deoxyribose backbone (Falk et al., 1963; Liquier et al., 1991; Zhou-Sun et al., 1997).

The infrared spectra of pDNA (F) at 1573.39 cm^{-1} (b), assigned to C=N, was disappeared that was showed in the infrared spectra of M/C/D nanocomposite (E). In addition, the infrared spectra of pDNA at 1239.3(c), 1093.58 cm^{-1}(d), assigned to PO_2^{-1}, was departed that was compared with the band at 1109.49 $cm^{-1}$of M/C/D nanocomposite. The regions that assigned to C=N and PO_2^{-1} groups of pDNA (F) were changed by interacting with M/C.

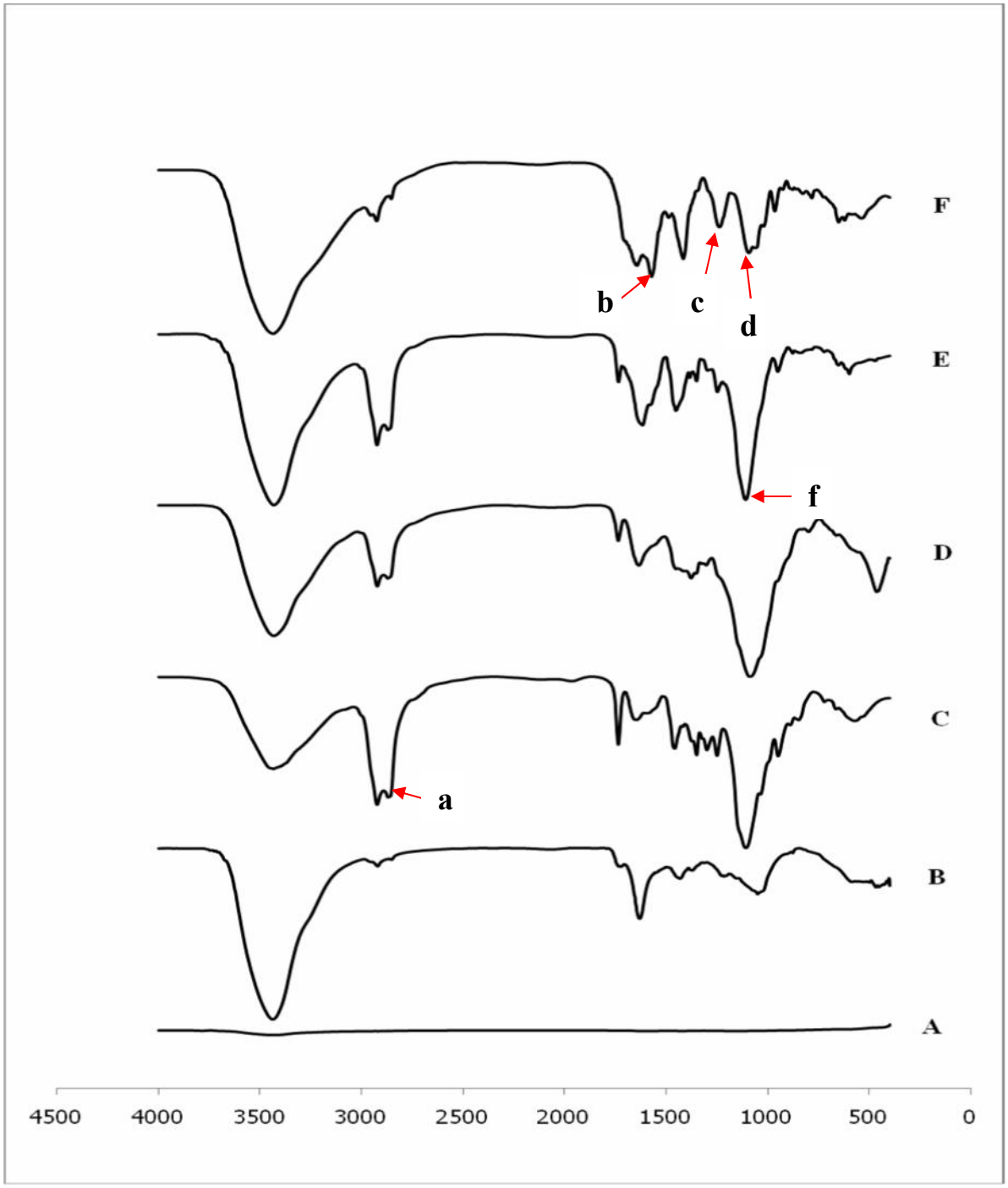

Figure 15 The infrared spectra of MWCNTs(A), f-MWCNTs(B), CS(C), f-MWCNTs/CS(D), f-MWCNTs/CS/pDNA(E) and pDNA(F)

4. Gel retardation assay

The f-MWCNTs/CS were then further formed complex with plasmid DNA. The complexation of f-MWCNTs/CS/pDNA was confirmed by the electrophoretic mobility analysis which revealed that f-MWCNTs/CS could efficiently immobilize pEGFP-C_2. f-MWCNTs/CS/pDNA was electrophoresed on an agarose gel. They were prepared at various formulations with chitosan, f-MWCNTs of f-MWCNTs/CS with 0.8 μg pDNA in figure 16a and 0.6 μg, 1 μg pDNA in figure 16b. The migration of pDNA was observed in lane 2. All formulations in lane 3 to 14 showed the effective retardation of DNA migration.

a

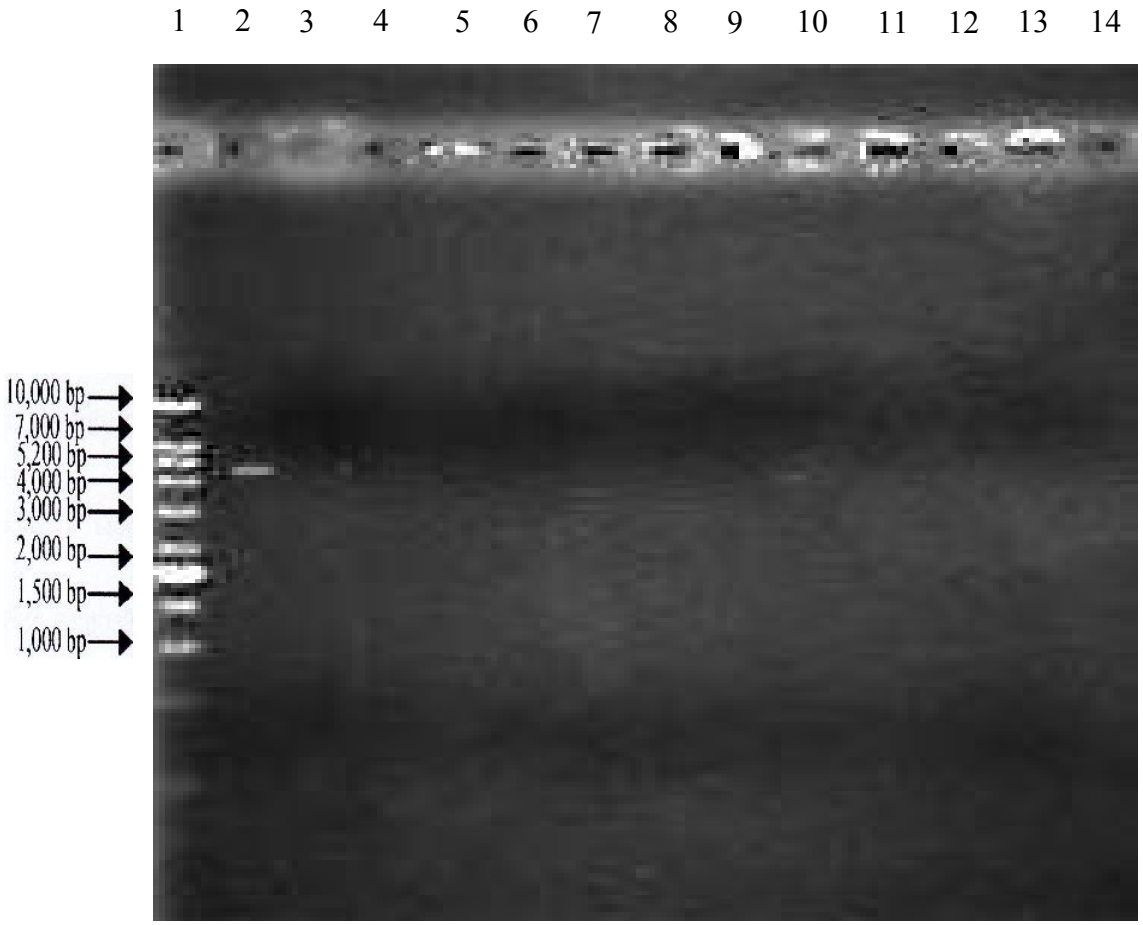
1 2 3 4 5 6 7 8 9 10 11 12 13 14
10,000 bp
7,000 bp
5,200 bp
4,000 bp
3,000 bp
2,000 bp
1,500 bp
1,000 bp

b

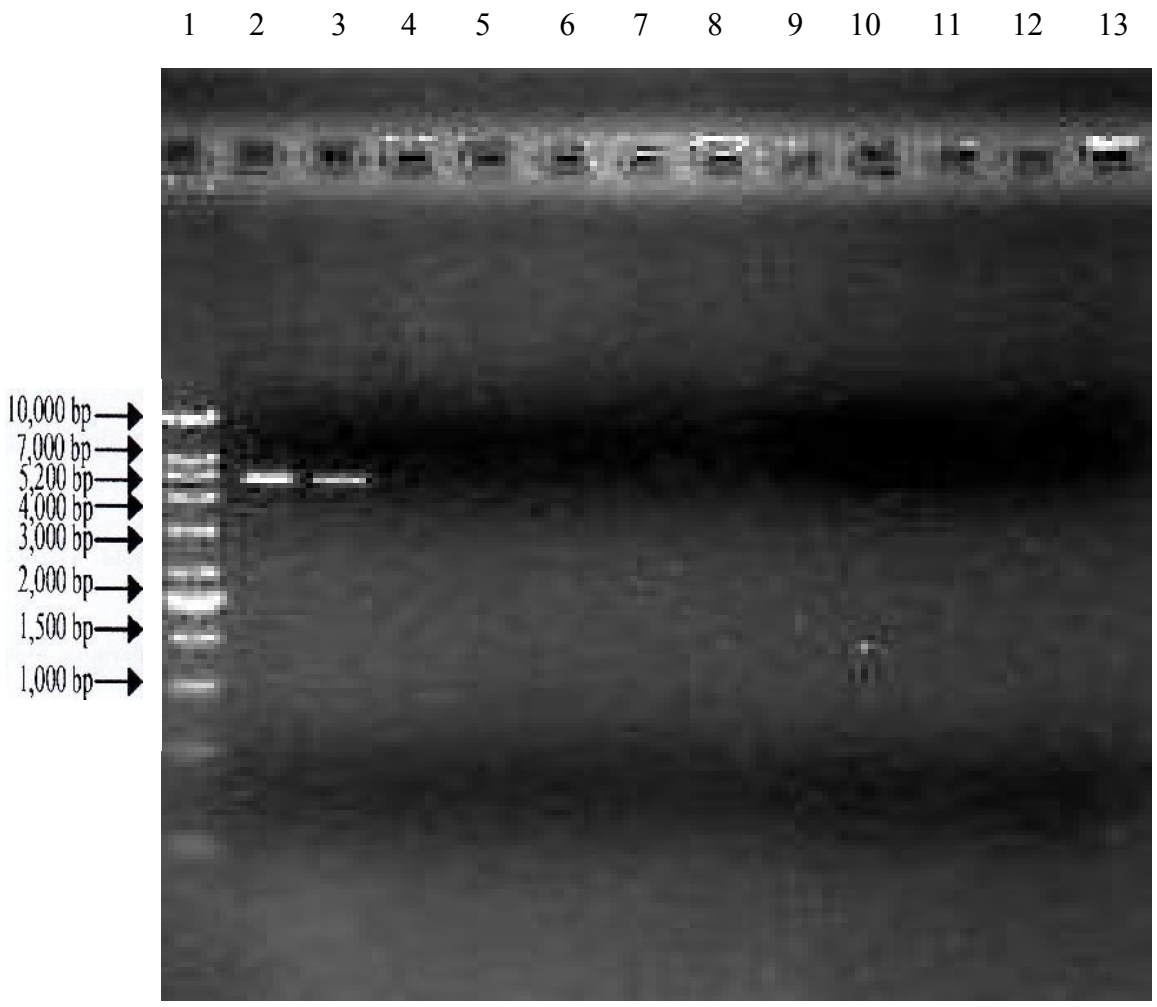

Figure 16 Gel retarding analysis of f-MWCNTs/CS/pDNA (a), Lane 1: DNA ladder (reference), Lane 2: 0.8 µg naked pDNA (pEGFP-C_2), Lanes 3-8: complexes prepared with 1:3 formulations 0.01%w/v f-MWCNTs/CS, Lanes 9-14: complexes prepared with 1:3 formulations 0.015%w/v f-MWCNTs/CS., Gel retarding analysis of f-MWCNTs/CS/pDNA (b), Lane 1: DNA ladder (reference), Lane 2: 1 µg naked pDNA(pEGFP-C_2), Lane 3: 0.6 µg naked pDNA(pEGFP-C_2), Lane 4: complexes prepared with 1:3 0.01%w/v f-MWCNTs/0.05%w/v CS/1 µg pEGFP-C_2 (sonicating

30min.), Lane 5: complexes prepared with 3:1 0.01%w/v f-MWCNTs/0.05%w/v CS/1 µg pEGFP-C_2, Lane 6: complexes prepared with 1:3 0.01%w/v f-MWCNTs/0.05%w/v CS/0.6 µg pEGFP-C_2, Lane 7: complexes prepared with 1:3 0.01%w/v f-MWCNTs/0.05%w/v CS/1µg pEGFP-C_2, Lane 8: complexes prepared with 1:3 0.015%w/v f-MWCNTs/0.05%w/v CS/1µg pEGFP-C_2, Lane 9: complexes prepared with 1:3 0.01%w/v f-MWCNTs/0.25%w/v CS/1µg pEGFP-C_2, Lane 10: complexes prepared with 3:1 0.01%w/v f-MWCNTs/0.25%w/v CS/1µg pEGFP-C_2, Lane 11: complexes prepared with 1:3 0.01%w/v f-MWCNTs/0.25%w/v CS/0.6µg pEGFP-C_2, Lane 12: complexes prepared with 1:3 0.01%w/v f-MWCNTs/0.25%w/v CS/1µg pEGFP-C_2, Lane 13: complexes prepared with 1:3 0.015%w/v f-MWCNTs/0.25%w/v CS /1µg pEGFP-C_2.

5. Cytotoxicity of f-MWCNTs, CS, pDNA and commercial vectors.

5.1 Morphology of HeLa cells observed by inverted microscope

The morphology of HeLa cells were showed in figure 17 after incubation with the nanoparticles of pDNA, M/C, M/C/D, Lipofectamine® and Lipofectamine®-pDNA complexes in the 5% CO_2 humidified incubator at 37°C for 72 hours. pDNA, 3:1 M/C and the ratio of 3:1:1 ,1:11:1, 1:13:1, 1:15:1, 1:17:1 M/C/D nanoparticles presented no noticeable modify the morphology of HeLa cells. The cells have a slightly elongated shape (figure 12b-h). In previous study, Weiling et al. (2011) reported that the morphological studies of HeLa cells incubated with MWCNT-PAMAM hybrid at different concentrations showed that cells lived better than those incubated with pure PAMAM or Lipofectamine 2000; the number of HeLa cells had no obvious decrease until the concentration was larger than 15 µg/mL.

HeLa cells culture in figures 17b-h were agreed with ATCC®. HeLa cells from ATCC® have an epithelial-like morphology. The cells have a slightly elongated shape at low density, but become more cobblestone-like in appearance as cultures approach confluence. Viable, round cells may be present in rising numbers as cell density increases; and, it is not uncommon for HeLa cells to slough completely off the vessel when cultures are overgrown.

Lipofectamine® and Lipofectamine®-pDNA revealed that HeLa cells reform to round cells at low density. HeLa cells incubating with Lipofectamine® and Lipofectamine®-pDNA were death because of Lipofectamine® was toxic during transfection(figure 17i-j). Zhong et al.(2008) reported that prolonged culture of the transfected cells caused significant increases in early apoptotic cells ($P<0.05$) and in the damaged or necrotic cells ($P<0.001$), and resulted in reduced viable cells ($P<0.01$); these changes became obvious after a 48-hour culture, which also increased the ratio of G(0)/G(1) phase cells ($P<0.05$) and decreased those of G(2)/M phase cells ($P<0.01$), S phase cells ($P<0.01$), and the late apoptotic cells ($P<0.05$).

a

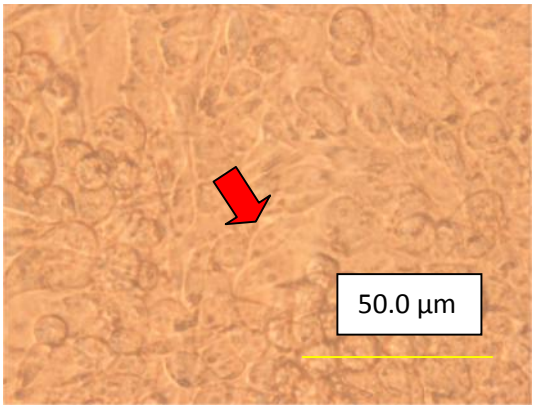

b

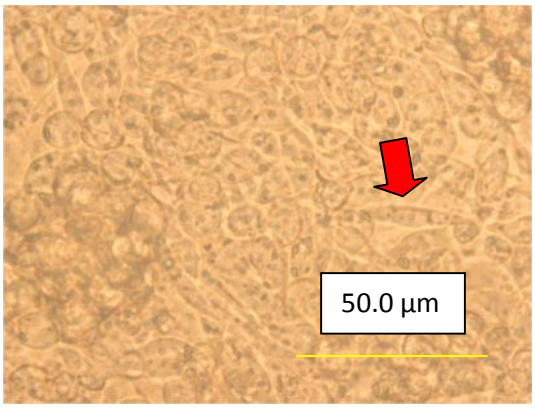

c

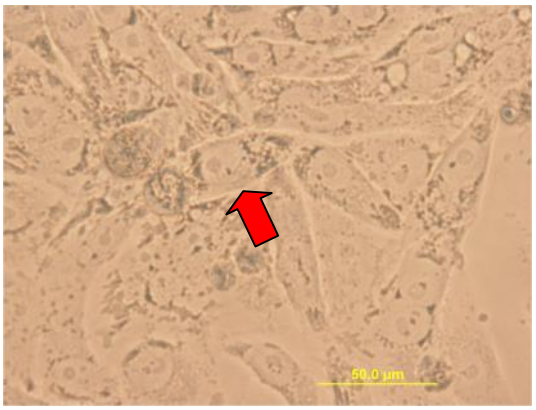

d

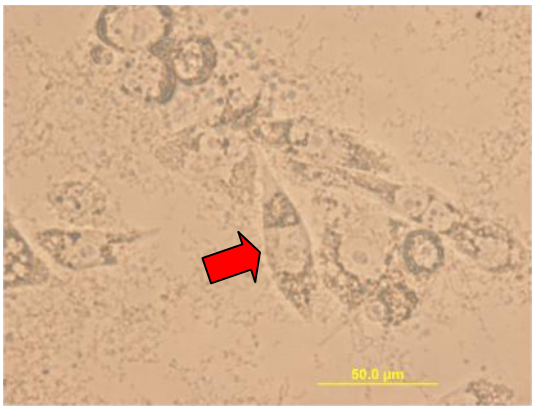

e

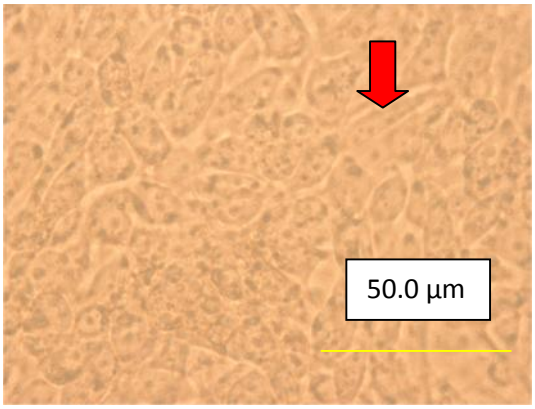

f

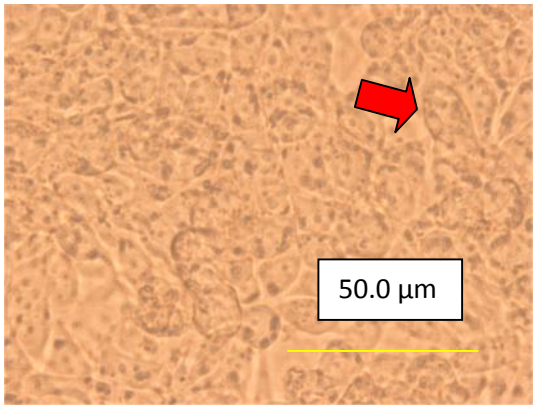

g

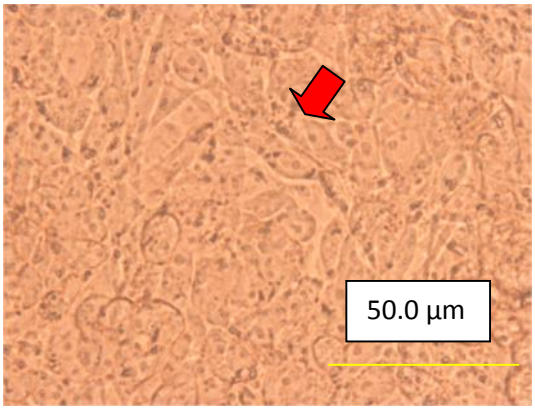

h

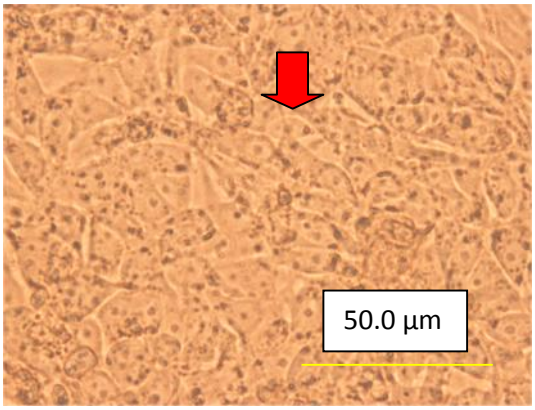

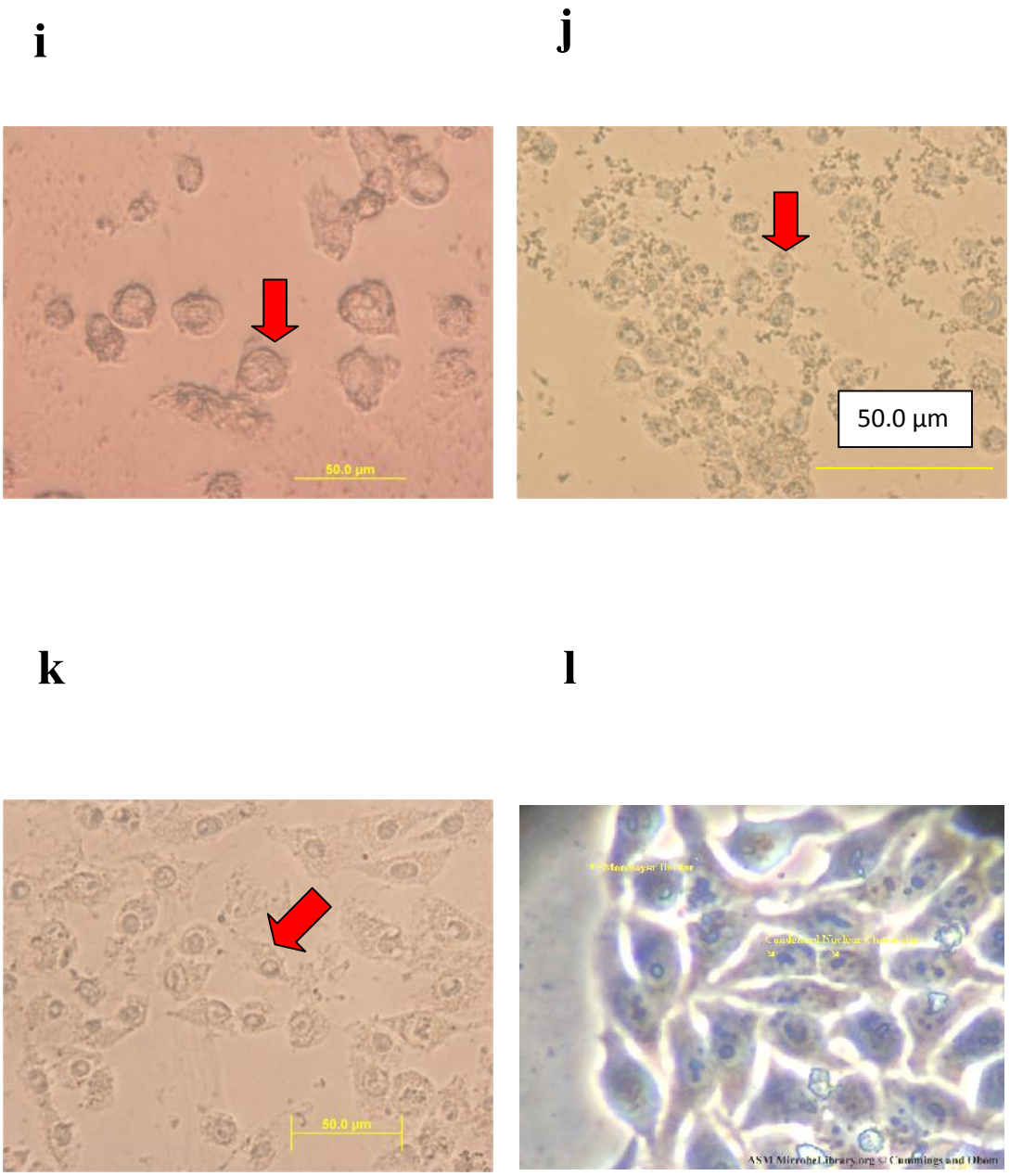

Figure 17 HeLa cells were incubated with solutions in the 5% CO_2 humidified incubator at 37°C for 72 hours (400x); HeLa cells in DMEM (a), HeLa cells were incubated with naked pDNA (b), HeLa cells in 3:1 M/C nanoparticle formulation (c), HeLa cells in 3:1:1 M/C/D nanoparticle formulation (d), HeLa cells in 1:11:1 M/C/D nanoparticles formulation (e), HeLa cells in 1:13:1 M/C/D nanoparticles formulation (f), HeLa cells in 1:15:1 M/C/D nanoparticles formulation (g), HeLa cells in 1:17:1 M/C/D nanoparticles formulation (h), HeLa cells in Lipofectamine® reagent (i), HeLa cells in 2:1(µl:µg) Lipofectamine® reagent-pDNA (j), HeLa cells in 6.7:1(µl:µg) PolyFect® reagent-pDNA (k), HeLa cells (Patrick J. et al., 2007) (l)

5.2 Cell viability tests

% Cell viability of HeLa cell cultures of f-MWCNT were showed in figure 18a after incubated at difference concentration over 72 hours. HeLa cell culture after incubated with f-MWCNTs at concentration below 75 μg/ml was nearly 100% cell viability.

The cellular viability was calculated as percentage of each CS concentration (figure 18b). The M/C, M/C/D nanoparticles and commercial vectors-pDNA complexes were compared (figure 18c).

The M/C/D showed the best survival than those nanoparticles. HeLa cell culture after incubated with f-MWCNTs at concentration below 75 μg/ml over 72 hours was nearly 100% cell viability. This study agreed with Weiling et al., 2011. HeLa cell culture after incubated with f-MWCNTs at concentration below 10 μg/ml over 72 hours was about 40-70% cell viability. Weiling et al. reported that the cellular viability of HeLa cells curture is higher than those of Lipofectamine 2000 in the whole studied concentration range. In detail, the cellular MWCNT hybrid, being about 1.91 times as large as those of Lipofectamine 2000 (at the concentration of 15 μg/ml)

a

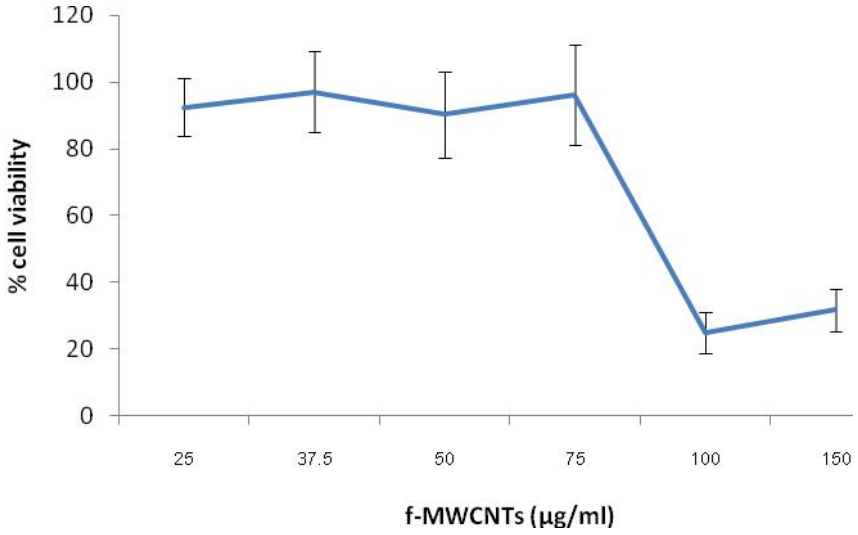
120
100
80
60
40
20
0
% cell viability
25
37.5
50
75
100
150
f-MWCNTs (µg/ml)

b

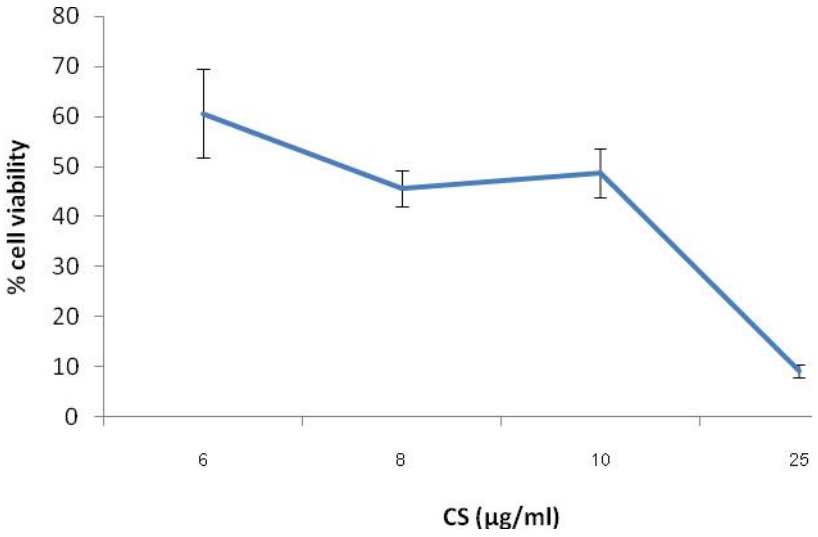
80
70
60
50
40
30
20
10
0
% cell viability
6
8
10
25
CS (µg/ml)

c

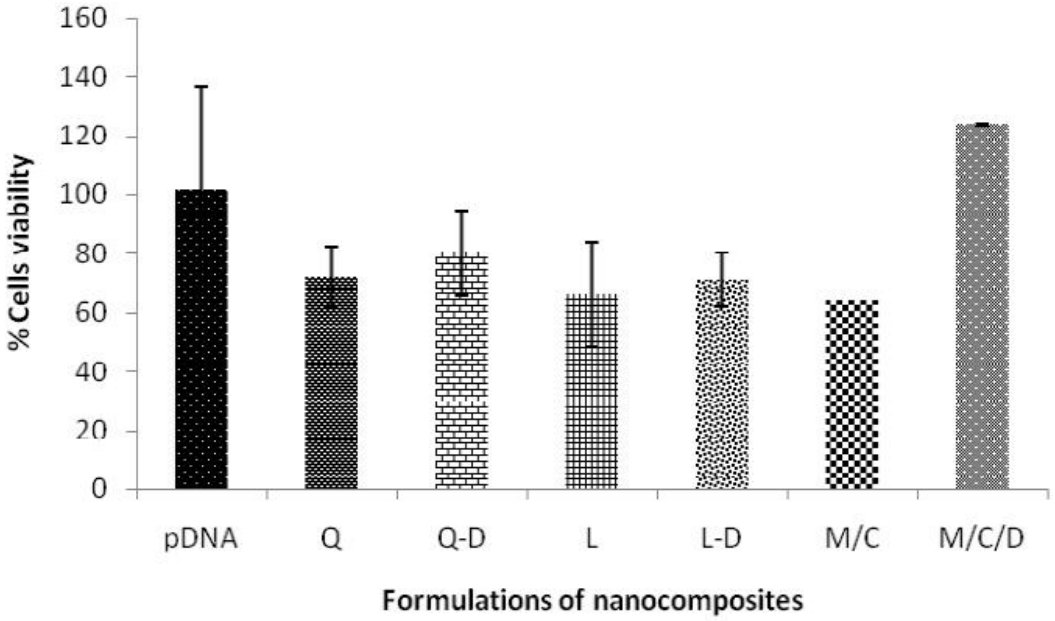

Figure 18 % Cell viability of HeLa cell culture after incubated with f-MWCNTs at different concentration over 72 hours (a), % Cell viability of HeLa cell culture after incubated with CS at different concentration over 72 hours (b), % Cell viability of HeLa cell culture after incubated with 3:1 of M/C, 3:1:1 of M/C/D nanoparticles and commercial vectors-pDNA complexes (Q=PolyFect®, L=Lipofectamine®) over 72 hours (c).

6. *In vitro* transfection in HeLa cells culture

Flow cytometry analysis of the expression of the green fluorescent protein (%GFP)

After HeLa cells culture were transfected with the control pEGFP-C_1, M/C/D, PolyFect®, Lipofectamine® for 48 hour, they were determined for GFP expression. The GFP-related fluorescence was quantified as the product of the mean fluorescence intensity (MFI) of the cell population displaying fluorescence (cells in region M1) above the autofluorescence limit, with the percentage of cells within the M1 region called % M1, according to the following equation:

$$\text{Amount of fluorescences} = (\text{MFI} \times \%\text{M1})/100 \qquad (3)$$

These two parameters were given by the flow cytometer CellQuest® software (Becton-Dickinson) (Jean-Luc T. et al., 2001).

The transfection efficiency of formulations was determined as the GFP-related fluorescence expression after incubated with formulations for 48 hours that were showed in table 5. Figure 19a presented the percentage of GFP comparison among pDNA, 1:9:1 M/C/D and 5:3:1 M/C/D. 5:3:1 M/C/D formulation that were significantly different from negative control (pDNA) ($P<0.05$). 1:9:1 M/C/D formulation was not significantly different from negative control (pDNA).

Figure 19 presented the cell population displaying fluorescence (cells in region M1). This figure showed the comparison between HeLa cells culture with DMEM (c), pEGFP-C_1 (d), 1:9:1 M/C/D (e), 5:3:1 M/C/D (f) formulation. In 1:9:1 M/C/D and 5:3:1 M/C/D formulation, there were more migration of M1 region than HeLa cells culture with DMEM and pEGFP-C_1. Whereas, 5:3:1 M/C/D formulation exhibited the high migration of M1 region. The results demonstrated that the most transfection efficiency was obtained from 5:3:1 M/C/D formulation.

PolyFect® is the activated dendrimers which are positively charged and resemble snowflakes in structure (David et al., 2010). Lipofectamine® is a polycationic liposome that is wildly used to be positive controls in many transfection studies (Weiling et al., 2011). In comparison with positive controls, PolyFect® and Lipofectamine® were used. Figure 19b presented the percentage of GFP comparison among 1:9:1 M/C/D, 5:3:1 M/C/D, PolyFect® (Q) and Lipofectamine® (L). PolyFect® and Lipofectamine® were revealed significantly different from 1:9:1 M/C/D and 5:3:1 M/C/D ($P<0.05$).

Comparison among 1:9:1 M/C/D (e), 5:3:1 M/C/D (f) formulation and PolyFect® (g), Lipofectamine® (h) in figure 19, PolyFect® and Lipofectamine® showed more migration of M1 region than 1:9:1 M/C/D and 5:3:1 M/C/D formulation. The PolyFect® exhibited the high migration of M1 region. M1 region area of Lipofectamine® was smaller than the others. Because Lipofectamine® modified the morphology of HeLa cells, many of cells death were observed.

Highly f-MWCNTs in nanocomposite could be improved the transfection efficiency even though the transfection efficiency of M/C/D formulation was still lower than PolyFect® and Lipofectamine. Functionalized carbon nanotubes are able to interact with plasmid DNA through the electrostatic interaction and penetrate cell membranes with low toxicity (Pantarotto et al, 2004) (Gao et al., 2006).

Table 5 *In vitro* expression of the green fluorescent protein (%GFP)

sample	% GFP
pEGFP-C_1	-0.07±0.91
1:9:1 M/C/D	3.44±2.78
5:3:1 M/C/D	3.92±1.57
PolyFect®	43.19±5.9
Lipofectamine®	14.87±1.77

a

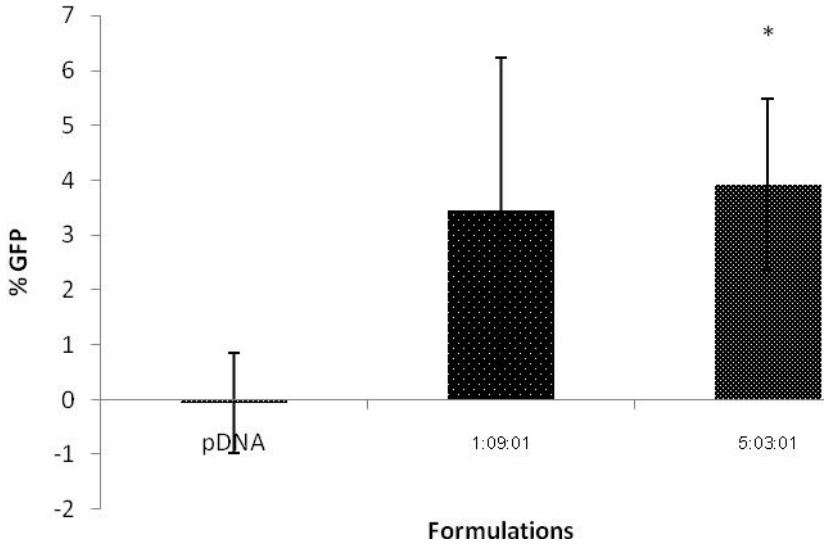
7
6
5
4
3
2
1
0
-1
-2
% GFP
*
pDNA
1:09:01
5:03:01
Formulations

b

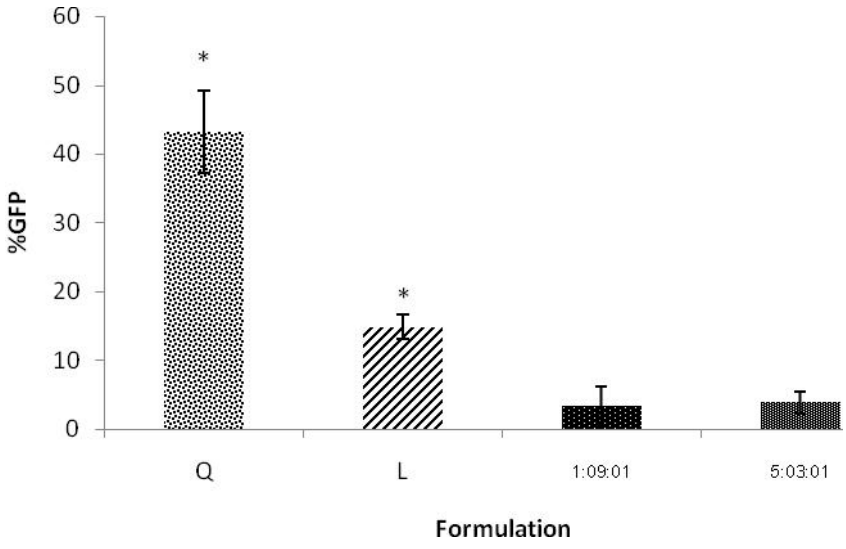
60
50
40
30
20
10
0
%GFP
*
*
Q
L
1:09:01
5:03:01
Formulation

c

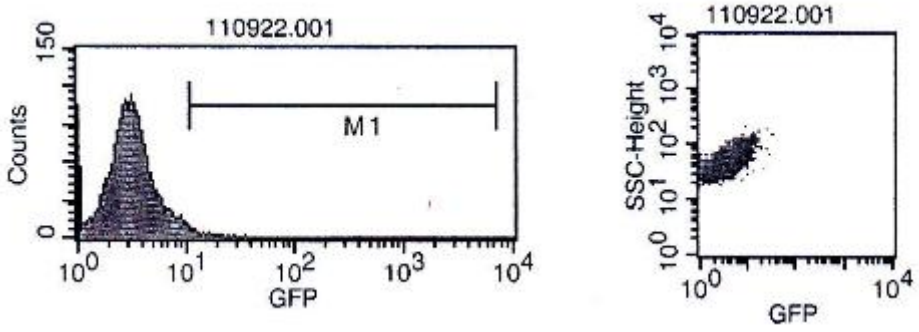
110922.001
Counts
150
0
M1
10^0 10^1 10^2 10^3 10^4
GFP
110922.001
SSC-Height
10^0 10^1 10^2 10^3 10^4
10^0 10^4
GFP

d

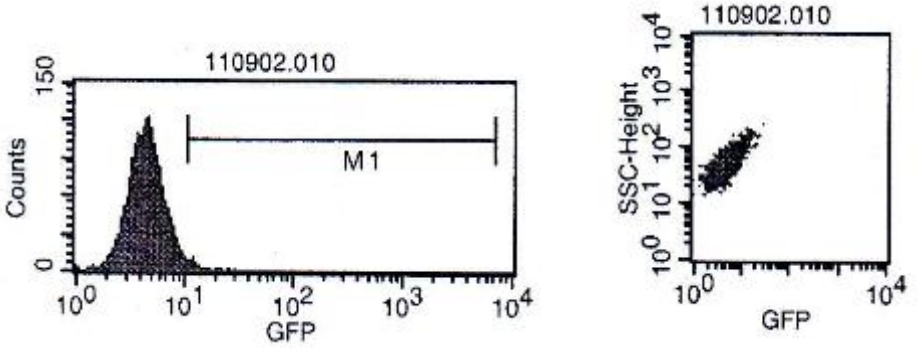
110902.010
Counts
150
0
M1
10^0 10^1 10^2 10^3 10^4
GFP
110902.010
SSC-Height
10^0 10^1 10^2 10^3 10^4
10^0 10^4
GFP

e

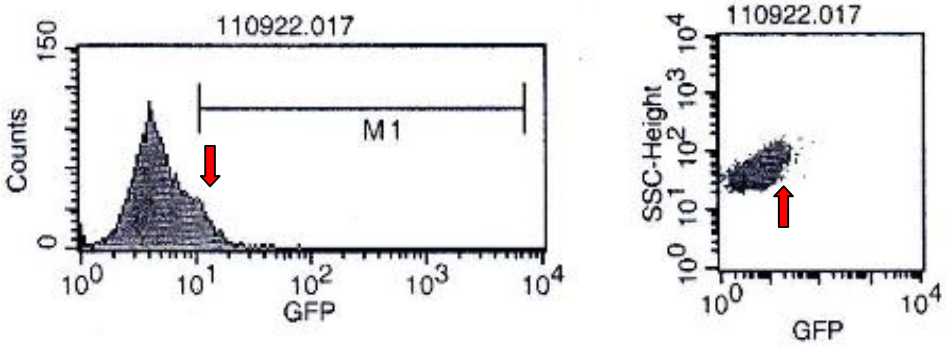
110922.017
Counts
150
0
M1
10^0 10^1 10^2 10^3 10^4
GFP
110922.017
SSC-Height
10^0 10^1 10^2 10^3 10^4
10^0 10^4
GFP

f

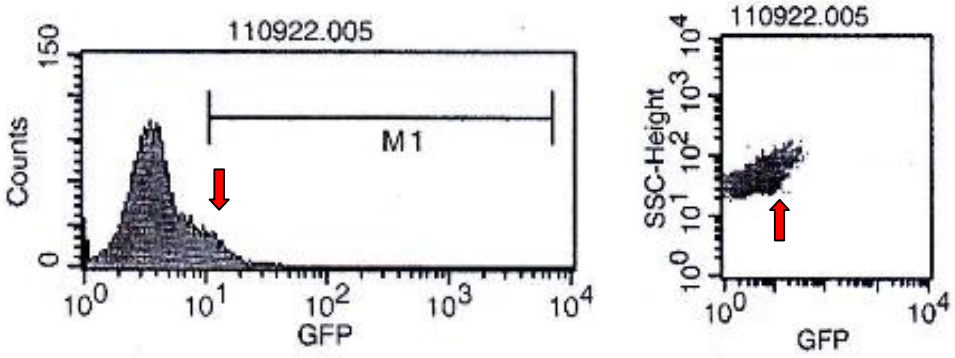
110922.005
Counts
150
0
M1
10^0 10^1 10^2 10^3 10^4
GFP
110922.005
SSC-Height
10^0 10^1 10^2 10^3 10^4
10^0
10^4
GFP

g

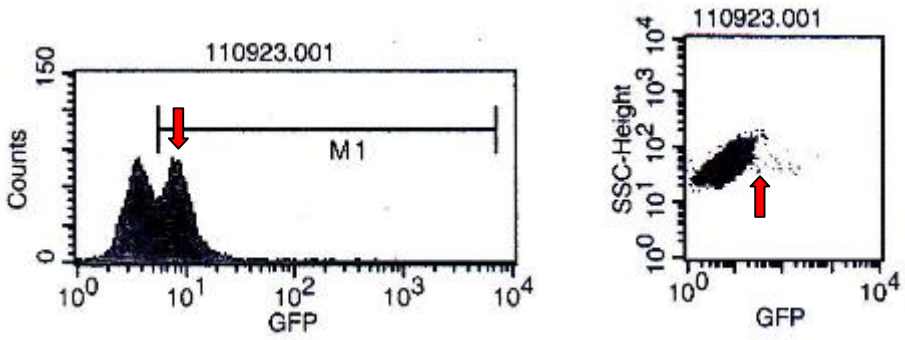
110923.001
Counts
150
0
M1
10^0 10^1 10^2 10^3 10^4
GFP
110923.001
SSC-Height
10^0 10^1 10^2 10^3 10^4
10^0
10^4
GFP

h

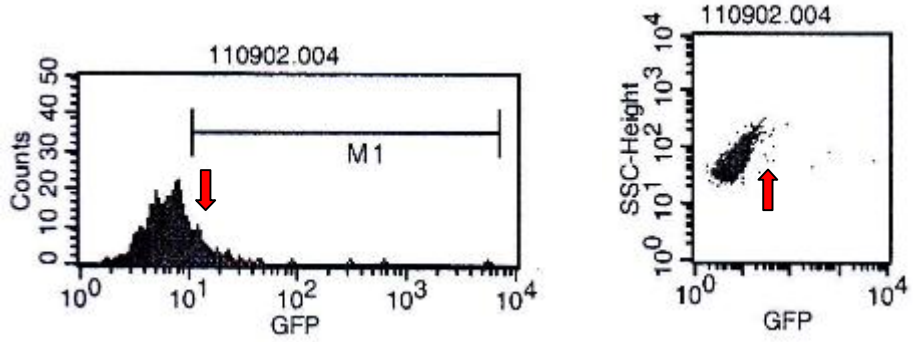
110902.004
Counts
0 10 20 30 40 50
M1
10^0 10^1 10^2 10^3 10^4
GFP
110902.004
SSC-Height
10^0 10^1 10^2 10^3 10^4
10^0
10^4
GFP

Figure 19 Comparison of pDNA, 1:9:1 M/C/D, 5:3:1 M/C/D, the *In vitro* expression of the green fluorescent protein (%GFP) (a), Comparison of 1:9:1 M/C/D, 5:3:1 M/C/D, PolyFect® (Q) and Lipofectamine® (L), the *In vitro* expression of the green fluorescent protein (%GFP) (b), The expression of the green fluorescent protein (%GFP) were examined after incubated with the control HeLa cells culture with DMEM (c), pEGFP-C_1(d), 1:9:1 M/C/D (e), 5:3:1 M/C/D (f), PolyFect® (g), Lipofectamine® (h) over 48 hours.

CHAPTER V

CONCLUSION

The M/C/D nanoparticles were prepared by using electrostatic interaction. Multiwalled carbonnanotube(MWCNTs) were functionalized by treating with concentrated sulfuric acid and concentrated nitric acid to improve solubilization and to obtain anionic particles. Negative charges were resulted from the functionalization of carboxylic group. MWCNTs sonicated for 6 hours (Seung-Hoon et al.) and 12 hours (Ajeet et al.) were compared in this study. The production yield percentage of each f-MWCNTs in the mixture solvents of H_2SO_4/HNO_3 for 12 hours was 100.82-101.4%. These were related to the exposure time that the pristine MWCNTs were contacted to oxidizing agent (the mixture solvents of H_2SO_4/HNO_3).

The average particle size of functionalized MWCNTs (f-MWCNTs) was 68 to 84 nm and zeta potential was -22.44 to -9.58 mV. The 0.010%w/v f-MWCNTs (68 nm; -22.44 mV) could exhibit higher stability when compared with 0.015%w/v f-MWCNTs (84 nm; -9.58 mV). The smallest particles size and the lower zeta potential were attributed to the lower agglomeration of the pristine MWCNTs that were contacted to oxidizing agent (the mixture solvents of H_2SO_4/HNO_3).

The obtained f-MWCNTs were then attached with cationic chitosan nanoparticles (CS) by stirring overnight. f-MWCNTs/CS complexes were prepared by electrostatic interactions using two types of CS; 0.05%w/v and 0.25%w/v chitosan. Highly protonated chitosan backbone leaded to the spontaneous formation. Chitosan nanoparticles were harmonized with f-MWCNTs for pDNA binding. Ionic interaction of f-MWCNTs/CS complexes among carboxyl moieties and amine groups was enhanced with a decrease in f-MWCNTs/CS that showed the condensation of pDNA with the small particle sizes(<150 nm). The electrostatic interactions between f-MWCNTs/CS and pDNA were confirmed by the broader size distribution and the lower zeta potential.

Based on the method of negative stain, uranyl ions will bind to modified surface charge of nucleic acid phosphate groups or carboxyl groups. TEM images of f-MWCNTs interacting with chitosan nanoparticles-coated indicated the complex formation verified by their ionic charge.

The f-MWCNTs/CS were then further formed complex with plasmid DNA. The complexation of f-MWCNTs/CS/pDNA was confirmed by the electrophoretic mobility analysis.

HeLa cells incubated with the nanoparticles of pDNA, M/C, M/C/D, Lipofectamine® and Lipofectamine®-pDNA complexes in the 5% CO_2 humidified incubator at 37°C for 72 hours. pDNA, 3:1 M/C and the ratio of 3:1:1 ,1:11:1, 1:13:1, 1:15:1, 1:17:1 M/C/D nanoparticles presented no noticeable morphology

modification. Lipofectamine® and Lipofectamine®-pDNA revealed that HeLa cells reformed to round cells and resulted in cell death.

HeLa cell culture incubated with f-MWCNTs at concentration below 75 μg/ml over 72 hours showed nearly 100% cell viability. HeLa cell culture incubated with f-MWCNTs at concentration below 10 μg/ml over 72 hours showed about 40-70% cell viability. The M/C, M/C/D nanoparticles and commercial vectors-pDNA complexes were compared and the M/C/D showed the maximum of cell survival.

The transfection efficiency of formulations was determined by the GFP-related fluorescence expression after incubating HeLa cells with formulations for 48 hours. 1:9:1 M/C/D and 5:3:1 M/C/D formulation indicated higher cell population when compared with HeLa cells incubated with DMEM and pEGFP-C_1. This improvement would be ascribed to the negative control (pDNA) .

This study suggested that f-MWCNTs could help improve the transfection efficiency even though the transfection efficiency of M/C/D formulation was still lower than that of PolyFect® and Lipofectamine. Functionalized are able to interact with plasmid DNA due to the electrostatic interaction. Such complex would penetrate cell membranes with low toxicity.

REFERENCES

Alberto Bianco, Kostas Kostarelos and Maurizio Prato. Applications of carbon nanotubes in drug delivery. Current Opinion in Chemical Biology 2005, 9:674–679.

Alberto, B., Wei, W., Giorgia, P., Cedric, K., Lara, L., Charalambos, D. P., Kostas, K., and Maurizio, P., 2007. Carbon Nanotube-based Vectors for Delivering Immunotherapeutics and Drugs. Nanotechnologies for the Life Sciences vol 10: 85-142.

Alcamo,I.E. DNA technology:The awesome skill 2nded.San Diego:Harcourt Academic Press,2001.

Amit K. Jain, MPharm, Vaibhav Dubey, MPharm, Neelesh Kumar Mehra, MPharm,Neeraj Lodhi, MPharm, Manoj Nahar, MPharm,Dinesh K. Mishra, MPharm, Narendra K. Jain, PhD. Carbohydrate-conjugated multiwalled carbon nanotubes: development and characterization. Nanomedicine: Nanotechnology, Biology, and Medicine 5(2009):432–442.

ATCC ® CCL-2: Morphology. Availablefrom: http://atcc.custhelp.com/app/answers/detail/a_id/442/~/atcc%E2%AE-ccl-2-%3A-morphology [2011 July 24]

Ce´dric Klumpp,Kostas Kostarelos,Maurizio Prato, Alberto Bianco.Functionalized

carbon nanotubes as emerging nanovectors for the delivery of therapeutics.Biochimica et Biophysica Acta 1758 (2006) :404 – 412.

Chularat Iamsamai, Supot Hannongbua, Uracha Ruktanonchai, Apinan Soottitantawat, Stephan T. Dubas. The effect of the degree of deacetylation of chitosan on its dispersion of carbon nanotubes. CARBON 48 (2010):25-30.

Colin W. Pouton, Leonard W. Seymour. Key issues in non-viral gene delivery.Advanced Drug Delivery Reviews 46(2001):187–203.

Constantine P. Firme III,Prabhakar R. Bandaru.Toxicity issues in the application of carbon nanotubes to biological systems . Nanomedicine: Nanotechnology, Biology, and Medicine xx (2010) xxx–xxx.

Coué, G.,Feijen, J., Engbersen, J.F.J.,2008..Development of biodegradable poly(amidoamine)s for protein delivery. Journal of Controlled Release 132:e2 e3.

Dann J.A. Crommelin and Robert D. Sideler.Pharmaceutical Biotechnology An Introduction for Pharmacist and Pharmaceutical Scientists. London:Tayler & Francis Group,2002.

G.Coué,J. Feijen, J.F.J. Engbersen.Development of biodegradable poly(amidoamine)s for protein delivery. Journal of Controlled Release 132(2008):e2-e3.

GaryWalsh.Biopharmaceuticals Biochemistry and

Biotechnology.England: John&Wiley&Sons Ltd.,2003.

Jean-Pierre.Purification of the phage DNA.Available from:http://genemol.org/genemol/firstweek/Wednesday1.html [2011, May 7]

Kayser, O., and Muller R.H.,2004. Pharmaceutical Biotechnology Drug Discovery and Clinical Applications.Germany:WILEY-VCH Verlag GmbH&Co.

Kostas kostarelos, Lara lacerda, Giorgia pastorin, Wei wu, Se´ bastien wieckowski, Jacqueline luangsivilay, Sylvie godefroy, Davide pantarotto, Jean-paul briand, Sylviane muller, Maurizio prato and Alberto bianco.Cellular uptake of functionalized carbon nanotubes is independent of functional group and cell type.nature nanotechnology 2(2006):108 – 113.

Kostas kostarelos.Carbon nanotube cellular interaction, binding & internalization: a case of 'nanosyringe'?.Nanobioeurope(2008).

Lara Lacerda, Simona Raffa, Maurizio Prato, Alberto Bianco, Kostas Kostarelos.Cell-penetrating CNTs for delivery of therapeutics.nanotoday 2(2007):38-43.

Marianna Foldvari, Mukasa Bagonluri, Carbon nanotubes as functional excipients for nanomedicines:I. pharmaceutical properties. Nanomedicine: Nanotechnology, Biology, and Medicine 4(2008):173–182.

Marianna Foldvari, Mukasa Bagonluri, Carbon nanotubes as functional excipients for nanomedicines: II. Drug delivery and biocompatibility issues. Nanomedicine:Nanotechnology, Biology, and Medicine 4(2008):183–200.

Michael J. Groves. Pharmaceutical Biotechnology 2nd ed. New York and

London:Tayler & Francis Group,2006.

Moseley,A.B.,and Caskey,C.T.Human genetic disease and the medical need for somatic gene therapy.Advanced Drug Derivery Reviews.12(1993):131 -142.

Nadine Wong Shi Kam, Zhuang Liu, and Hongjie Dai. Carbon Nanotubes as Intracellular Transporters for Proteins and DNA: An Investigation of the Uptake Mechanism and Pathway. Angew. Chem. Int. Ed.44(2005):1–6.

O. Kayser and R.H. Muller. Pharmaceutical Biotechnology Drug Discovery and Clinical Applications.Germany:WILEY-VCH Verlag GmbH&Co.,2004.

Ravi Singh,Davide Pantarotto, David McCarthy, Olivier Chaloin,Johan Hoebeke,Charalambos D. Partidos,Jean-Paul Briand,Maurizio Prato,Alberto Bianc and Kostas Kostarelos.Binding and Condensation of Plasmid DNA onto Functionalized Carbon Nanotubes: Toward the Construction of Nanotube-Based Gene Delivery Vectors. J.AM.CHEM. SOC.127(2005):4388-4396.

Rodney J.Y.HO and Milo Gibaldi.Biotechnology and Biopharmaceuticals Transforming proteins and Genes into Drugs.England:John&Wiley&Sons Ltd.,2003.

Seung-Hoon Baek, Bumsu Kim, Kyung-Do Suh. Chitosan particle/multiwall carbon

nanotube composites by electrostatic interactions. Colloids and Surfaces A: Physicochem. Eng. Aspects 316 (2008): 292–296.

Sullivan,S.M. Introduction to gene therapy and guidelines to pharmaceutical development.In A. Rolland and S.M.(eds.),Pharmaceutical gene delivery system,.pp.1-16.New York:Marcel Dekker,2003.

Weiling Qin, Keqin Yang, Hao Tang, Liang Tan, Qingji Xie, Ming Ma, Youyu Zhang, Shouzhuo Yao. Improved GFP gene transfection mediated by polyamidoamine dendrimer-functionalized multi-walled carbon nanotubes with high biocompatibility.colliods and surfaces B Biointersurface84 (2011):206–213.

X. Deng,G. Jia,H. Wang,H. Sun,X. Wang,S. Yang,T. Wang,Y. Liu. Translocation and fate of multi-walled carbon nanotubes in vivo. Carbon 45 (2007):1419–1424.

Xiaoke Zhang, Xuefeng Wang, Qinghua Lu, Chuanlong Fu. Influence of carbon nanotube scaffolds on humancervical carcinoma HeLa cell viability and focal adhesion kinase expression.carbon46(2008):453–460

Ye Liu, Dr., De-Cheng Wu, Wei-De Zhang, Dr., Xuan Jiang, Chao-Bin He, Dr., Tai Shung Chung, Prof., Suat Hong Goh, Prof., Kam W. Leong, Prof.Polyethylenimine-Grafted Multiwalled Carbon Nanotubes for Secure Noncovalent Immobilization and Efficient Delivery of DNA. Angew. Chem. Int. Ed.44(2005):4782 – 4785.

Zhenzi Li, Zhenyu Wu, Kang Li. The high dispersion of DNA–multiwalled carbon nanotubes and their properties. Analytical Biochemistry 387(2009):267–270.

Zhong YQ, Wei J, Fu YR, Shao J, Liang YW, Lin YH, Liu J, Zhu ZH. Toxicity of cationic liposome Lipofectamine 2000 in human pancreatic cancer Capan-2 cells. Nan Fang Yi Ke Da Xue Xue Bao. 2008 Nov; 28(11):1981-4.

APPENDICES

APPENDIX A

PLASMID DNA AND PREPARATION OF PLASMID DNA

DNA concentration and purity determination by UV spectrophotometry

pDNA batch 1

Measuring Mode: Abs.

Scan Speed: Fast

Slit Width: 2.0

Sampling Interval: 0.1

No.	Wavelength (nm.)	Abs.
1	260.00	2.018
2	280.00	0.793

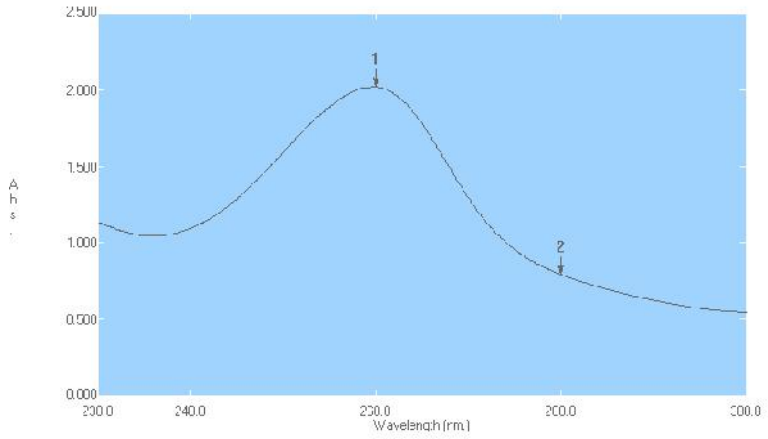

Measuring Mode: Abs.

Scan Speed: Fast

Slit Width: 2.0

Sampling Interval: 0.1

No.	Wavelength (nm.)	Abs.
1	260.00	2.020
2	280.00	0.794

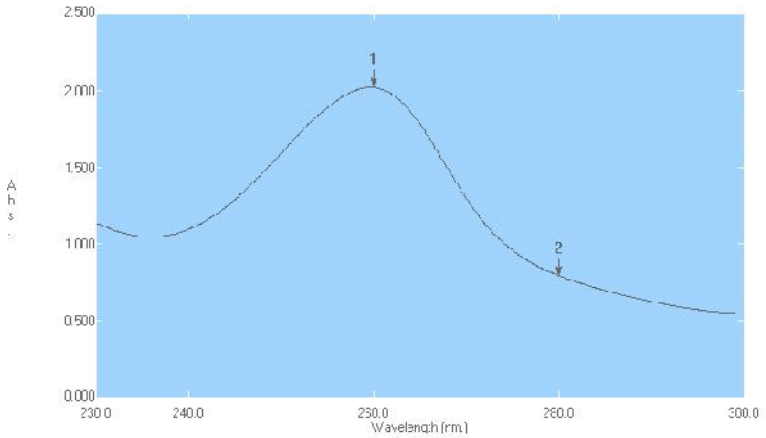

Measuring Mode: Abs.

Scan Speed: Fast

Slit Width: 2.0

Sampling Interval: 0.1

No.	Wavelength (nm.)	Abs.
1	260.00	2.014
2	280.00	0.794

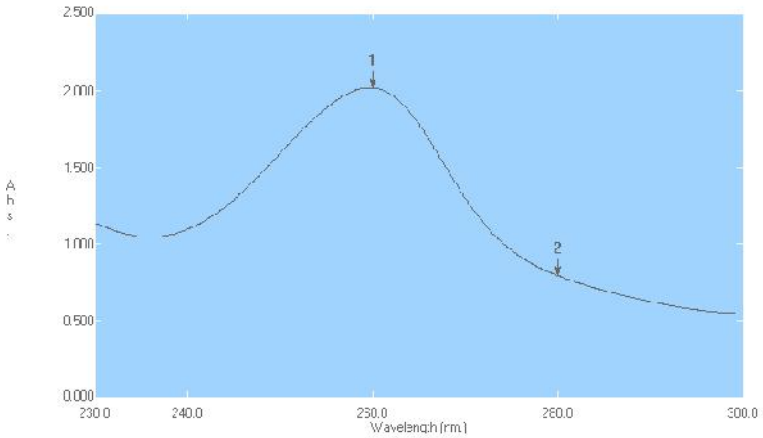

pDNA batch 2

Measuring Mode: Abs.

Scan Speed: Fast

Slit Width: 2.0

Sampling Interval: 0.1

No.	Wavelength (nm.)	Abs.
1	260.00	1.961
2	280.00	1.226

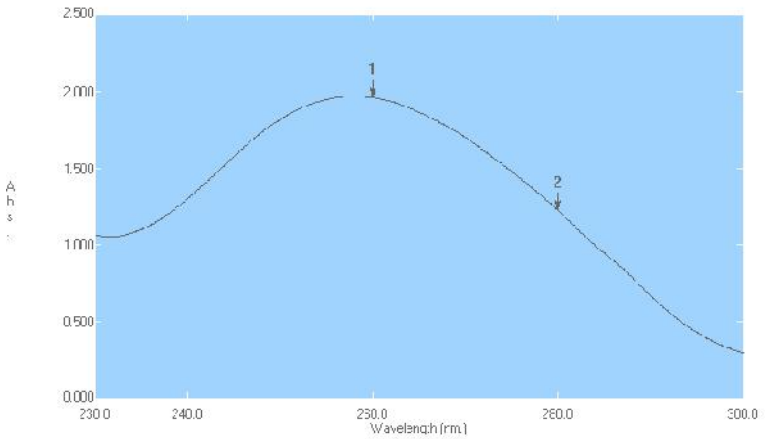

Measuring Mode: Abs.

Scan Speed: Fast

Slit Width: 2.0

Sampling Interval: 0.1

No.	Wavelength (nm.)	Abs.
1	260.00	1.956
2	280.00	1.219

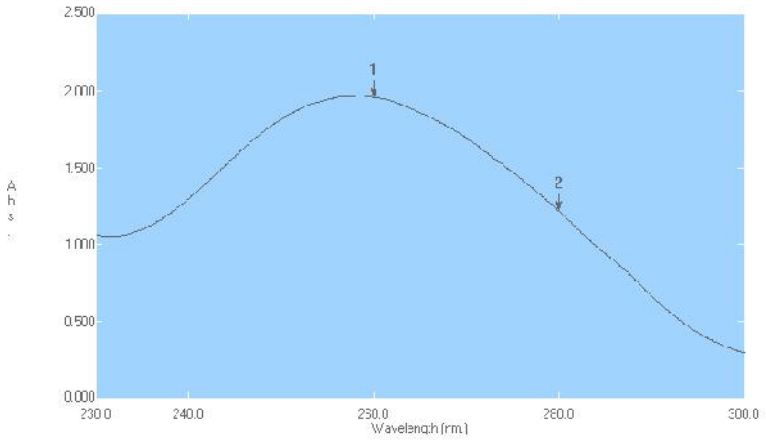

Measuring Mode: Abs.

Scan Speed: Fast

Slit Width: 2.0

Sampling Interval: 0.1

No.	Wavelength (nm.)	Abs.
1	260.00	1.956
2	280.00	1.218

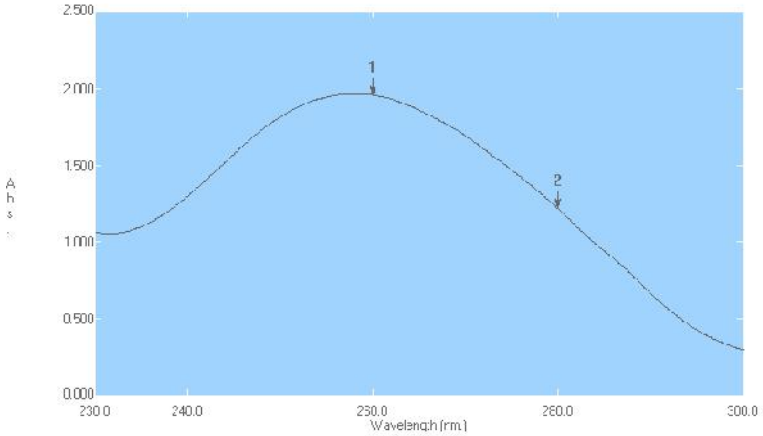
2.500
2.000
1.500
1.000
0.500
0.000
A
b
s
.
1
2
230.0
240.0
250.0
260.0
300.0
Wavelength (nm.)

DNA concentration and purity determination

pDNA No.	OD-260	OD-280	OD260x50(conc.) (µg/ml)	OD260/OD280(purity)
1-1	2.018	0.793	100.85	2.54
1-2	2.020	0.794		
1-3	2.014	0.794		
Mean 1	2.017	0.794		
2-1	1.961	1.216	97.9	1.61
2-2	1.956	1.219		
2-3	1.956	1.218		
Mean 2	1.958	1.218		

The production yield percentage of each f-MWCNTs in the mixture solvents of H_2SO_4/HNO_3 for 12 hours

Formulation (mg/100ml)	% yield f-MWCNTs	Mean±SD
5	94.2, 108.6, 101.4	101.4±10.18
10	109.6, 103.9, 102.77	102.77±7.46
15	102.67, 102.73, 100.82	100.82±3.26
20	99.55, 102.4, 102.4	100.98±2.02

Test of homogeneity of variances of the production yield percentage of each f-MWCNTs in the mixture solvents of H_2SO_4/HNO_3 for 12 hours.

YIELD

Levene Statistic	df1	df2	Sig.
1.978	3	8	.196

The one way analysis of variance of the production yield percentage of each f-MWCNTs in the mixture solvents of H_2SO_4/HNO_3 for 12 hours.

ANOVA

YIELD

Source of variation	Sum of Squares	df	Mean Square	F	Sig.
Between Groups	33.031	3	11.010	.637	.612
Within Groups	138.258	8	17.282		
Total	171.289	11			

Multiple Comparisons of the production yield percentage of each f-MWCNTs in the mixture solvents of H_2SO_4/HNO_3 for 12 hours.

Multiple Comparisons

Dependent Variable: YIELD

	(I) FORMULAT	(J) FORMULAT	Mean Difference (I-J)	Std. Error	Sig.	95% Confidence Interval	
						Lower Bound	Upper Bound
LSD	5mg	10mg	-4.0233	3.39434	.270	-11.8507	3.8040
		15mg	-.6733	3.39434	.848	-8.5007	7.1540
		20mg	-.0500	3.39434	.989	-7.8774	7.7774
	10mg	5mg	4.0233	3.39434	.270	-3.8040	11.8507
		15mg	3.3500	3.39434	.353	-4.4774	11.1774
		20mg	3.9733	3.39434	.275	-3.8540	11.8007
	15mg	5mg	.6733	3.39434	.848	-7.1540	8.5007
		10mg	-3.3500	3.39434	.353	-11.1774	4.4774
		20mg	.6233	3.39434	.859	-7.2040	8.4507
	20mg	5mg	.0500	3.39434	.989	-7.7774	7.8774
		10mg	-3.9733	3.39434	.275	-11.8007	3.8540
		15mg	-.6233	3.39434	.859	-8.4507	7.2040

APPENDIX B

MEASUREMENT OF PARTICLE SIZE AND ZETA POTENTIAL

Particle size of chitosan nanoparticles at 100% transmission

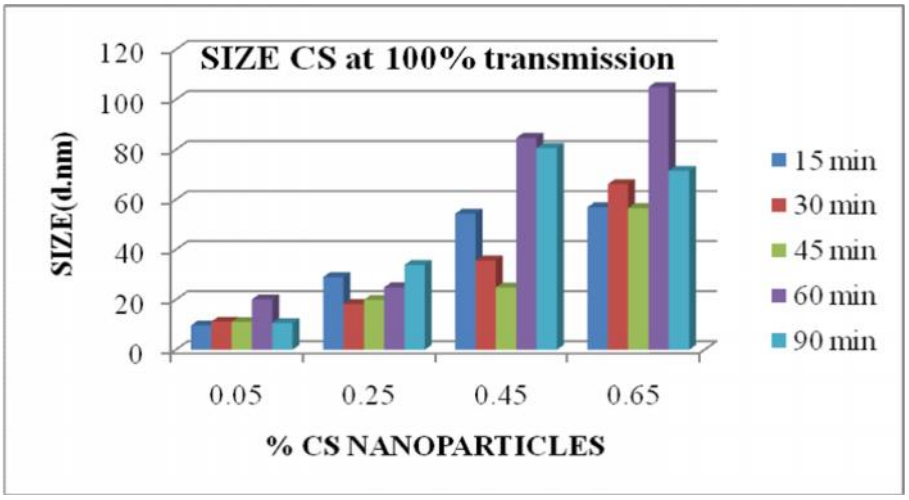

Particle size of chitosan nanoparticles at 120% transmission

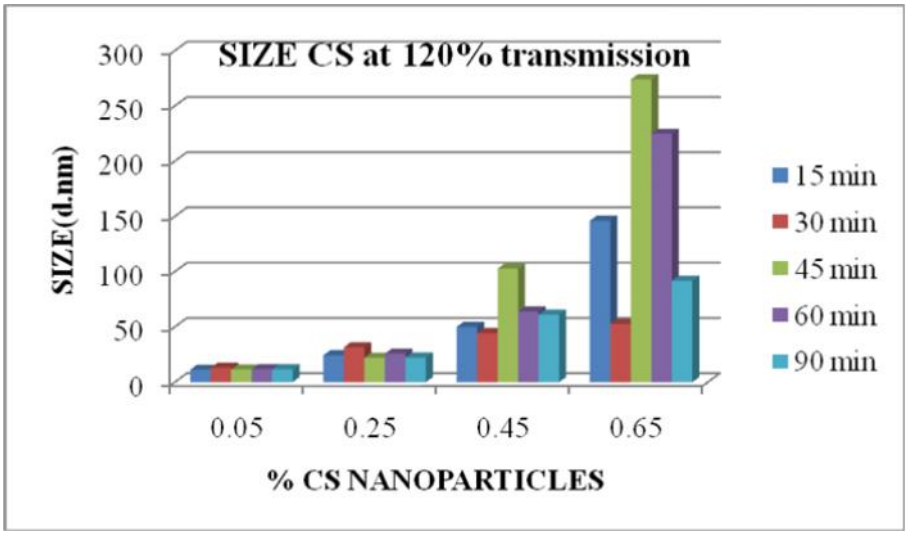

Particle size of chitosan nanoparticles at 140% transmission

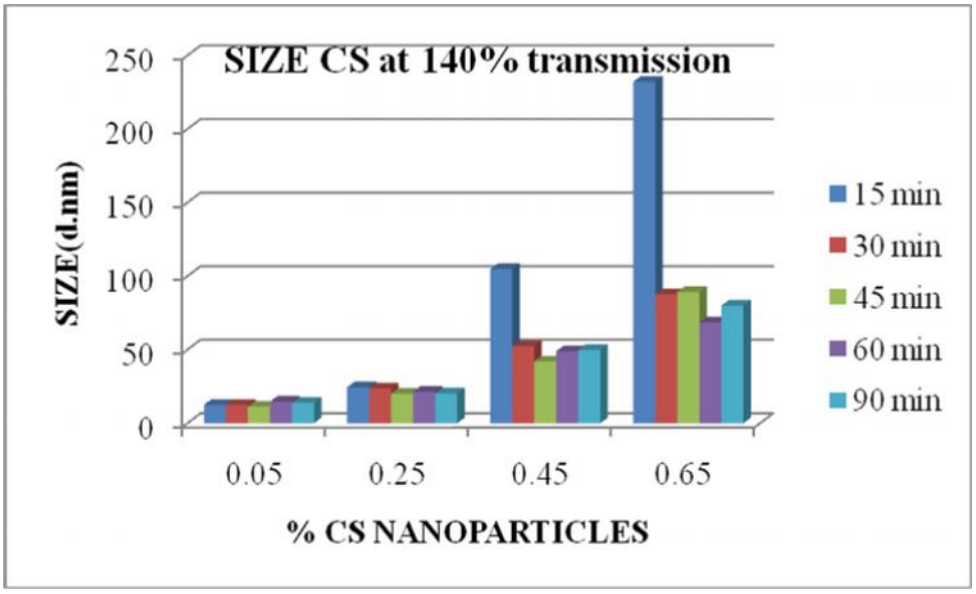

Zeta potential of chitosan nanoparticles at 100% transmission

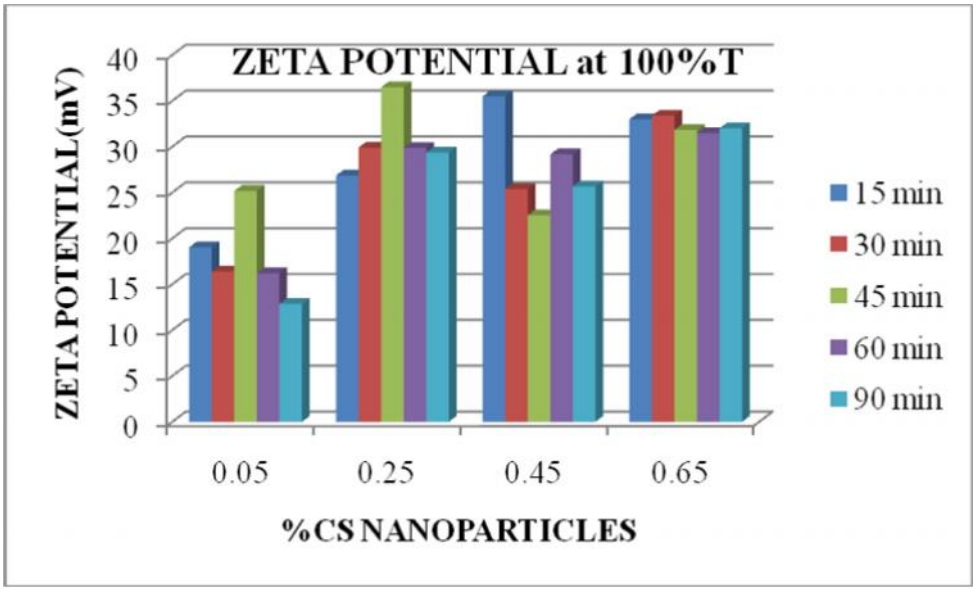

Zeta potential of chitosan nanoparticles at 120% transmission

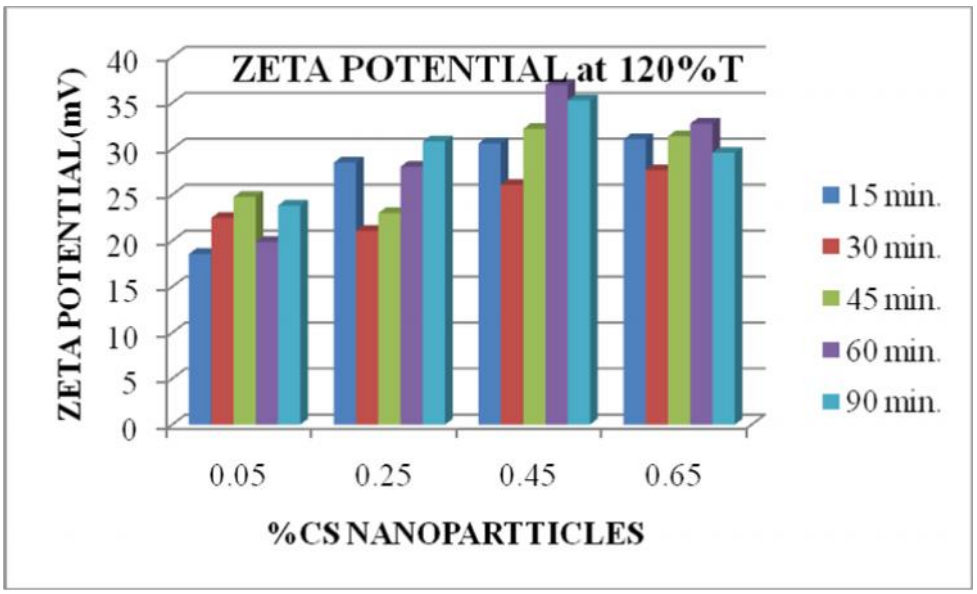

Zeta potential of chitosan nanoparticles at 140% transmission

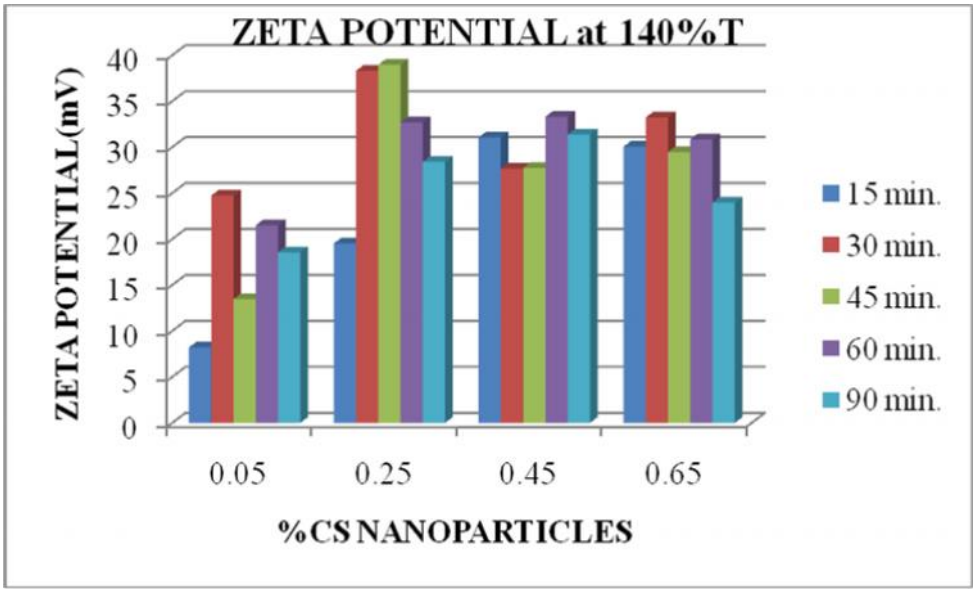

The comparison of particle size of 0.005% chitosan nanoparticles (n=3)

Time (min.)	% ultrasound power		
	100	120	140
15	9.96, 9.37, 9.78	11.26, 11.21,11.22	11.29, 11.88, 14.34
30	11.86, 10.52, 11.27	10.77, 13.13, 15.18	12.59, 12.85, 12.00
45	11.56, 11.04, 10.75	11.86, 11.04, 11.60	10.7, 12.44, 10.9
60	20.51, 10.69, 29.25	11.99, 11.15, 12.16	21.31, 11.37, 11.44
90	10.24, 10.62, 11.14	11.95, 11.40, 11.42	19.19, 11.73, 10.99

The comparison mean±SD of particle size of 0.005% chitosan nanoparticles (n=3)

Time (min.)	Mean±SD		
	% ultrasound power		
	100	120	140
15	9.70±0.03	11.23±0.02	12.50±1.62
30	11.22±0.67	13.03±2.21	12.48±0.44
45	11.12±0.41	11.50±0.42	11.35±0.95
60	20.15±9.28	11.77±0.54	14.71±5.72
90	10.66±0.45	11.59±0.31	13.97±4.54

The two way analysis of variance of 0.005% chitosan nanoparticles size

Univariate Analysis of Variance

Between-Subjects Factors

		Value Label	N
FORMULA	1	CS100	15
	2	CS120	15
	3	CS140	15
TIME	1	15	9
	2	30	9
	3	45	9
	4	60	9
	5	90	9

Test of homogeneity of variances of 0.005% chitosan nanoparticles size.

Levene's Test of Equality of Error Variances

Dependent Variable: SIZE

F	df1	df2	Sig.
4.524	14	30	P<0.05

a Design: Intercept+FORMULA+TIME+FORMULA * TIME

Tests of Between-Subjects Effects

Dependent Variable: SIZE

Source	Type III Sum of Squares	df	Mean Square	F	Sig.
Corrected Model	257.648(a)	14	18.403	1.846	.078
Intercept	6990.808	1	6990.808	701.189	p<0.05
FORMULA	10.723	2	5.361	.538	.590
TIME	114.177	4	28.544	2.863	.040
FORMULA * TIME	132.749	8	16.594	1.664	.149
Error	299.098	30	9.970		
Total	7547.555	45			
Corrected Total	556.746	44			

a R Squared = .463 (Adjusted R Squared = .212)

Multiple Comparisons of particle size of 0.005% chitosan nanoparticles at 100, 120 and 140% ultrasound power

Multiple Comparisons

Dependent Variable: SIZE

	(I) % ultrasound power	(J) % ultrasound power	Mean Difference (I-J)	Std. Error	Sig.	95% Confidence Interval	
						Lower Bound	Upper Bound
Dunnett C	CS100	CS120	.7507	1.39852	p>0.05	-2.9097	4.4110
		CS140	-.4307	1.58757	p>0.05	-4.5858	3.7244
	CS120	CS100	-.7507	1.39852	p>0.05	-4.4110	2.9097
		CS140	-1.1813	.85088	p>0.05	-3.4083	1.0457
	CS140	CS100	.4307	1.58757	p>0.05	-3.7244	4.5858
		CS120	1.1813	.85088	p>0.05	-1.0457	3.4083

Based on observed means.

Multiple Comparisons of particle size of 0.005% chitosan nanoparticles at 15, 30, 45, 60 and 90 min. by sonication

Dependent Variable: SIZE

	(I) TIME	(J) TIME	Mean Difference (I-J)	Std. Error	Sig.	95% Confidence Interval	
						Lower Bound	Upper Bound
Dunnett C	15	30	-1.0956	.68112	p>0.05	-3.4487	1.2576
		45	-.1756	.52619	p>0.05	-1.9934	1.6423
		60	-4.3911	2.24992	p>0.05	-12.1640	3.3818
		90	-.9300	1.03003	p>0.05	-4.4885	2.6285
	30	15	1.0956	.68112	p>0.05	-1.2576	3.4487
		45	.9200	.51258	p>0.05	-.8508	2.6908
		60	-3.2956	2.24678	p>0.05	-11.0576	4.4665
		90	.1656	1.02314	p>0.05	-3.3691	3.7002
	45	15	.1756	.52619	p>0.05	-1.6423	1.9934
		30	-.9200	.51258	p>0.05	-2.6908	.8508
		60	-4.2156	2.20476	p>0.05	-11.8324	3.4013
		90	-.7544	.92723	p>0.05	-3.9578	2.4489
	60	15	4.3911	2.24992	p>0.05	-3.3818	12.1640
		30	3.2956	2.24678	p>0.05	-4.4665	11.0576
		45	4.2156	2.20476	p>0.05	-3.4013	11.8324
		90	3.4611	2.37593	p>0.05	-4.7471	11.6693
	90	15	.9300	1.03003	p>0.05	-2.6285	4.4885
		30	-.1656	1.02314	p>0.05	-3.7002	3.3691
		45	.7544	.92723	p>0.05	-2.4489	3.9578
		60	-3.4611	2.37593	p>0.05	-11.6693	4.7471

Based on observed means.

The comparison of zeta potential of 0.005% chitosan nanoparticles

Time (min.)	% ultrasound power		
	100	120	140
15	10.34, 23.6, 23.17	14.15, 25.18, 16.37	5.61, 7.17, 11.82
30	5.34, 18.33,25.47	32.47, 20.92, 14.03	40.2, 26.2, 7.77
45	18.55, 34.55, 22.43	21.68, 28.73, 23.87	21.57, 12.54, 6.29
60	11.37, 29.73, 7.47	21.94, 11.15, 26.53	26.47, 6.68, 31.37
90	9.48, 6.46, 22.6	38.5, 21.77, 11.22	23.97, 18.48, 13.19

The comparison mean±SD of zeta potential of 0.005% chitosan nanoparticles

Time (min.)	Mean±SD		
	% ultrasound power		
	100	120	140
15	19.04±7.53	18.57±5.83	8.20±3.23
30	16.38±10.20	22.48±9.32	24.73±16.26
45	25.18±8.35	24.76±3.61	13.47±7.68
60	16.19±11.89	19.88±7.90	21.51±13.07
90	12.85±8.58	23.83±13.75	18.55±5.39

The two way analysis of variance of 0.005% chitosan nanoparticles zeta potential

Univariate Analysis of Variance

Between-Subjects Factors

		Value Label	N
TIME	1	15	9
	2	30	9
	3	45	9
	4	60	9
	5	90	9
FORMULA	1	CS100	15
	2	CS120	15
	3	CS140	15

Test of homogeneity of variances of 0.005% chitosan nanoparticles zeta potential.

Levene's Test of Equality of Error Variances

Dependent Variable: ZETA

F	df1	df2	Sig.
1.142	14	30	.365

a Design: Intercept+TIME+FORMULA+TIME * FORMULA

Tests of Between-Subjects Effects

Dependent Variable: ZETA

Source	Type III Sum of Squares	df	Mean Square	F	Sig.
Corrected Model	1040.336(a)	14	74.310	.817	.646
Intercept	16310.807	1	16310.807	179.253	p<0.05
TIME	213.036	4	53.259	.585	.676
FORMULA	187.374	2	93.687	1.030	.369
TIME * FORMULA	639.927	8	79.991	.879	.545
Error	2729.795	30	90.993		
Total	20080.938	45			
Corrected Total	3770.131	44			

a R Squared = .276 (Adjusted R Squared = -.062)

Multiple Comparisons of zeta potential of 0.005% chitosan nanoparticles at 100, 120 and 140% ultrasound power

Multiple Comparisons

Dependent Variable: ZETA

	(I) % ultrasound power	(J) % ultrasound power	Mean Difference (I-J)	Std. Error	Sig.	95% Confidence Interval	
						Lower Bound	Upper Bound
LSD	CS100	CS120	-3.9747	3.48316	.263	-11.0882	3.1389
		CS140	.6373	3.48316	.856	-6.4762	7.7509
	CS120	CS100	3.9747	3.48316	.263	-3.1389	11.0882
		CS140	4.6120	3.48316	.195	-2.5016	11.7256
	CS140	CS100	-.6373	3.48316	.856	-7.7509	6.4762
		CS120	-4.6120	3.48316	.195	-11.7256	2.5016

Based on observed means.

Multiple Comparisons of zeta potential of 0.005% chitosan nanoparticles at 15, 30, 45, 60 and 90 min. by sonication

Multiple Comparisons

Dependent Variable: ZETA

	(I) TIME	(J) TIME	Mean Difference (I-J)	Std. Error	Sig.	95% Confidence Interval	
						Lower Bound	Upper Bound
LSD	15	30	-5.9244	4.49674	.198	-15.1080	3.2591
		45	-5.8667	4.49674	.202	-15.0502	3.3169
		60	-3.9222	4.49674	.390	-13.1058	5.2614
		90	-3.1400	4.49674	.490	-12.3236	6.0436
	30	15	5.9244	4.49674	.198	-3.2591	15.1080
		45	.0578	4.49674	.990	-9.1258	9.2414
		60	2.0022	4.49674	.659	-7.1814	11.1858
		90	2.7844	4.49674	.540	-6.3991	11.9680
	45	15	5.8667	4.49674	.202	-3.3169	15.0502
		30	-.0578	4.49674	.990	-9.2414	9.1258
		60	1.9444	4.49674	.669	-7.2391	11.1280
		90	2.7267	4.49674	.549	-6.4569	11.9102
	60	15	3.9222	4.49674	.390	-5.2614	13.1058
		30	-2.0022	4.49674	.659	-11.1858	7.1814
		45	-1.9444	4.49674	.669	-11.1280	7.2391
		90	.7822	4.49674	.863	-8.4014	9.9658
	90	15	3.1400	4.49674	.490	-6.0436	12.3236
		30	-2.7844	4.49674	.540	-11.9680	6.3991
		45	-2.7267	4.49674	.549	-11.9102	6.4569
		60	-.7822	4.49674	.863	-9.9658	8.4014

Based on observed means.

The comparison of particle size of 0.025% chitosan nanoparticles (n=3)

Time (min.)	% ultrasound power		
	100	120	140
15	14.53, 21.87, 50.75	17.11, 23.41, 32.48	23.77, 23.03, 26.41
30	13.91, 20.87, 20.11	46.62, 23.38, 24.86	27.92, 23.11, 20.15
45	18.81, 17.63, 23.4	19.89, 24.74, 21.56	17.51, 16.77, 26.09
60	14.22, 20.71, 39.93	32.56, 23.07, 21.76	21.58, 20.52, 22.14
90	30.79, 17.77, 53.16	19.26, 19.34, 28.19	18.26, 21.13, 21.67

The comparison mean±SD of particle size of 0.025% chitosan nanoparticles (n=3)

Time (min.)	Mean±SD		
	% ultrasound power		
	100	120	140
15	29.05±19.15	24.33±7.72	24.40±1.77
30	18.30±3.82	31.62±13.01	23.73±3.92
45	19.95±3.05	22.06±2.46	20.13±5.18
60	24.95±13.37	25.80±5.89	21.42±0.82
90	33.91±17.90	22.26±5.13	20.35±1.83

The two way analysis of variance of 0.025% chitosan nanoparticles size

Univariate Analysis of Variance

Between-Subjects Factors

		Value Label	N
TIME	1	15	9
	2	30	9
	3	45	9
	4	60	9
	5	90	9
FORMULA	1	CS100	15
	2	CS120	15
	3	CS140	15

Test of homogeneity of variances of 0.025% chitosan nanoparticles size.

Levene's Test of Equality of Error Variances(a)

Dependent Variable: SIZE

F	df1	df2	Sig.
4.227	14	30	P<0.05

a Design: Intercept+TIME+FORMULA+TIME * FORMULA

Tests of Between-Subjects Effects

Dependent Variable: SIZE

Source	Type III Sum of Squares	df	Mean Square	F	Sig.
Corrected Model	829.796(a)	14	59.271	.720	.739
Intercept	26245.013	1	26245.013	318.709	p<0.05
TIME	153.012	4	38.253	.465	.761
FORMULA	103.621	2	51.811	.629	.540
TIME * FORMULA	573.162	8	71.645	.870	.552
Error	2470.434	30	82.348		
Total	29545.242	45			
Corrected Total	3300.229	44			

a R Squared = .251 (Adjusted R Squared = -.098)

Multiple comparisons of 0.025% chitosan nanoparticles size by vary 100, 120 and 140% ultrasound power

Multiple Comparisons

Dependent Variable: SIZE

	(I) % ultrasound power	(J) % ultrasound power	Mean Difference (I-J)	Std. Error	Sig.	95% Confidence Interval	
						Lower Bound	Upper Bound
Dunnett C	CS100	CS120	.0153	3.81213	p>0.05	-9.9621	9.9927
		CS140	3.2267	3.39605	p>0.05	-5.6617	12.1151
	CS120	CS100	-.0153	3.81213	p>0.05	-9.9927	9.9621
		CS140	3.2113	2.09248	p>0.05	-2.2653	8.6879
	CS140	CS100	-3.2267	3.39605	p>0.05	-12.1151	5.6617
		CS120	-3.2113	2.09248	p>0.05	-8.6879	2.2653

Based on observed means.

Multiple Comparisons of the zeta potential of 0.025%w/v chitosan nanoparticles by vary % ultrasound power at 15, 30, 45, 60 and 90 min.

Dependent Variable: SIZE

	(I) TIME	(J) TIME	Mean Difference (I-J)	Std. Error	Sig.	95% Confidence Interval	
						Lower Bound	Upper Bound
Dunnett C	15	30	1.3811	4.67058	p>0.05	-14.7546	17.5168
		45	5.2178	3.71839	p>0.05	-7.6283	18.0639
		60	1.8744	4.35192	p>0.05	-13.1603	16.9092
		90	.4211	5.17196	p>0.05	-17.4467	18.2889
	30	15	-1.3811	4.67058	p>0.05	-17.5168	14.7546
		45	3.8367	3.24996	p>0.05	-7.3911	15.0645
		60	.4933	3.95917	p>0.05	-13.1846	14.1713
		90	-.9600	4.84613	p>0.05	-17.7022	15.7822
	45	15	-5.2178	3.71839	p>0.05	-18.0639	7.6283
		30	-3.8367	3.24996	p>0.05	-15.0645	7.3911
		60	-3.3433	2.77256	p>0.05	-12.9218	6.2352
		90	-4.7967	3.93664	p>0.05	-18.3968	8.8034
	60	15	-1.8744	4.35192	p>0.05	-16.9092	13.1603
		30	-.4933	3.95917	p>0.05	-14.1713	13.1846
		45	3.3433	2.77256	p>0.05	-6.2352	12.9218
		90	-1.4533	4.53981	p>0.05	-17.1372	14.2306
	90	15	-.4211	5.17196	p>0.05	-18.2889	17.4467
		30	.9600	4.84613	p>0.05	-15.7822	17.7022
		45	4.7967	3.93664	p>0.05	-8.8034	18.3968
		60	1.4533	4.53981	p>0.05	-14.2306	17.1372

Based on observed means

The comparison of zeta potential of 0.025% chitosan nanoparticles

Time (min.)	% ultrasound power		
	100	120	140
15	6.89, 37.7, 35.93	23.97, 35.9, 25.63	24.3, 20.23, 14.03
30	23.7, 29.83, 36.17	15.47, 17.1, 30.63	38.6, 44.97, 31.37
45	34.4, 39.63, 35.4	17.05, 17.4, 34.53	36.7, 42.2, 38.03
60	38.9, 21.2, 29.47	21.0, 30.37, 32.8	30.93, 28.0, 39.2
90	33.57, 29.57, 24.93	26.47, 33.9, 32.03	27.13, 34.07, 23.97

The comparison mean±SD of zeta potential of 0.025% chitosan nanoparticles

Time (min.)	Mean±SD		
	% ultrasound power		
	100	120	140
15	26.84±17.30	28.50±6.46	19.52±5.17
30	29.90±6.23	21.07±8.32	38.31±6.80
45	36.48±2.78	22.99±9.99	38.98±2.87
60	29.86±8.86	28.06±6.23	32.71±5.81
90	29.36±4.32	30.80±3.87	28.39±5.17

The two way analysis of variance of 0.025% chitosan nanoparticles zeta potential

Univariate Analysis of Variance

Between-Subjects Factors

		Value Label	N
TIME	1	15	9
	2	30	9
	3	45	9
	4	60	9
	5	90	9
FORMULA	1	CS100	15
	2	CS120	15
	3	CS140	15

Test of homogeneity of variances of 0.025% chitosan nanoparticles zeta potential

Levene's Test of Equality of Error Variances (a)

Dependent Variable: ZETA

F	df1	df2	Sig.
2.446	14	30	.019

(a)Design: Intercept+TIME+FORMULA+TIME * FORMULA

Tests of Between-Subjects Effects

Dependent Variable: ZETA

Source	Type III Sum of Squares	df	Mean Square	F	Sig.
Corrected Model	1358.610(a)	14	97.044	1.714	.105
Intercept	39029.791	1	39029.791	689.294	P<0.05
TIME	289.994	4	72.499	1.280	.300
FORMULA	234.697	2	117.349	2.072	.144
TIME * FORMULA	833.918	8	104.240	1.841	.108
Error	1698.684	30	56.623		
Total	42087.085	45			
Corrected Total	3057.295	44			

a R Squared = .444 (Adjusted R Squared = .185)

Multiple Comparisons of the zeta potential of 0.025%w/v chitosan nanoparticles by vary at 100, 120 and 140% ultrasound power

Multiple Comparisons

Dependent Variable: ZETA

	(I) % ultrasound power	(J) % ultrasound power	Mean Difference (I-J)	Std. Error	Sig.	95% Confidence Interval	
						Lower Bound	Upper Bound
Dunnett C	CS100	CS120	4.2027	2.90184	p>0.05	-3.3923	11.7976
		CS140	-1.0960	3.15765	p>0.05	-9.3604	7.1684
	CS120	CS100	-4.2027	2.90184	p>0.05	-11.7976	3.3923
		CS140	-5.2987	2.91384	p>0.05	-12.9250	2.3277
	CS140	CS100	1.0960	3.15765	p>0.05	-7.1684	9.3604
		CS120	5.2987	2.91384	p>0.05	-2.3277	12.9250

Based on observed means.

Multiple Comparisons of the zeta potential of 0.025%w/v chitosan nanoparticles by vary % ultrasound power at 15, 30, 45, 60 and 90 min.

Multiple Comparisons

Dependent Variable: ZETA

	(I) TIME	(J) TIME	Mean Difference (I-J)	Std. Error	Sig.	95% Confidence Interval	
						Lower Bound	Upper Bound
Dunnett C	15	30	-4.8067	4.75467	p>0.05	-21.2329	11.6195
		45	-7.8622	4.63631	p>0.05	-23.8795	8.1551
		60	-5.2544	4.09536	p>0.05	-19.4029	8.8940
		90	-4.5622	3.73057	p>0.05	-17.4504	8.3260
	30	15	4.8067	4.75467	p>0.05	-11.6195	21.2329
		45	-3.0556	4.45695	p>0.05	-18.4532	12.3421
		60	-.4478	3.89116	p>0.05	-13.8908	12.9952
		90	.2444	3.50518	p>0.05	-11.8651	12.3540
	45	15	7.8622	4.63631	p>0.05	-8.1551	23.8795
		30	3.0556	4.45695	p>0.05	-12.3421	18.4532
		60	2.6078	3.74561	p>0.05	-10.3324	15.5479
		90	3.3000	3.34287	p>0.05	-8.2488	14.8488
	60	15	5.2544	4.09536	p>0.05	-8.8940	19.4029
		30	.4478	3.89116	p>0.05	-12.9952	13.8908
		45	-2.6078	3.74561	p>0.05	-15.5479	10.3324
		90	.6922	2.53996	p>0.05	-8.0827	9.4672
	90	15	4.5622	3.73057	p>0.05	-8.3260	17.4504
		30	-.2444	3.50518	p>0.05	-12.3540	11.8651
		45	-3.3000	3.34287	p>0.05	-14.8488	8.2488
		60	-.6922	2.53996	p>0.05	-9.4672	8.0827

Based on observed means.

APPENDIX C

IN VITRO TRANSFECTION IN HeLa CELL CULTURE

Comparison of pDNA, 1:9:1 M/C/D, 5:3:1 M/C/D, the *In vitro* expression of the green fluorescent protein (%GFP)

Formulation	pDNA	M/C/D	
		1:9:1	5:3:1
1	-0.1	2.06	5.59
2	-0.96	6.64	3.69
3	0.85	1.62	2.48
Mean±SD	-0.07±0.91	3.44±2.78	3.92±1.57

Test of homogeneity of variances of %GFP of pDNA, 1:9:1 and 5:3:1 M/C/D.

Test of Homogeneity of Variances

GFP

Levene Statistic	df1	df2	Sig.
3.077	2	6	.120

The one way analysis of variance of the green fluorescent protein (%GFP), pDNA, 1:9:1 and 5:3:1 M/C/D, were incubated for 48 hours in the 5% CO_2 humidified incubator at 37°C

ANOVA

GFP

Source of variation	Sum of Squares	df	Mean Square	F	Sig.
Between Groups	28.471	2	14.235	3.880	.083
Within Groups	22.012	6	3.669		
Total	50.482	8			

Multiple Comparisons of the green fluorescent protein (%GFP), PolyFect®, Lipofectamine®, 1:9:1 and 5:3:1 M/C/D, were incubated for 48 hours in the 5% CO_2 humidified incubator at 37°C

Multiple Comparisons

Dependent Variable: GFP
LSD

(I) FORMULAT	(J) FORMULAT	Mean Difference (I-J)	Std. Error	Sig.	95% Confidence Interval	
					Lower Bound	Upper Bound
pDNA	1:9:1 M/C/D	-3.5100	1.56388	.066	-7.3367	.3167
	5:3:1 M/C/D	-3.9900(*)	1.56388	.043	-7.8167	-.1633
1:9:1 M/C/D	pDNA	3.5100	1.56388	.066	-.3167	7.3367
	5:3:1 M/C/D	-.4800	1.56388	.769	-4.3067	3.3467
5:3:1 M/C/D	pDNA	3.9900(*)	1.56388	.043	.1633	7.8167
	1:9:1 M/C/D	.4800	1.56388	.769	-3.3467	4.3067

* The mean difference is significant at the .05 level.

Comparison of 1:9:1 M/C/D, 5:3:1 M/C/D, PolyFect®, Lipofectamine®, the *In vitro* expression of the green fluorescent protein (%GFP)

Formulation	PolyFect®	Lipofectamine®	M/C/D	
			1:9:1	5:3:1
1	47.8	13.7	2.06	5.59
2	45.23	16.9	6.64	3.69
3	36.55	14.0	1.62	2.48
Mean±SD	43.19±5.9	14.87±1.77	3.44±2.78	3.92±1.57

Test of homogeneity of variances of %GFP of PolyFect®, Lipofectamine®, 1:9:1 and 5:3:1 M/C/D.

Test of Homogeneity of Variances

GFP

Levene Statistic	df1	df2	Sig.
3.806	3	8	.058

The one way analysis of variance of the green fluorescent protein (%GFP), PolyFect®, Lipofectamine®, 1:9:1 and 5:3:1 M/C/D, were incubated for 48 hours in the 5% CO_2 humidified incubator at 37°C

ANOVA

GFP

Source of variation	Sum of Squares	df	Mean Square	F	Sig.
Between Groups	3131.798	3	1043.933	86.863	p<0.05
Within Groups	96.146	8	12.018		
Total	3227.944	11			

Multiple Comparisons of the green fluorescent protein (%GFP), PolyFect®, Lipofectamine®, 1:9:1 and 5:3:1 M/C/D, were incubated for 48 hours in the 5% CO_2 humidified incubator at 37°C

Multiple Comparisons

Dependent Variable: GFP
LSD

(I) FORMULAT	(J) FORMULAT	Mean Difference (I-J)	Std. Error	Sig.	95% Confidence Interval	
					Lower Bound	Upper Bound
Q	L	28.3250(*)	2.83057	p<0.05	21.7977	34.8523
	1:9:1 M/C/D	39.7533(*)	2.83057	p<0.05	33.2260	46.2806
	5:3:1 M/C/D	39.2733(*)	2.83057	p<0.05	32.7460	45.8006
L	Q	-28.3250(*)	2.83057	p<0.05	-34.8523	-21.7977
	1:9:1 M/C/D	11.4283(*)	2.83057	.004	4.9010	17.9556
	5:3:1 M/C/D	10.9483(*)	2.83057	.005	4.4210	17.4756
1:9:1 M/C/D	Q	-39.7533(*)	2.83057	p<0.05	-46.2806	-33.2260
	L	-11.4283(*)	2.83057	.004	-17.9556	-4.9010
	5:3:1 M/C/D	-.4800	2.83057	.870	-7.0073	6.0473
5:3:1 M/C/D	Q	-39.2733(*)	2.83057	p<0.05	-45.8006	-32.7460
	L	-10.9483(*)	2.83057	.005	-17.4756	-4.4210
	1:9:1 M/C/D	.4800	2.83057	.870	-6.0473	7.0073

* The mean difference is significant at the .05 level.

APPENDIX D

CONCEPTUAL FRAMEWORK

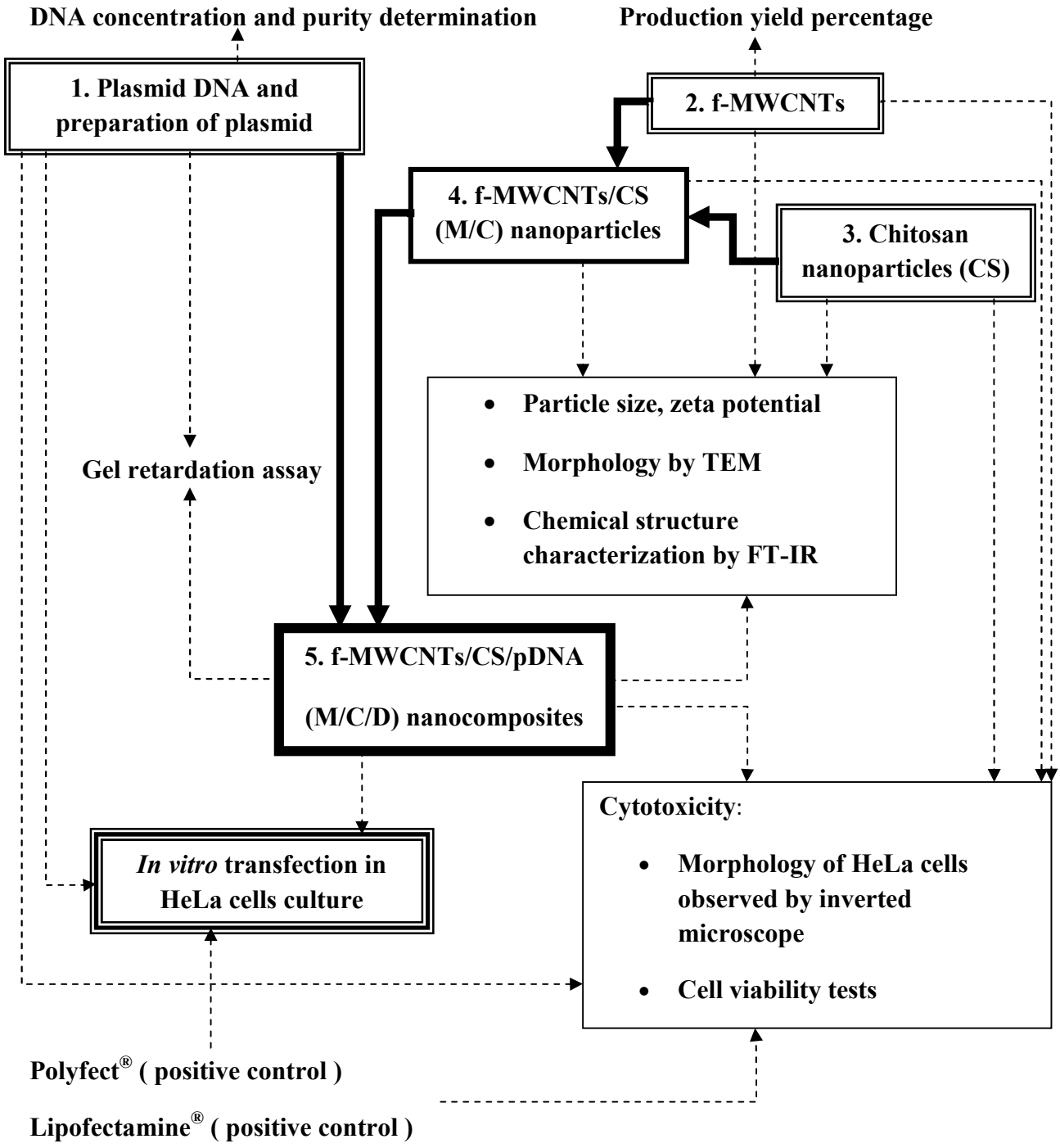

VITA

Miss Orrapan Jai-ut was born on October 31, 1983 in Chiangmai, Thailand. She received her Bacheler Degree of Pharmacy in 2007 from Faculty of Pharmacy, Chiangmai University, Thailand.